TURUN
YLIOPISTO
UNIVERSITY
OF TURKU

LABEL-FREE METHODS FOR STUDYING PROTEIN-PROTEIN INTERACTIONS

Salla Valtonen

TURUN YLIOPISTON JULKAISUJA – ANNALES UNIVERSITATIS TURKUENSIS
SARJA – SER. AI OSA – TOM. 661 | ASTRONOMICA – CHEMICA – PHYSICA – MATHEMATICA | TURKU 2021

TURUN
YLIOPISTO
UNIVERSITY
OF TURKU

LABEL-FREE METHODS FOR STUDYING PROTEIN-PROTEIN INTERACTIONS

Salla Valtonen

TURUN YLIOPISTON JULKAISUJA – ANNALES UNIVERSITATIS TURKUENSIS
SARJA - SER. AI OSA – TOM. 661 | ASTRONOMICA – CHEMICA – PHYSICA – MATHEMATICA | TURKU 2021

University of Turku

Faculty of Science
Department of Chemistry
Chemistry of Drug Development
Doctoral Programme in Physical and Chemical Sciences

Supervised by

Docent Harri Härmä, PhD
Department of Chemistry
University of Turku
Turku, Finland

Kari Kopra, PhD
Department of Chemistry
University of Turku
Turku, Finland

Reviewed by

Professor Kevan Shokat
Department of Chemistry
University of California
Berkeley, CA, USA

Professor Hanns-Christian Mahler
University of Frankfurt/Main
Frankfurt, Main, Germany

Opponent

Professor Ali Tavassoli
Department of Chemistry
University of Southampton
Southampton, England, UK

ISBN 978-951-29-8723-8 (PRINT)
ISBN 978-951-29-8724-5 (PDF)
ISSN 0082-7002 (Print)
ISSN 2343-3175 (Online)
Painosalama, Turku, Finland 2021

Look how far we've come.

UNIVERSITY OF TURKU
Faculty of Science
Department of Chemistry
Chemistry of Drug Development
SALLA VALTONEN: Label-Free Methods for Studying Protein-Protein Interactions
Doctoral Dissertation, 148 pp.
Doctoral Programme in Physical and Chemical Sciences
December 2021

ABSTRACT

Proteins are the building blocks of life, and mainly perform their roles through protein-protein interactions (PPIs). Thus, PPIs are essential to the normal function of the cells and the body, and disturbances in these interactions are an underlying cause for many diseases. Because PPIs are so vital, multiple methods have been developed to study these interactions. Typically, the methods are based on reporter molecules, although label conjugation may disrupt PPIs. Several label-free methods have also been introduced, which can be categorized into surface-based and solution-based approaches. Surface-based methods are often very sensitive, but they require protein conjugation to a solid surface. Solution-based methods, on the other hand, are fully conjugation-free but suffer from low sensitivity.

In this thesis, a label-free, solution-based Protein-Probe method with nanomolar sensitivity was developed for studying protein thermal stability and interactions. The method is based on an external probe peptide, the Eu-probe, and it does not require conjugation to the interacting proteins, avoiding potential disruption of the reactions. The Eu-probe does not significantly bind to native, intact proteins, and the time-resolved luminescence signal of the free probe is quenched by a modulator in the Protein-Probe solution. When denaturation reveals hydrophobic amino acids or binding events increase the overall surface area, the change in the protein structure enables the Eu-probe binding. Binding to the proteins protects the probe from the modulator and leads to a signal increase.

The Protein-Probe was first applied to studying protein-ligand interactions and PPIs by observing their effect on protein thermal stability in thermal shift assays. PPIs were also monitored based on interaction-induced signal increase at elevated temperatures without a thermal shift, and in competitive thermal shift assays with small molecular ligands. The formation of large protein complexes and aggregates was successfully monitored at room temperature. The developed label-free Protein-Probe method has improved sensitivity over the current solution-based PPI detection techniques. The method enables monitoring different interaction types, as the external probe binds to a wide variety of proteins in multiple assay concepts. Thus, the Protein-Probe is a promising new method for PPI studies.

KEYWORDS: protein-protein interactions, label-free, time-resolved luminescence, Protein-Probe

TURUN YLIOPISTO
Matemaattis-luonnontieteellinen tiedekunta
Kemian laitos
Lääkekehityksen kemia
SALLA VALTONEN: Leimavapaat menetelmät proteiinien välisten vuorovaikutusten tutkimiseen
Väitöskirja, 148 s.
Fysikaalisten ja kemiallisten tieteiden tohtoriohjelma
joulukuu 2021

TIIVISTELMÄ

Proteiinit ovat yksi elämän rakennuspalikoista, ja ne toimivat pääasiassa proteiinien välisten vuorovaikutusten (PPI:t) kautta. Tämän vuoksi PPI:t ovat elintärkeitä solujen ja kehon normaalille toiminnalle, ja häiriöt vuorovaikututuksissa ovat usean sairauden takana. Koska PPI:t ovat niin keskeisiä, niiden tutkimiseen on kehitetty useita menetelmiä. Tyypillisesti menetelmät perustuvat reportterimolekyyleihin, vaikka niiden kiinnitys saattaa häiritä PPI:tä. On olemassa myös useita leimavapaita menetelmiä, jotka voidaan jakaa pintapohjaisiin ja liuospohjaisiin menetelmiin. Pintapohjaisilla menetelmillä on usein hyvä herkkyys, mutta niiden heikkous on että proteiini täytyy konjugoida kiinteään pintaan. Liuospohjaiset menetelmät taas eivät vaadi ollenkaan konjugaatiota, mutta kärsivät usein huonosta herkkyydestä.

Tässä työssä kehitettiin leimavapaa, liuospohjainen ”Protein-Probe” menetelmä, jonka herkkyys on nanomolaarisella alueella. Menetelmä perustuu ulkoiseen koetinpeptidiin, Eu-koettimeen, joten tutkittavia proteiineja ei konjugoida. Eu-koetin ei sitoudu merkittävästi natiivirakenteisiin proteiineihin, ja Protein-Probe-liuoksessa oleva modulaattori sammuttaa vapaan koettimen aikaerotteisen luminesenssi-signaalin. Muutokset proteiinien rakenteessa, kuten denaturaatiosta johtuva hydrofobisten aminohappojen paljastuminen ja vuorovaikutuksia seuraava pinta-alan kasvu, mahdollistavat Eu-koettimen sitoutumisen. Sitoutuminen proteiineihin suojaa koetinta modulaattorilta ja johtaa näin signaalin kasvuun.

Protein-Probe-menetelmällä tutkittiin proteiini-ligandi- ja proteiini-proteiini-vuorovaikutuksia seuraamalla niiden vaikutusta proteiinien lämpöstabiilisuuteen ”thermal shift” määrityksissä. Vuorovaikutuksia havainnoitiin myös perustuen sitoutumisen aikaansaamaan signaalin nousuun korkeassa lämpötilassa, ja kilpailevissa thermal shift määrityksissä pienten ligandimolekyylien kanssa. Suurten proteiinikompleksien ja aggregaattien muodostuminen havaittiin huoneenlämmössä. Kehitetty leimavapaa Protein-Probe menetelmä on herkempi kuin nykyiset liuospohjaiset tekniikat, ja sillä on mahdollista tutkia erilaisia vuorovaikutuksia, koska ulkoinen koetin sitoutuu moneen eri proteiiniin useassa määritystyypissä. Protein-Probe-menetelmä on siis lupaava uusi menetelmä PPI-tutkimukseen.

ASIASANAT: proteiinien väliset vuorovaikutukset, leimavapaa, aikaerotteinen luminesenssi, Protein-Probe

Table of Contents

Abbreviations

ANS	1-anilinonaphthalene-8-sulfonate
ATP	Adenosine triphosphate
AZA	Acetazolamide
Bio-BSA	Biotinylated bovine serum albumin
BLI	Biolayer interferometry
BSA	Bovine serum albumin
CA	Carbonic anhydrase
CD	Circular dichroism
CRP	C-reactive protein
DARPin	Designed ankyrin repeat protein
DNA	Deoxyribonucleic acid
DLS	Dynamic light scattering
DPI	Dual polarization interferometry
DSC	Differential scanning calorimetry
DSF	Differential scanning fluorimetry
EC_{50}	Half-maximal effectivity concentration
eIF4A	Eukaryotic initiation factor 4A
eIF4H	Eukaryotic translation initiation factor 4H
EIS	Electrochemical impedance spectroscopy
FRET	Förster resonance energy transfer
GDP	Guanosine diphosphate
GMPPNP	5'-Guanylyl imidodiphosphate
GTP	Guanosine triphosphate
HIDC	1,1,3,3,3′,3′-hexamethylindodicarbocyanine iodide
HTS	High-throughput screening
ITC	Isothermal titration calorimetry
mAb	Monoclonal antibody
NMR	Nuclear magnetic resonance
PAGE	Polyacrylamide gel electrophoresis
PBS	Phosphate-buffered saline
PDCD4	Programmed cell death protein 4

PLI	Protein-ligand interaction
PPI	Protein-protein interaction
QCM	Quartz crystal microbalance
QCM-D	Quartz crystal microbalance-dissipation monitoring
qPCR	Quantitative polymerase chain reaction
QRET	Quenching resonance energy transfer
RNA	Ribonucleic acid
RT	Room temperature
RWG	Resonant waveguide grating
SA	Streptavidin
S/B	Signal-to-background ratio
SD	Standard deviation
SLS	Static light scattering
SPR	Surface plasmon resonance
TE	Transverse electric
TICT	Twisted intramolecular charge transfer
TIRE	Total internal reflection ellipsometry
T_m	Melting temperature
TM	Transverse magnetic
TRL	Time-resolved luminescence
UV	Ultraviolet
WT	Wild type

List of Original Publications

This dissertation is based on the following original publications, which are referred to in the text by their Roman numerals:

I Vuorinen, E., Valtonen, S., Eskonen, V., Kariniemi, T., Jakovleva, J., Kopra, K. & Härmä, H. Sensitive label-free thermal stability assay for protein denaturation and protein-ligand interaction studies. *Analytical Chemistry*, 2020; 92(5): 3512–3516.

II Valtonen, S., Vuorinen, E., Kariniemi, T., Eskonen, V., Le Quesne, J., Bushell, M., Härmä, H. & Kopra, K. Nanomolar protein-protein interaction monitoring with a label-free Protein-Probe technique. *Analytical Chemistry*, 2020; 92(24): 15781–15788.

III Valtonen, S., Vuorinen, E., Eskonen, V., Malakoutikhah, M., Kopra, K. & Härmä, H. Sensitive, homogeneous, and label-free protein-probe assay for antibody aggregation and thermal stability studies. *mAbs*, 2021; 13(1): 1955810.

IV Kopra, K., Valtonen, S., Mahran, R., Kapp, J., Hassan, N., Gillette, W., Westover, K., Plückthun, A. & Härmä, H. Critical evaluation of the thermal shift assay suitability for small GTPase stability screening. *Manuscript*.

1 Introduction

As one of the essential macromolecule classes that form the basis of life, proteins have a variety of functions; from acting as structural supports to relaying intra- and intercellular signals. Often they perform these functions in complexes with other proteins, and protein-protein interactions (PPIs) have been studied for decades.[1] Because proteins control and mediate the normal function of the body on a cellular level, they can often cause malfunction: the impaired structure, absence, or overexpression of proteins may all lead to disease.

Although a single mutated protein species can cause illness, the disease mechanism often relies on changes in the interactions. For example, in cancer, one mutated protein might activate a long signaling cascade despite the inhibitory and feedback mechanisms in the cell, if the mutation disrupts the PPI between the inhibiting compound and the mutated protein. The induced uncontrolled chain of PPIs might result in excessive proliferation of the cell and lead to tumor formation and cancer. Because PPIs are an important part of the progression of many diseases, the interacting proteins are also very interesting as drug targets.[2]

Due to PPIs having such important biological functions, computational, cell-based, and *in vitro* methods have been developed to study these interactions. Computational methods rely on the vast protein databases readily available today. These databases can be used to quickly and efficiently screen for novel PPIs, find new binding patterns, and elucidate the binding mechanisms. The results obtained with computational methods are not applicable to actual proteins in all cases, so the findings must be experimentally validated. Cell-based methods provide information on the PPI function under their natural, physiological conditions, and these methods may also be applicable for PPI screening. There are disadvantages to using living cells, however, such as laborious cell culturing and maintenance.

Methods using purified proteins are, in a sense, a compromise between computational and cell-based methods. The PPIs are examined in laboratory experiments with actual proteins, but not necessarily under physiological conditions and in the presence of assisting proteins, post-translational modifications, and so on. Studying purified proteins is often the method of choice in drug development, for example, in which it is necessary to screen a vast number of potential drug candidates

in a cost-effective and timely manner. These *in vitro* methods may be roughly divided into label-based and label-free approaches. Label-based methods, which mainly utilize fluorescent labels, have been popular for decades and enable sensitive PPI detection. However, labels can interfere with the interactions; a disadvantage that can be overcome by label-free methods. A wide variety of label-free methods have been developed for studying PPIs, and these methods can be further categorized into surface-based and solution-based approaches, which have their own advantages and disadvantages. Despite the great quantity of existing methods, there is still an unfilled niche for novel techniques with improved sensitivity and precision, increased throughput, and better cost-effectiveness.

2 Review of Literature

2.1 Proteins

Proteins, along with carbohydrates and nucleic acids, are a major class of biomolecules that govern all organisms. Proteins function as carriers for other molecules in the bloodstream, have structural roles both inside and outside of cells, are an important part of the immune system in the form of antibodies, mediate complex cell signaling cascades, catalyze reactions as enzymes, and much more.[1] It is estimated that humans have several million different protein species, when all the modified forms are taken into account.[3]

Proteins are macromolecules that consist of smaller "building blocks", known as amino acids. There are twenty natural amino acids genetically encoded in eukaryotes.[4] All amino acids have the same backbone structure: an amine group and a carboxyl group on either side of a central carbon that carries a side chain group. These side chains are what make different amino acids unique from each other. Based on their side chains, amino acids can be categorized into nonpolar (aliphatic), polar uncharged, positively charged, negatively charged, and aromatic amino acids. The properties of these side chains are the basis of protein structure and function.[5]

In a cell, the protein-making translation machinery links amino acids by catalyzing an amide type peptide bond linkage between the amine and carboxyl groups. Several amino acids are linked into chains called peptides in a sequence determined by the DNA of the cell, forming the protein primary structure (Fig. 1). The peptides then fold into secondary structures, most commonly α-helices and β-sheets, based on the properties of the amino acid side chains (Fig. 1).[4] The peptide chains may also undergo post-translational modifications, in which the side chains of the amino acids or the terminal ends of the peptide chain are modified. These modifications affect the activity, stability, and localization of the proteins.[6] Finally, the peptide chains with their secondary structures are further folded into the tertiary structure, which is also determined by the properties of the amino acid side chains (Fig. 1). The tertiary structure is formed via both covalent and non-covalent interactions. Correct folding into the tertiary structure often requires assistance by several chaperone proteins in the cells.

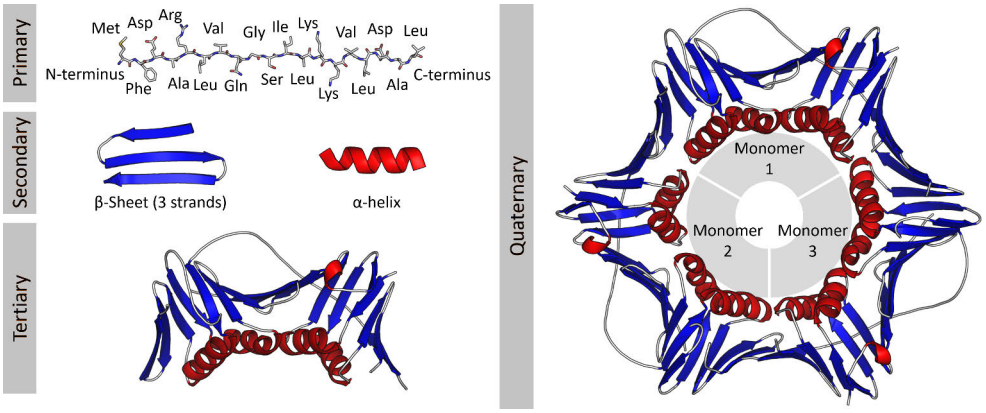

Figure 1. The structure of a model protein, proliferating cell nuclear antigen, which has a role in DNA replication. The primary structure of the protein consists of a chain of amino acids and is folded to secondary structures, such as β-sheets and α-helices. The secondary structures then come together to form the tertiary structure. Many proteins are functional upon achieving the tertiary structure. In some cases, the full functionality is gained only after forming a quaternary structure. Picture modified from the original.[7]

Proteins can be roughly categorized to globular, fibrous, and membrane proteins based on their tertiary structure. Globular proteins are somewhat soluble in water because their outer surface mostly consists of hydrophilic amino acids, and the hydrophobic amino acids are buried in the core of the protein. Globular proteins have many roles in the body, including as enzymes.[8] Fibrous proteins are much less water soluble because they consist of long polypeptide chains that form fibrils or sheet-like structures. Fibrous proteins often have cytoskeletal, structural roles.[9] Membrane proteins either interact with or are a part of the membranes of a cell. These proteins may be permanently embedded into the membranes or attach transiently and they function, for example, as transmembrane receptors or ion channels.[10]

When the protein tertiary structure has been achieved, the functional protein can be released from the protein-making machinery and transported to an appropriate location. In some cases, however, several individual proteins attach non-covalently to form a quarternary structure (Fig. 1). The quaternary structure of proteins consists of identical or different subunits, and the subunit number varies from protein to protein.[4] For example, C-reactive protein (CRP), which is active in inflammation, consists of five identical subunits. In contrast, hemoglobin, which carries oxygen in the blood, consists of two subunits with different structures.

The protein structure is quite stable once the complex protein folding process is completed, but it is not completely resistant to change. Some conformational changes are required for protein function, such as the allosteric activation by ligands, but the protein structure may also become non-functional due to external stressors. Proteins are especially susceptible to environmental conditions once they are purified and

handled outside the self-balancing environment of the cell or body. Conditions such as high temperatures or changes in pH can lead to a loss of structure, i.e., denaturation. In the denaturation process, the amino acid sequence usually stays intact, but the protein structure is (partially) lost on the quaternary, tertiary, and/or secondary levels. Denaturation is reversible in some cases: once the denaturing factor has been removed, renaturation may take place. However, irreversible denaturation is also possible and may lead to a permanent loss of function.[4,11] Harsh conditions, such as very high temperatures, may also lead to loss of function through protein degradation, in which deamidation or oxidation of the amino acid side chains occur. The conformational integrity of a protein may affect the resistance to thermal degradation, so denatured proteins are in some cases more susceptible to thermal degradation than native proteins.[12]

Protein folding into the correct native form is a precarious process guided by the amino acid composition of the peptide, and a mutation of even one critical amino acid might make the folding impossible. Changes in the cell environment, such as pH fluctuation, can also affect the folding process negatively. Incorrect folding often brings hydrophobic amino acids to the exterior of the protein, forming a "sticky" surface that may lead to unwanted aggregation, i.e., self-association of protein molecules into stable complexes.[4,13] Although the aggregation process often requires at least partial mis-/unfolding of proteins, correctly folded proteins may also aggregate due to inherent fluctuations of the local structure revealing sequences prone to aggregation.[13,14] Fortunately, cells have mechanisms in plate to ensure that proteins are re-folded correctly (chaperones) or defective complexes are disposed of (e.g., proteasomes).[15,16] If these mechanisms fail, protein aggregates may compromise the function of the cell and lead to several neurodegenerative diseases.[17] However, even when non-mutated proteins interact as intended, the structure can unfold in a small, controlled area to create the interaction interface of PPIs.

2.2 Protein-protein interactions

The mechanisms of PPIs and the structures of the interaction interfaces are introduced in the next section. The roles of PPIs and their relevance as a research target will also be discussed.

2.2.1 Mechanisms of protein-protein interactions

There are thousands of different protein interaction types, and it is estimated that hundreds of thousands of different binary PPIs take place in the human body.[18–20] Taking multi-protein complexes into account brings the number of distinct interactions even higher. Protein complexes can be homo-oligomers consisting of

identical proteins, or hetero-oligomers, where several different proteins form a complex. PPIs can also be divided into reversible and permanent interactions.

Reversible, transient PPIs may constantly associate and disassociate, but the proteins might also stay associated until a specific signal is received through, e.g., a cellular signaling cascade.[21] KRAS and RAF proteins, for example, bind transiently in one step of a signaling chain that activates DNA transcription and, eventually, cell proliferation. KRAS is a small GTPase that is activated by nucleotide exchange from guanosine diphosphate (GDP) to guanosine triphosphate (GTP), and after the activation KRAS can interact with the RAS-binding domain (RBD) of RAF (Fig. 2). The GTP-KRAS binding activates RAF, a protein kinase that phosphorylates the next protein in the signaling chain. As the GTP is hydrolyzed to GDP, KRAS dissociates from RAF until the next cascade is initiated.[22,23]

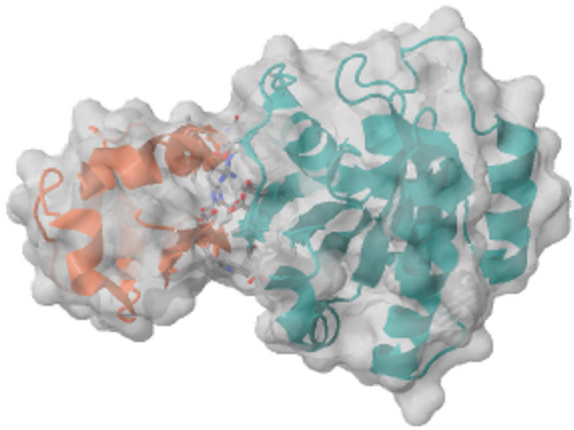

Figure 2. The interaction between the RAS protein (green) and RAS-binding domain (orange) of RAF. The interaction area is relatively flat and large, and most of the interacting amino acids are buried in the middle of the interaction interface. Picture modified from the original.[24]

As opposed to transient PPIs, Permanent PPIs do not normally dissociate once formed, except if the protein structure is lost due to, e.g., denaturation. For example, the bonds between protein subunits can be said to be permanent. Some proteins form so called “obligate complexes”, in which case the individual proteins are not stable enough to exist in the unbound state. For example, the heavy and light chains of antibodies practically always exist as a complex in the body.[21] PPIs are also the basis for the aggregation of proteins: the proteins form non-native dimers that initiate the nucleation, followed by polymerization and aggregate growth.[24]

The type of the PPI is tightly linked to the amino acid composition of the interaction surface and the bond preference of the amino acids. Thus, it may be possible to predict if the PPI is reversible or permanent based on the amino acids

found at the interaction interface. Equally, knowing the interaction type might enable prediction of what kind of bonds the amino acids will form—homo-oligomer domains, for example, have been observed to preferentially form bonds between identical amino acids.[26] A wide variety of protein and protein pair structures have been characterized and deposited in databases such as the Protein Data Bank. These databases make it possible to computationally analyze a massive amount of data to determine trends in PPIs and interface structures, and to gain insight into the amino acid behavior at binding sites.[26,27] The computational approach to studying PPIs will be discussed more in depth in section 2.4.

In general, PPI interfaces are large and flat in shape, as seen in the interaction between RAS and RBD (Fig. 2).[28,29] The interfaces consist of a core area, which is not in contact with the solvent during the interaction, and an outer rim, which is partly buried and shields the core from water. The buried interface core has hydrophobic properties, but not to the same extent as the interior of the protein. The composition of the rim is similar to that of the protein surface.[30] Certain amino acids are found in the PPI interfaces more often than others: leucine is the most common amino acid, followed by arginine, which forms cation-π bonds with the aromatic rings of tryptophan and tyrosine. Aromatic amino acids, despite not often being present on the surface of the protein, are important components of the interfaces.[31] Specific groups of amino acids, called hot spots, contribute a large amount of binding energy, and the structures are often conserved across orthologous proteins that participate in PPIs. These hot spots contain predominantly tyrosine, tryptophan, and arginine, and are situated in the middle of the interface.[31,32]

In addition to the protein structure, the binding environment of the PPI also affects the formation. Cell homeostasis often ensures that the conditions are suitable for PPIs *in vivo* and the interactions can take place as intended. However, when proteins are handled *in vitro*, the environmental conditions may have more drastic effects. One important factor is pH, as proteins have an ideal pH range where they function optimally, and changes in the pH can prevent the protein function and interactions with other proteins.[33,34] Besides pH, ionic strength and salt concentration have an impact on PPIs, and an excessive salt concentration may disrupt the protein-protein binding. Metal ions are also essential for some interactions, such as the formation of the hexameric insulin structure required for storing inactive insulin in the body.[35,36]

Changes in the protein concentration affect what types of chemical bonds mediate PPIs. For example, electrostatic interactions are more important in dilute solutions than at high concentrations, whereas van der Waal's forces are considerably more prominent when the protein concentration is high. Proteins work successfully in the crowded cell environment, but once a protein is isolated, a high concentration of the single protein species may cause problems, such as

aggregation.[37,38] Additives (i.e., excipients) are required in the protein storage solution to keep the protein stable. Sometimes not only the stability, but the correct function of a protein relies on other molecules, such as nucleic acids. DNA, for example, can mediate PPIs during the process of DNA repair.[39] Protein interactions may also be facilitated by scaffold structures, as is the case with eukaryotic initiation factor 4F (eIF4F), a protein complex promoting translation initiation. eIF4F consists of three proteins: eukaryotic initiation factor 4A (eIF4A; RNA helicase), eukaryotic translation initiation factor 4E (eIF4E; RNA-cap-binding protein), and eukaryotic translation initiation factor 4G (eIF4G; scaffold protein). eIF4G has binding domains for eIF4A, eIF4E, and other assisting proteins and it also binds directly to RNA. The eIF4F complex and the assisting proteins recruit the small ribosomal subunit to initiate mRNA translation—a function which the individual proteins are not capable of performing on their own.[40,41]

2.2.2 The role of protein-protein interactions

As previously mentioned, PPIs carry out an astonishingly wide variety of processes in cells, associating and dissociating as required. PPIs both initiate and inhibit complicated processes, and disrupting either role may lead to malfunctions in the cell.[42] If an important process is not initiated, the function of the cell may be compromised, leading, for example, to metabolic disorders.[43,44] On the other hand, if PPI regulation does not function due to a mutation, the result could be overactive cell signaling promoting uncontrolled proliferation, potentially leading to cancer.[45] Neurofibromatosis type 1, for example, can be caused by inherited or *de novo* mutations in the *NF1* gene and, thus, the neurofibromin protein. Neurofibromatosis type 1 is the most common human disease predisposing to tumor formation, and the symptoms range from tumors of the nervous system to learning disabilities. Neurofibromin is a GTPase-activating protein, and one of its roles is to inactivate RAS by accelerating the hydrolysis of the bound GTP, leading to downregulation of the RAS signaling chain that promotes cell proliferation. Therefore, the absence of neurofibromin may lead to uncontrolled cell division and tumor formation. The constantly active RAS signaling chain may also adversely affect synapse plasticity and is one of the reasons behind the learning difficulties exhibited by neurofibromatosis patients. Neurofibromin has also other roles besides controlling RAS function, such as positive regulation of phosphorylation pathways related to cyclic adenosine monophosphate. Therefore, mutations in this one protein lead to defects both in the inhibition and initiation of essential processes.[46]

As PPI malfunctions can cause several diseases, they are obviously interesting drug targets. However, the large size of protein-protein interfaces makes them difficult to target with small drug molecules, more so than the ligand binding sites

participating in protein-ligand interactions (PLIs). PLIs often enable using the ligand structure as a basis for the small molecule drug, but PPIs do not necessarily have such templates available. PPI interfaces often consist of amino acids that are not adjacent in the peptide chain, because the proteins are folded into secondary and tertiary structures (Fig. 2). For example, in α-helices, neighboring amino acids may be on the opposite sides of the helical structure, and not all of them necessarily contribute to the protein-protein binding. Furthermore, more than one domain of the protein may take part in the PPI, and amino acids that are nearby each other in the interaction interface may be very far apart in the peptide sequence. Therefore, isolating a peptide sequence from one of the interacting proteins to create a potential binder and drug candidate is usually not viable.[47–51] In general, small molecule PPI drugs are also favored over large peptides because small molecules have a better bioavailability: they enter the systemic circulation more rapidly than large peptide molecules, and thus reach their target destination faster.[47,52]

Despite the challenges, it has not been impossible to find PPI drugs. KRAS, which is mutationally activated in approximately 30 % of human cancers, was considered undruggable for decades, but in recent years several small molecule inhibitors have been developed and entered clinical trials.[53,54] The first KRAS inhibitor was approved for clinical use by the FDA in 2021.[55] This inhibitor, called AMG-510 or sotorasib, selectively targets KRAS mutant G12C, and it is intended for the treatment of non-small-cell lung cancer.[55,56] The development of KRAS inhibitors has been enabled, in part, by identifying new potential binding pockets in the KRAS structure, such as the allosteric switch-II pocket.[57] Developing allosteric molecules that affect the protein structure—and thus the binding affinity—may enable inhibiting PPIs indirectly even if the interaction interface is difficult to target. Allosteric modulation of PPIs has also been used successfully with transcriptional cofactor Med25, which contributes to tumorigenesis and has large, hydrophobic interaction interfaces that are challenging targets for small molecules.[58] Although many PPI drugs still function through PLIs, understanding and detecting the formation of the targeted PPIs is of utmost importance in evaluating properties such as selectivity and potency of drug molecules.

2.3 Label-based methods in *in vitro* PPI studies

Studying the interactions of purified proteins in *in vitro* assays is a convenient way to research PPIs, as recombinant proteins can often be purchased relatively easily without needing to culture cells in-house. Fluorescence-based methods are the most popular approach for verifying and studying PPIs in a laboratory setting and may be divided into heterogeneous and homogeneous assays. In heterogeneous assays, such as enzyme-linked immunosorbent assay, the unbound label molecules must be

removed from the sample before measurement, which complicates the assay by adding extra steps. Homogeneous assays are performed with a mix-and-measure concept, which makes them simpler for the end user and more popular in PPI studies than heterogeneous assays. This chapter will focus on homogeneous label-based assays. First, the principles of fluorescence are briefly introduced, followed by discussion about fluorescence-based PPI detection. Examples of methods based on non-fluorescent labels are also given.

Fluorescence takes place when a label molecule absorbs a photon and is excited to a higher energy state, then returns to the ground state and releases the photon, which is observed as emission (Fig. 3A). Due to internal conversions between the vibrational states of the excited molecule, the photon loses some of its energy, leading to emission at a longer wavelength compared to the excitation wavelength. The fluorescence emission intensity at the chosen wavelength is monitored with a fluorescence reader instrument, commonly a microtiter plate reader. The relaxation of the label molecules only takes nanoseconds, so continuous excitation is utilized to obtain several measurements.

In *in vitro* assays, the fluorescent labels are often organic dyes, although labels such as quantum dots may also be used. The labels are commonly conjugated to purified proteins through reactive thiol or amine groups. The thiol groups of cysteines are a convenient target for labeling, as cysteines are not found in proteins very frequently, and site-specific labeling is enabled by mutationally introducing a cysteine to the protein. Maleimide is a widely used molecule that reacts with free cysteines in a highly specific manner and thus functions as a linker between the protein and the label. In the case of IgG_1 antibodies, for example, maleimide does not react with intact sulfur bridges, but links the label to free thiol groups elsewhere in the antibody structure. The N-terminal amine group of proteins offers another possibility for site-specific labeling, although the pH of the labeling reaction must be chosen carefully to avoid conjugation to lysine side chains. For example, succinimidyl esters or isothiocyanates are used as the linker groups for attaching labels to the amines.[59]

The most common fluorescence-based method for studying PPIs is Förster resonance energy transfer (FRET). FRET relies on the energy transfer between a donor molecule and an acceptor molecule (Fig. 3B). The donor emission spectrum overlaps with the acceptor absorbance spectrum, so the donor excites the acceptor molecule when they are in proximity. Upon return to the ground state, the acceptor molecule emits fluorescence at a wavelength longer than the donor emission. The energy transfer between the donor and acceptor occurs through a resonance-based dipole-dipole interaction instead of radiation. For the FRET energy transfer to take place, the donor and acceptor must be within 1-10 nm of each other, which enables studying PPIs with FRET.[60,61]

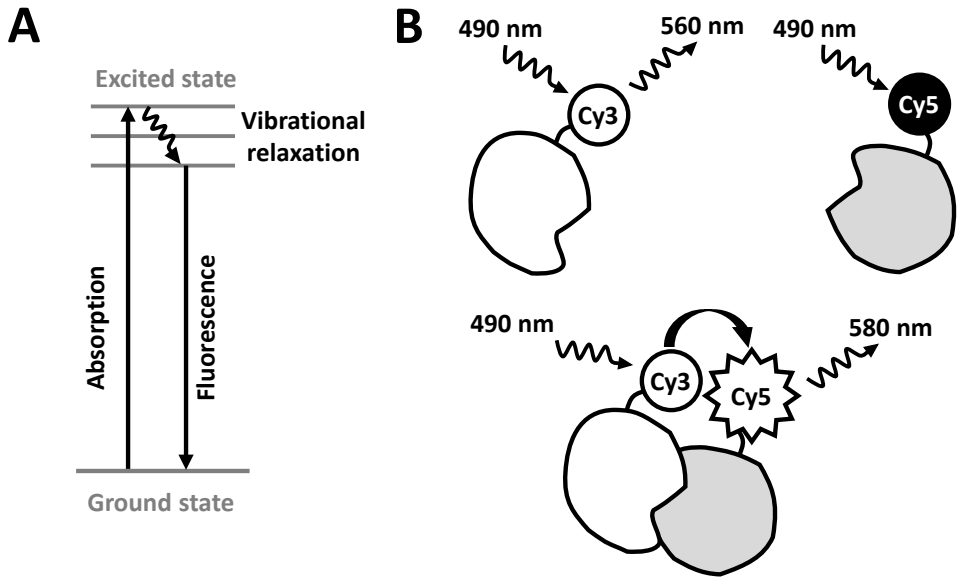

Figure 3. Fluorescence and FRET in PPI monitoring. **A.** Jablonski diagram for conventional fluorescence. The absorption of a photon excites an electron to a higher energy state, and the subsequent return to ground state is observed as the emission of a photon on a longer wavelength. **B.** A model FRET system for monitoring PPIs, using cyanine dyes Cy3 and Cy5. When proteins labeled with a donor molecule (Cy3) and an acceptor molecule (Cy5) are far apart, there is no energy transfer between the labels. Upon protein interaction, the labels are brought into close proximity, enabling the energy transfer and acceptor emission.

FRET is commonly monitored through signal intensity and lifetime. In the signal intensity approach, measuring the acceptor emission is the most reliable and least error-prone approach, as the acceptor produces a fluorescence signal only if the distance to the donor is small enough. Separate measurement of the donor fluorescence can be used as a control.[62,63] In the lifetime approach, the time it takes for the fluorescent molecule to return from excited to ground state is observed. This is often performed by monitoring the emission decay of the donor molecule, as the donor decay is accelerated by energy transfer to the acceptor. Thus, decreased donor lifetime can be interpreted as a close proximity of the labels, i.e., the studied proteins interacting.

There are also proximity-based PPI detection methods that do not use fluorescent labels, but instead utilize, e.g., radioactivity or chemiluminescence. In scintillation proximity assays, one protein is labeled with a radioactive atom, and another is labeled with a microscopic scintillant bead. When the radioactivity decays, the atom emits β-particles that can excite the scintillant and trigger light emission. However, the energy of the β-particles dissipates in water, so the scintillant and radioactive

atom must be within a specific distance of each other for the scintillant excitation to take place. The appropriate distance depends on which radioactive atom is used. Tritium, for example, must be within 1.5 µm of the scintillant bead. The advantage of scintillation proximity assays is that they are sensitive, and the long scintillation distance enables monitoring large protein complexes. The flip side is that the long distance may also lead to false positives, as the labeled proteins may come within the scintillation distance even when not interacting. Another issue is that handling and disposing of the radioactive components is difficult.[64,65]

The AlphaScreen method relies on chemiluminescence. The interacting proteins are conjugated with latex particles: one bead contains a photosensitizer and the other chemiluminescent compounds. Irradiating the sample with a laser at 680 nm leads to the formation of singlet oxygen near the photosensitizer bead. If the beads are in close proximity, i.e., the labeled proteins interact, the singlet oxygen excites the chemiluminescent label, and a luminescence signal can be observed. The beads must be within 200 nm of each other for the singlet oxygen to reach the chemiluminescent compound, making it possible to monitor larger protein complexes than with FRET. However, the long distance may cause problems with false positives, similarly to scintillation proximity assays. The chemiluminescence emission is measured at a lower wavelength than what is used for the excitation, which removes the concern of autofluorescence and leads to a low background signal and high sensitivity. However, there are other sources of interference, such as the quenching of the singlet oxygen by antioxidants or metal ions.[66,67]

In vitro methods do not usually measure PPIs under the physiological conditions, so it is likely that the obtained results do not directly correspond to interactions inside cells. Nevertheless, the techniques introduced above provide sensitive methods for studying PPIs, and they are very widely used. A common property of all these techniques is that one or more of the interacting proteins must be labeled with a fluorophore, an enzyme, or even a relatively large bead. The disadvantage of labeling the proteins is that the label might disrupt of prevent PPIs due to changes in the electrostatic charges compared to unlabeled proteins or by altering the binding sites, among other things. Even if the label is targeted precisely and does not disrupt the binding interface, large labels can cause steric hindrance. For example, the scintillant beads are extremely large compared to proteins, with diameters of 2–10 µm (whereas an average protein has a diameter below 10 nm), and the size of the AlphaScreen beads is approximately 250 nm.[68]

2.4 Computational and cell-based PPI studies

The next section briefly discusses computational methods in the context of PPI studies. The chapter also introduces how cell- and lysate-based methods can be used in PPI research.

2.4.1 Computational methods

Computational methods for studying PPIs rely on the biological databases that nowadays are readily available. Because the relevant protein structure data has already been studied elsewhere and uploaded to the databases, computational PPI research does not necessarily require experimental work in the laboratory; however, the computational findings must always be experimentally verified.

Computational methods aim to predict PPIs through a wide variety of techniques. These may be divided into network-, genome-, sequence-, structure-, and domain-based methods. The network-based approach assumes that if two proteins have several common interaction partners, these two proteins also interact with each other.[69] In genome-based methods, the genome of the organism is analyzed, and PPIs are predicted based on links between the genes coding the proteins. For example, if two genes are consistently found together in several organisms, the proteins they code could be PPI partners.[69]

Sequence-based methods assume that if proteins with a homologous sequence interact in one species, they also form PPIs in other species. Structure-based methods employ the same strategy from the perspective of folded proteins: proteins that form similar structural domains are assumed to also have similar interactions.[69] Comparing only the sequence or structure might not always tell the whole truth, however. For example, two paralogs of the RNA helicase protein eIF4A, eIF4A1 and eIF4A2, share a 90 % sequence homology and very conserved structures, but the function and interactions of these two proteins still differ.[70–72] Homologous domains may also have very different sequences, so studying both aspects may be advantageous. Domain-based methods combine protein sequence and structure information to find patterns of interaction and recognition. These methods are limited, however, in that they usually focus on one individual domain at a time and do not take the effects of the other participating structures into account.[69] In focusing on the specific structural information of the interacting proteins, sequence-, structure-, and domain-based methods use more detailed information than the network- or genome-based techniques. Domain-based studies of PPIs especially focus closely on the amino acid composition and the structural details of the PPI interface at the molecular level.

At the amino acid level, computational methods aim to predict, discover, and understand the binding site structural patterns. Thousands of protein-protein

interface structures that have been resolved and uploaded to databases can be analyzed to determine which amino acids are the most common at a given type of interaction interface. In addition, the interactions of currently uncharacterized proteins may be predicted by comparing their sequence to the known binding site structures. Finding a kinase domain enables assigning a protein to the kinase protein family and may guide the interaction studies to the right direction, for example.[26,27] It may also be possible to assess the effects of mutations on PPIs without having to produce and test each mutated protein separately, and to screen for PPI drugs, though usually only in the context of finding small molecule inhibitors through PLIs.[73,74]

Computational methods are an excellent starting point when searching for new PPIs, as they enable screening novel interactions from a vast amount of data without the need to acquire every protein. They are, however, the most powerful when used in combination with experimental studies, which are required to validate findings with real proteins.

2.4.2 Cell- and lysate-based methods

In contrast to the theoretical, calculation-based computational methods and the *in vitro* measurements with purified proteins, studying PPIs with *in vivo* methods can reveal information about cell function outside of a theoretical or lab setting. The term "cell-based methods" can refer to methods that study PPIs *inside* cells or *using* cells. The former group focuses on elucidating PPIs in living cells, cell function, and the impact of protein modifications on interactions. The latter group uses cells as tools for studying PPIs and does not necessarily give information on the function of PPIs inside cells in real time. Such methods are often used for screening for novel PPIs from large, artificial libraries, for example.

FRET is the most common method for observing PPIs naturally taking place inside living cells, and it is used in cells similarly to *in vitro* assays, though there are differences. The most advantageous way to label the proteins in *in vivo* FRET studies is to directly produce recombinant fusion proteins in the cells, where the "label" protein naturally produces a bright fluorescent signal when exposed to excitation light. The first discovered fluorescent protein was green fluorescent protein, but since then several variants with different excitation and emission wavelengths have been produced and utilized in cellular FRET studies.[75] Expressing two proteins of interest fused to reporters with compatible excitation and emission spectra enables taking FRET PPI measurements inside living cells in real time.[62,75,76] Additionally, cellular FRET measurements are often performed under a microscope, enabling visualization of the cells and, thus, localization of the interaction. In fluorescence lifetime imaging assays, for example, the donor lifetime decay can be simultaneously

monitored in all pixels of the image, producing a comprehensive map of the PPIs in the cell.[77,78]

Fluorescence correlation spectroscopy is another technique based on fluorescent labels that enables real-time measurements in cells. The method tracks the movement of fluorescently labeled molecules under a focused laser beam using a microscope. The number of labeled molecules in the measurement area determines the fluorescence intensity, and therefore it is possible to monitor diffusion of the labeled proteins. Protein complex formation is detected based on the effects on the diffusion, as large complexes have slower diffusion speed than individual proteins. It is also possible to calculate the binding kinetics of the interaction.[79,80] If two interacting proteins are conjugated with distinct labels, the diffusion of both protein species can be recorded and cross-correlated, in which case the technique is called fluorescence cross-correlation spectroscopy.[80,81] Both fluorescence correlation and cross-correlation spectroscopy can achieve single-molecule sensitivity.[79,81]

The label-related problems from which *in vitro* assays suffer, such as steric hindrance and interference with protein binding, also affect cell-based assays, especially when more than one protein is labeled. Additionally, both FRET and fluorescence (cross) correlation spectroscopy enable studying only a small number of interactions at any one time, as proteins of interest must be produced as fusion proteins inside the cells, complete with appropriate fluorescent labels. These methods are the most suitable for studying how the modification of one binding partner affects a known protein complex.

Cells can also be used for high-throughput PPI screening with methods such as the two-hybrid method and phage display. The two-hybrid method is based on the two-domain structure of a transcription factor required for the transcription of a reporter gene. The screened proteins, bait and target, are produced as fusion proteins with the two domains of the transcription factor, often in yeast or bacterial cells. PPI between the bait and target brings the transcription factor domains into close enough contact that they gain functionality and enable the transcription of a reporter gene. Several kinds of reporter genes can be used, such as genes essential for survival or ones producing detectable reporter molecules.[82,83] The two-hybrid method enables verifying PPIs in the cell environment, and millions of interactions can be screened relatively easily.[84,85]

Phage-display is another cell-based method that makes it possible to screen large protein libraries for PPIs. In this approach, the genes of the studied proteins are fused with the coat protein genes of a bacteriophage, and the proteins are consequently displayed on the surface of the phages. These phages are produced in bacteria in large amounts, then exposed to immobilized bait protein. PPIs attach some of the phages to the bait, and the rest are washed away. The remaining phages are collected, and the process is repeated several times to enrich the interacting proteins, followed

by sequencing the genomes of the remaining phages to identify the binding proteins. To facilitate the expression on the phage surface, peptide fragments are often used instead of whole proteins.[86–88] Phage display libraries can contain up to tens of billions of distinct protein fragments that are screened for interactions.[89] In phage display, the screened interactions take place in a non-physiological environment, unlike in the two-hybrid methods, in which the proteins interact inside cells.

In addition to using cells and phages as the screening vector, cells are also used in PPI screening in the form of lysates. Novel PPIs are screened from cell lysates using several immunoprecipitation-based techniques. The original form of (co-) immunoprecipitation, also called pull-down, uses antibodies to pull the interacting proteins out of the sample. A protein of interest is targeted with an antibody linked to a resin. As the target protein is pulled down, the interacting components come with it and can then be identified using, e.g., mass spectrometry.[90] Affinity tagging functions in a similar way, but instead of using antibodies, the target protein is recombinantly produced with an affinity tag that is used for the pull-down.[91] Another version of affinity tagging is tandem affinity purification, which utilizes a protease-cleaved tag. After cell lysis and protein complex collection with the first tag, another purification can be performed using the second tag. This way, binders with a higher affinity can be obtained.[92] Pull-down and affinity tagging methods make it possible to discover a variety of binding partners for one protein of interest and may enable identifying functional complexes consisting of multiple different proteins.

Proximity labeling has a similar principle to affinity tagging assays, except that in proximity labeling more than one protein is tagged. In this method, proteins are labeled inside a living cell using, for example, a promiscuous biotin ligase produced as a fusion protein with a protein of interest. The ligase attaches biotin to proteins in a proximity-dependent manner, meaning that only the proteins from the specific area are biotinylated and separated from the cell lysate in the following affinity purification step. Identifying the biotinylated proteins with methods such as mass spectrometry provides information on which proteins usually function in close proximity in the cell environment. The biotinylated proteins may not all be direct interaction partners, as the promiscuous ligase does not differentiate between interacting proteins and those that are simply near each other in the cell, but the obtained results aid in discovering interaction networks.[93]

Various forms of electrophoresis are also used to analyze cell lysates and detect and identify membrane protein complexes, for example. The cell lysate can be analyzed with native polyacrylamide gel electrophoresis (PAGE) to separate the protein complexes based on their size and charge. The same samples may then be denatured and run on a denaturing PAGE gel—now at a 90° angle compared to the first assay—to separate the subunits of the protein complexes. Electrophoresis-based methods are suitable for discovering protein pairs, followed by identification with,

e.g., mass spectrometry.[94,95] PAGE may also be combined with blotting methods, such as western blotting, in which the proteins are transferred to a membrane and probed with labeled antibodies. Far western blotting, in which the protein of interest is used as the labeled probe instead of antibodies, enables screening for novel PPI pairs, but also confirming interactions.[96]

All in all, studying PPIs inside cells may provide valuable information about the interactions in the physiological context where they take place. Cell-based screening methods also enable searching for novel PPIs from large protein libraries or even the whole proteome of the cell in more or less physiological conditions, depending on the method. Not all laboratories have the capability and expertise to work with live cells, however, and in early screening studies it might not even be necessary.

2.5 Label-free surface-based methods in PPI studies

The next section introduces surface-based label-free methods for PPI monitoring. In this thesis, "label-free" is used to refer to a method where none of the interacting protein components are tagged with a label molecule, such as a fluorophore. "Surface-based" refers to methods where one of the binding partners is immobilized on a solid surface for the binding measurement. It could be argued that methods where coupling to surfaces is required should not be deemed label-free, but in this context label-free is only considered to exclude labeled proteins.

2.5.1 Surface plasmon resonance

Surface plasmon resonance (SPR) is a popular optical method for detecting PPIs. In SPR, a studied interacting protein is immobilized onto a thin metal film, often made of gold. The immobilization can be achieved directly, through adsorption or covalent binding, or via linker or binder molecules.[97] If linkers are used, they are first directly coupled to the metal surface, and the studied protein may be attached to the linker molecule either covalently or through a more transient interaction. Covalent coupling can be achieved with amino-reactive groups, such as activated carboxyl groups.[98,99] On the other hand, proteins with tags such as biotin or a polyhistidine tail can be bound to a surface of streptavidin (SA) or Ni^{2+}-nitrilotriacetic acid, respectively.[100,101] Liquid containing the studied protein moves over the sensor surface in a flow cell, as depicted in Fig. 4A.

On the opposite side of the metal film is a glass prism, through which polarized light travels to the backside of the film. Evanescent waves are formed under the right conditions and excite the surface electrons—plasmons—of the metal film, leading to resonance. For the SPR phenomenon to occur, the light must enter at a certain

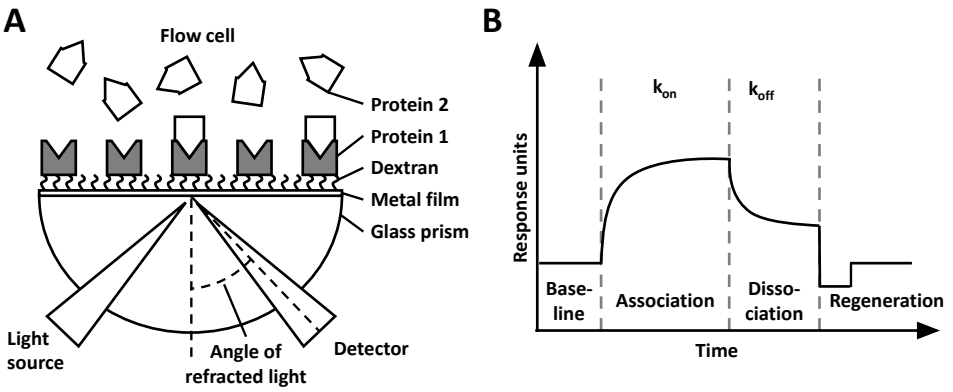

Figure 4. Surface plasmon resonance in monitoring PPIs. **A.** SPR detects protein binding based on mass increase at the sensor surface. One protein is conjugated to a thin metal film, often through an intermediate molecule such as dextran, and the interacting partner flows past the immobilized target protein. The light reflecting from the chip surface is monitored at a certain angle, and binding events are detected as a decrease in the intensity of the reflected light, because protein binding changes the refractive index of the surface. **B.** A schematic representation of typical SPR data with one protein concentration. The studied protein binds to its interaction partner in the association phase, with the binding gradually saturating. Flowing buffer solution over the chip leads to dissociation. The kinetic rate constants are usually calculated from several curves obtained with different analyte concentrations.

angle that is predominantly defined by the refractive index of the liquid adjacent to the metal film. The refractive index, and thus the resonance angle, are altered by protein binding at the sensor surface. This is observed as a decrease in the reflection intensity at the previously optimal angle, which is recorded by the detector. The refractive index changes caused by the analyte mass density are linearly proportional to the number of bound molecules, which enables quantification of the interacting proteins.[97,102] Because SPR is a mass sensor, studying the interactions of both small and large proteins is possible. The effective probing distance of the evanescent waves is affected by the wavelength of the SPR incident light, and while PPI measurements are usually performed in the visible or near-visible range (e.g., the Biacore instrument uses 760 nm), infrared wavelengths may be required for studying cells.[103]

SPR measurements can be monitored in real time, and the kinetics of the interaction, i.e., the association and dissociation rates, can be calculated from the results (Fig. 4B). Because different solutions can be circulated in the flow cell, successive binding events can be easily monitored with buffer washes in between.[102,104] The sensitivity of SPR is in the pico- to nanomolar range and can be further improved with materials other than gold as the sensor surface.[102,105–107] One disadvantage of SPR is that it does not usually have very high throughput. However,

new assay formats and setups are constantly developed to increase the throughput through autosamplers and chips with several channels, for example.[104,108]

2.5.2 Resonant waveguide grating

Resonant waveguide grating (RWG) is another method that monitors the changes in the refractive index of the sensor surface, and it relies on a waveguide structure. The incident light is directed to the substrate layer at the bottom of the RWG sensor. On top of the substrate layer lies a two-dimensional grating with a high refractive index, made from, e.g., titanium oxide. The topmost cover layer fills the gaps of the grating material, and the studied proteins are conjugated to the liquid-exposed side of the cover layer using similar approaches as with SPR sensors. When the refractive indices of both the substrate and the cover layer are lower than that of the grating, a waveguide is created.[109,110] Waveguides guide the light in a transverse pattern (i.e., perpendicular to the direction to which the light travels), relying on total internal reflection.[111] The incident light is coupled into the waveguide and then reflected back to a detector. Changes to the thickness and composition of the biolayer change the wavelength of the reflected light, enabling PPI monitoring.[109,110]

A special characteristic of RWG sensors is that they can be built on plastic films and incorporated to microtiter plates. This makes RWG a high-throughput method, as the assays can be performed on 96- or 384-well microtiter plates with a simultaneous measurement of all wells.[110] Performing the assays in the microtiter plate format reduces the interferences caused by liquid flow and enables steady state analysis of the binding. Thus, RWG may detect low-affinity interactions that SPR might fail to accurately measure.[112] The sensitivity of RWG sensors is in the pico- to nanomolar range and the measurements can be performed in real time, but endpoint measurements are more common in high-throughput screening (HTS).[110,113,114] However, RWG does not produce as detailed information about the binding kinetics as SPR does. Therefore, RWG is more suitable for the initial large-scale screening of PPIs, instead of detailed studies of known protein pairs.[112]

2.5.3 Ellipsometry

Ellipsometry is an optical method that is often used in a similar context as SPR, but instead of utilizing evanescent waves and resonance, ellipsometric measurements are based on monitoring the reflection of polarized light from a sensor surface. Incident light polarized both perpendicular (transverse electric, TE) and parallel (transverse magnetic, TM) to the plane of incidence is monitored, and the direction of the polarization affects how the light is reflected from the sensor surface. The surface often consists of silicon and silicon dioxide and is modified to enable the coupling

of proteins of interest. Protein binding is detected based on changes in the ratio of the reflections of the TM- and TE-polarized light.[115,116] In spectroscopic ellipsometry, measurements are performed on several wavelengths to obtain more data and therefore more precise information.[117]

Ellipsometry is suitable for observing the binding kinetics and quantification of the sample and detects picomolar protein concentrations. Both the amplitude and phase of the reflected light are measured, and they can be combined through algorithms and equations to acquire more information on the protein binding and orientation compared to methods such as SPR.[117–119] The downside of ellipsometry is that the beam of light must pass through the sample liquid, unlike in SPR and related methods, which might set limitations for the sample material composition regarding properties such as opacity.[115] Ellipsometry is also most suited for analyzing flat, uniform surfaces, so data interpretation may be challenging when studying uneven protein surfaces with varying thickness.[117]

The measurement principle and setup of ellipsometry can also be combined with the components of SPR assays, in which case the method is called total internal reflection ellipsometry (TIRE). Namely, the stacked structure containing a prism, a metal film coated to a glass slide, and a flow cell are used. The proteins of interest are conjugated to the flow cell side of the metal film, similarly to SPR. Incident light that passes through the prism to the other side of the metal film is coupled to the film in a way defined by the properties of the sensing surface, i.e., proteins bound to the surface. The monitored property is still the change in the incident light polarization caused by the reflection. In TIRE, the incident light does not pass through the sample liquid, which enables the use of a wider variety of media. TIRE has a roughly 30-fold higher sensitivity compared to ellipsometry, and the sensitivity can also exceed that of SPR. TIRE enables measuring binding affinities and kinetics with high accuracy.[120–122] Although TIRE is suitable for PPI studies, the improved sensitivity may be more useful when studying the binding of relatively small molecules (M_w <1 kDa).[123] The complicated equipment required may also be expensive.

2.5.4 Dual polarization interferometry

Dual polarization interferometry (DPI) detects protein pairs and multiprotein complexes by utilizing two optical slab waveguides. One is the sensing waveguide, which is in contact with the sample, and the other one is a reference waveguide. They are separated by cladding material and stacked on silicon oxide (Fig. 5). Laser light directed into one end of the DPI sensor is coupled to the waveguide slabs that guide the light in a defined, transverse direction. At the opposite end of the sensor, the light passing through the two waveguides forms a two-dimensional interference pattern based on the interaction of the waves. The polarization of the laser is rapidly changed

between TE and TM, enabling the measurement of two different phase changes, similarly to ellipsometry.[124,125]

The properties of the reference waveguide remain constant during the measurement, because it does not contact the sample. The protein of interest is typically covalently coupled to the sensing waveguide, which is exposed to a flow cell.[126–128] When proteins immobilized to the sensor surface bind the studied proteins, the refractive index and the thickness of the molecule layer change, as does the phase of the light. This is recorded as alterations in the interference patterns with both polarities.[124,125] DPI simultaneously monitors the phase changes with both TE and TM polarizations, and two interference patterns are recorded at almost the same time. Combining the results enables calculating both the refractive index (mass) and thickness of the protein layer. Therefore, DPI also provides information about the conformation of the bound proteins, and binding-caused structural changes can be monitored to some extent.[125] This sets DPI apart from other mass-sensing methods such as SPR. Sub-picomolar sensitivity may be achieved with DPI.[129] The initial kinetics obtained with the relatively long (e.g., 15 mm) sensor might not be entirely accurate, however, as reaching the desired protein concentration in the flow chamber may take over 10 seconds. Therefore, methods such as SPR, which may detect binding in a spot smaller than 0.5 mm^2, might be more suitable for acquiring the initial binding kinetics.[130]

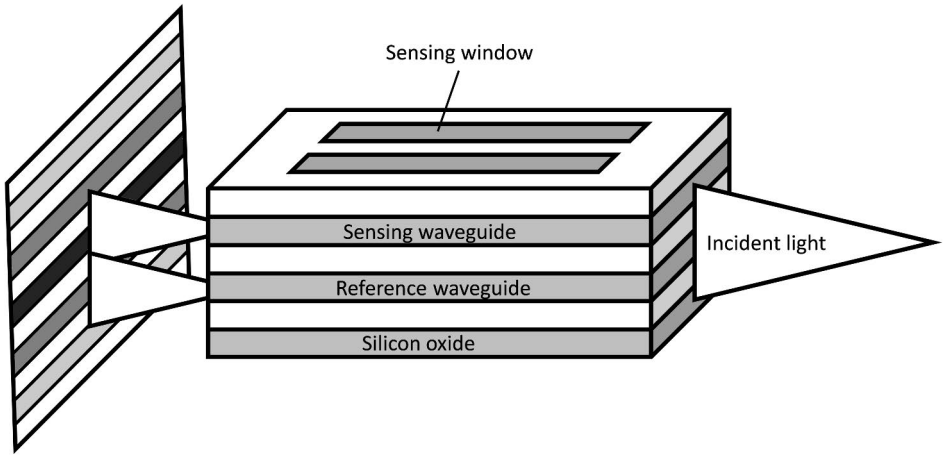

Figure 5. Dual polarization interferometry sensor. Two slab waveguides are stacked on top of each other, and the sensing waveguide is exposed to the sample material in a flow cell. Polarized light passes through both waveguides, and the molecules bound to the sensor surface affect the light traveling through the sensing waveguide. At the other end of the sensor, an interference pattern created by the two waveguides is monitored, giving information on protein binding. Rapidly altering the polarization enables measuring two separate phase changes.

2.5.5 Biolayer interferometry

Biolayer interferometry (BLI) is yet another method that enables studying both the interactions between protein pairs and the formation of multiprotein complexes in real time. In BLI, the studied protein is bound to a biocompatible surface located at the tip of a glass cylinder sensor (Fig. 6). Directly above the biocompatible layer is an internal reference layer, and when incident light moves down the biosensor fiber and reaches the tip, both layers reflect the light back. The reflection waves either add together or cancel each other, creating an interference pattern, similarly to DPI. When additional molecules are bound to the biocompatible layer, the thickness of the layer changes, and so does the reflection, changing the interference pattern. The BLI sensors are usually purchased with pre-prepared biocompatible surface. For example, SA and antibodies can be used as primary coatings. Similarly to other described methods, it is possible to observe more than one successive protein binding event, because each protein layer increases the thickness of the biolayer. BLI is also suitable for monitoring binding kinetics.[131] The result graphs obtained from BLI measurements are analogous to those of SPR assays (Fig. 4B) and the results are interpreted in a similar manner.

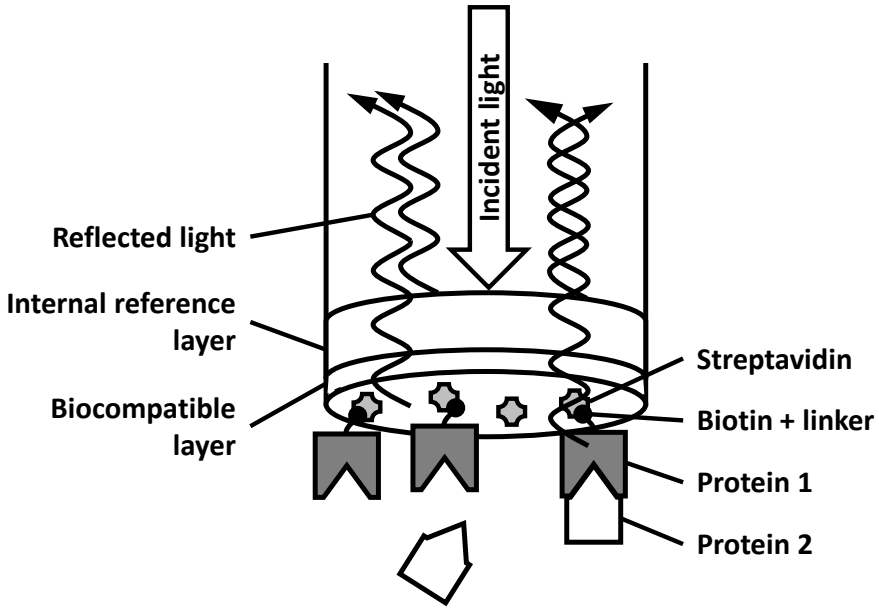

Figure 6. Biolayer interferometry principle in PPI detection. Incident white light travels through the sensor cylinder to the tip, where the internal reference layer and biocompatible layer reflect it back. These two reflections create an interference pattern that is determined by the thickness of the biocompatible layer, i.e., what molecules are bound to the layer. Thus, the binding of proteins is observed.

The glass cylinder with the sensing surface at the tip is a unique feature of BLI, compared to the other introduced surface-based methods. BLI assays use a dip-and-read concept, in which the sensor tips are dipped into solutions containing the studied proteins or wash buffers. Thus, the studied molecules are introduced to the sensor surface without the need for liquid flow, and it may be possible to collect and re-use the sample solution. The dip-and-read method can be performed on 96- or 384-well microtiter plates, which makes BLI an HTS-compatible method.[131] Because there is no liquid handling and only the tips are moved, solutions that might clog flow channels can potentially be analyzed.[114] However, not using liquid flow may affect the accuracy of the dissociation measurement, and the reproducibility of the assay might suffer.[132] BLI sensitivity is in the low nanomolar range for PPI measurements, not quite reaching that of SPR.[133] BLI is perhaps more suitable for HTS of interactions instead of detailed studies of one protein pair.

2.5.6 Quartz crystal microbalance

In quartz crystal microbalance (QCM) assays, much like in SPR assays, one protein of the studied PPI pair is attached to a gold surface either directly or via an intermediate binder molecule. QCM surfaces utilize similar conjugation methods as SPR chips, including SA/biotin and Ni^{2+}-nitrilotriacetic acid/histidine pairs.[134–136] Despite the similarities in the chip structure and preparation, the method of detection differs from SPR: instead of an optical measurement, QCM utilizes acoustic detection, and the gold surface is attached to a piezoelectric quartz crystal. When an alternating current is applied to the quartz crystal, it oscillates at a frequency defined by its mass. To measure PPIs, the gold surface coated with the target protein is exposed to a flow cell, and a solution containing the studied binding partner flows over the surface. PPIs change the mass of the quartz crystal, which leads to a shift in the oscillation frequency and detection of the binding (Fig. 7A).[134]

In addition to measuring only the frequency of the oscillation, it is possible to monitor the dissipation by momentarily cutting the current supply to the sensor (Fig. 7B). This approach is called quartz crystal microbalance with dissipation monitoring (QCM-D), which provides information on the viscoelastic properties of the molecules adsorbed to the sensor surface, i.e., the rigidity of the surface. This gives insight into the conformation of the bound molecules, but also into the amount of adsorbed water.[137,138] QCM and QCM-D are capable of monitoring PPIs and their kinetics, similarly to the other described surface-based methods. Both variants enable detecting sensor surface mass changes in the nanogram range, translating to picomolar sensitivity, but can also be applied to detecting very large objects, such as cells.[139–141] The application areas of QMC and QMC-D often overlap with that of SPR.

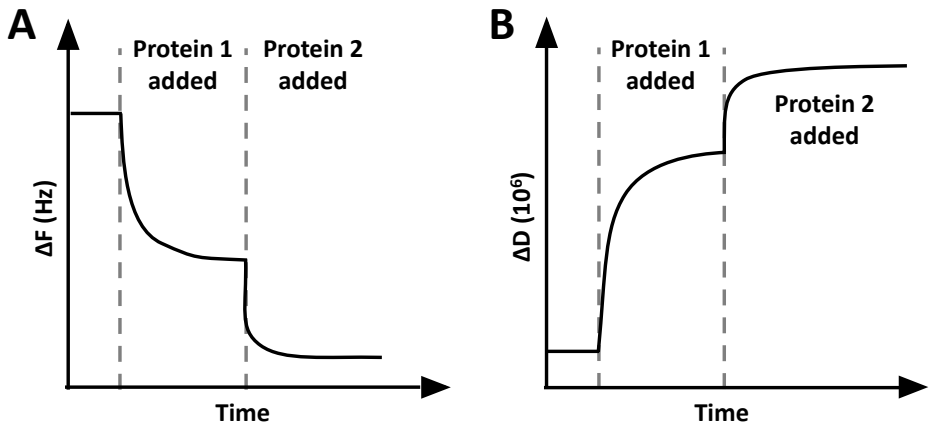

Figure 7. Schematic representations of QCM(-D) data. **A.** In a QCM measurement, protein binding is detected based on a decrease in the oscillation frequency of the sensor. The intensity of the change reflects the amount of bound protein. **B.** In QCM-D assays, also the dissipation of the oscillation is monitored after momentarily turning off the current supply. Protein binding makes the surface "softer" and increases the dissipation.

The advantage QCM-D has over QCM and optical methods is that it can detect and recognize solvent adsorbed to the sensor surface. Depending on whether the surface is rigid (less water) or soft (more water), different equations are required to accurately relate the oscillation frequency to sensor surface mass. Because QCM-D acquires more precise information about PPIs, it is more suited for quantifying the proteins than QCM.[137] QCM-D has a medium throughput, as there are instruments that can collect data simultaneously from several sensors.[142–144] The sensor chips are also relatively inexpensive. The disadvantage of QCM and QCM-D is that because the methods sense mass in a very sensitive manner, they are also sensitive to environmental conditions and susceptible to contaminations. Therefore, careful cleaning of the flow cells and chips is required before the measurement, and, e.g., the temperature of the measurement should be controlled.[137,145]

2.5.7 Electrochemical impedance spectroscopy

Electrochemical impedance spectroscopy (EIS) monitors PPIs based on changes in the sensor surface impedance. The sensor structure consists of two conductors and a non-conducting surface between them, which are in contact with a flow cell. One protein is immobilized to the non-conducting surface, commonly through binders such as SA and biotin, although self-assembling thiol layers on a gold surface have also been used. An interdigitated electrode configuration can improve the sensor performance and sensitivity (Fig. 8A). In this configuration, the two electrodes are

situated very close to each other, and proteins can be immobilized either between or on top of the electrodes.[146,147]

Protein binding and PPIs change the impedance properties of the sensor surface, and EIS enables measuring of the formation of multiprotein complexes. The monitored parameter is resistance, if there is a redox-active component present, such as a reducing or oxidizing enzyme. However, most proteins do not have redox-properties, and therefore PPI measurements are often performed by monitoring the capacitance in nonfaradaic EIS. The impedance is often determined at more than one frequency, and the results are commonly presented as a Nyquist plot, where each data point represents one measurement frequency (Fig. 8B).[146,148,149]

Different high-throughput strategies have been developed for EIS measurements, and EIS enables measuring binding events and their strength with femtomolar or even attomolar sensitivity.[149–151] The interdigitated electrode geometry enhances the impedance change monitoring at the solid-liquid interface of the sensor, where the protein binding takes place. Decreasing the gap between the electrodes further improves the sensitivity of the assay.[146,152] However, EIS is also very sensitive to non-specific changes in the impedance, such as those caused by non-specific adsorption to the sensor surface and contamination of the electrodes.[153]

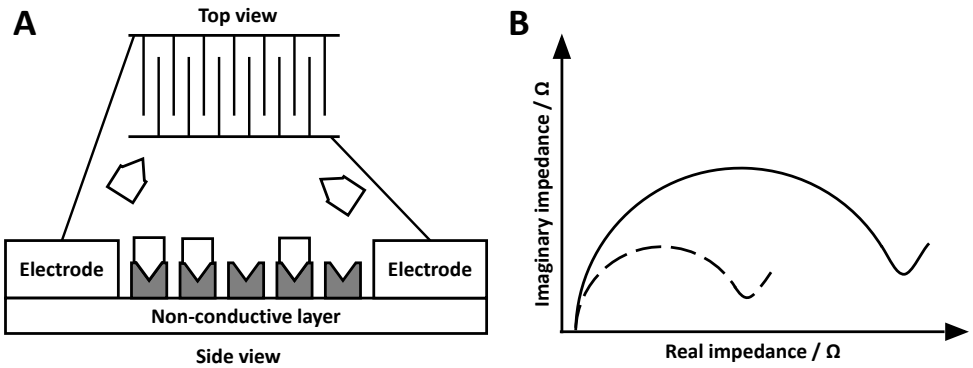

Figure 8. Electrochemical impedance spectroscopy principle for monitoring PPIs. **A.** The studied proteins are immobilized between electrodes on a non-conductive layer (side view). When additional proteins bind to the layer, the impedance properties of the sensor surface change, and the PPIs are detected. An interdigitated electrode configuration (top view) is used to improve the method functionality in bioanalysis. **B.** A schematic representation of EIS data, presented as a Nyquist plot. The dashed line represents the background signal produced by the sensor before protein binding, and the solid line represents the signal acquired upon PPI.

2.5.8 Protein microarrays

Protein microarrays have been used in PPIs studies for over two decades. Traditionally they utilize fluorescently labeled probes, but label-free approaches have also gained in popularity.[154–157] Resonance-, polarization-, and interference-based optical methods, such as SPR and ellipsometry, can be utilized for microarray detection. The basic functional principles behind the methods are the same but the detection is often combined with imaging, which drastically increases the throughput. Thousands of proteins may be printed onto a chip in distinct spots, the incident light can be directed to the whole array at once, and the response from all the protein spots can be recorded simultaneously with a charge-coupled device camera.[157,158] Automation further improves the throughput and makes protein microarrays a highly efficient tool for PPI research.

The properties of protein microarrays, for example suitability for different interaction types, depend on which detection method is used. For example, TIRE has improved sensitivity over ellipsometry also in a microarray setting. However, although the optical detection methods largely retain their capabilities in the microarray format, the sensitivity is often reduced compared to the traditional assays, and the specificity of the method may also suffer.[157] Producing microarray chips also requires specialized printing equipment, and the quality of the protein spots may vary. Furthermore, microarray measurements usually cannot be performed with the instruments designed for traditional label-free detection, and the instruments that are suitable for microarrays might not be interchangeable between different detection strategies. Protein microarrays are useful tools for screening PPIs with a high throughput, but the traditional forms of many label-free methods may be more suitable when only a relatively small number of interactions are studied.

2.6 Label-free solution-based methods in PPI studies

In this chapter, solution-based, label-free methods for monitoring PPIs are introduced. “Solution-based” method refers here to a technique where the interacting proteins are not immobilized on a surface and are instead free in the solution for interaction studies.

2.6.1 Calorimetry

Calorimetry measures the thermodynamics of chemical reactions, such as PPIs, by monitoring the heat produced or consumed by binding. Two common calorimetric methods for PPI detection are isothermal titration calorimetry (ITC) and differential scanning calorimetry (DSC). Both methods are based on two identical, temperature-

controlled cells, a sample cell and a reference cell, which are located inside an adiabatic, insulated structure.[159,160]

In ITC, the temperature of the system is kept constant. The reference cell contains buffer solution and the sample cell contains a protein of interest, and both cells are coupled to sensitive thermal detectors and heaters that keep the temperature constant between the two cells and the surrounding structure.[159,161] PPIs are measured by incrementally injecting the second studied protein into the sample cell containing the counter protein (Fig. 9). When the incrementally added protein contacts its interaction partner, the temperature of the sample cell changes, and the intensity and direction of the change depend on the interaction type. Subsequently, the heater feedback circuit activates and adjusts the temperature back to the constant level, and the energy consumption caused by the interaction is recorded. The amount of power required to keep the temperature constant is proportional to the amount of bound interacting proteins. Protein binding is observed as large heat changes at the beginning of the experiment, if the affinity is sufficient, as most of the injected protein interacts. As the system gradually saturates, the response decreases (Fig. 10A).[159,161]

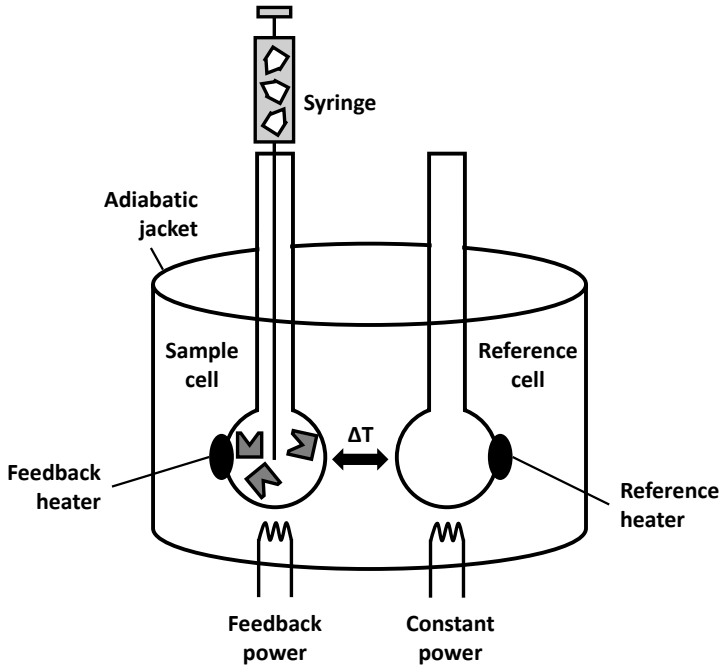

Figure 9. Isothermal titration calorimetry setup. The sample and reference cells are located inside an adiabatic jacket, where a constant power is applied to the reference cell. One interacting protein is inside the sample cell, and the other is slowly added with a syringe. The thermodynamics of the PPI change the sample cell temperature, followed by the feedback circuit equalizing the temperature with that of the reference cell. The PPI is observed by monitoring the fluctuation in the feedback power.

In DSC, calorimetry is combined to thermal ramping of the system. Constantly increasing the temperature leads to protein thermal denaturation, which consumes energy, and the thermal difference between the reference and sample cells is monitored. The measurement can be performed in two ways: power compensation and heat flux. The power compensation approach is similar to ITC detection. The sample and reference cells are not in contact, and separate heating and cooling elements control the temperature of each cell. The amount of energy required to maintain identical cell temperatures is monitored. In the heat flux approach, there is only one heater, and the cells are connected through a heat-conducting material. The temperature differences between the sample and reference cells result in a heat flow over the conducting material, which is measured.[162] A DSC measurement monitors the thermodynamic parameters of protein denaturation, producing characteristic thermal profiles for proteins, and does not directly provide information about the interaction status of the studied protein. However, DSC can be applied to PPI studies when the interaction affects the thermodynamic properties of the target protein, as in this case distinct thermal profiles can be acquired with and without the potential interaction partner (Fig. 10B).[163–165]

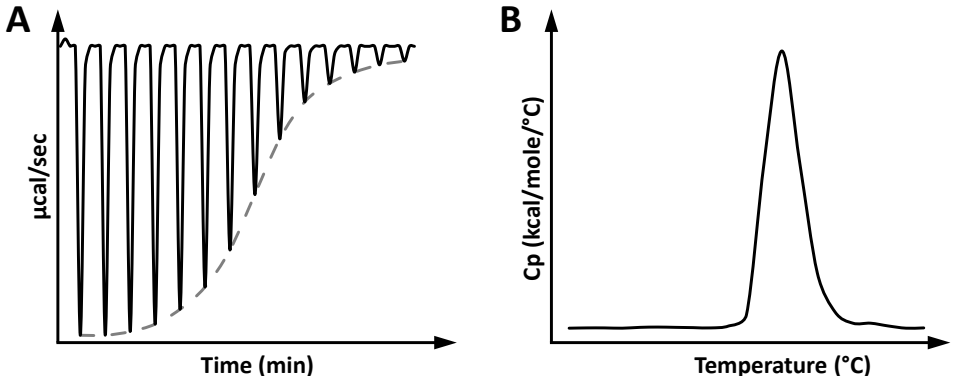

Figure 10. Schematic representation of calorimetry signals. **A.** In ITC data, each peak represents injection of the interacting protein (black, solid line). As the protein binding saturates, the peaks gradually become smaller. A curve is fitted on the peaks to calculate the stoichiometry, enthalpy, and affinity of the reaction (grey, dashed line). **B.** A DSC measurement produces a melting point peak for a protein. The melting temperature and enthalpy of the protein denaturation can be obtained through the curve fitting. PPIs that change the thermal profile may be detected with DSC.

ITC monitors the affinity and kinetics of the PPI and provides information on the enthalpy and stoichiometry, obtained by fitting a curve to the individual peaks (Fig. 10A). DSC can be used to determine the affinity and kinetics of a PPI reaction through comparing the thermal profiles of individual and complexed proteins. The method also measures the enthalpy of the denaturation and enables determining

melting temperatures (T_m) and temperatures of onset for the proteins or protein complexes. T_m is the temperature at which half of the protein or protein complex is denatured, whereas temperature of onset denotes the temperature where thermal changes begin to take place.[159,160,166] The problem with DSC is that the PPI must affect the thermal stability of the protein in some manner to be detected. ITC, which is commonly regarded as the gold standard method of PPI studies, is also not without disadvantages. Both ITC and DSC traditionally suffer from high sample consumption in the micromolar range, as well as low throughput. However, advances have been made in both regards with nanocalorimeters, which consume less sample, and array calorimeters, which improve the throughput.[164,167,168] That calorimetry is susceptible to minor differences in the sample materials is also a significant issue, as the method records such small temperature changes. For example, if the buffers of the two studied proteins are not identical regarding pH or salt concentration, the measurement may be disrupted.[169] Exchanging the buffer of the studied proteins with two different methods might already lead to notable changes, so the experiments must be controlled carefully.

2.6.2 Non-covalent external dyes

Methods using fluorescent detection are well-established in solution-based PPI studies but, as previously discussed, conjugating labels to the target molecules may distort the assay results. External dyes, which are often environmentally sensitive, are an alternative way to utilize fluorescence without labeling the interacting molecules. Some of these dyes can also be covalently attached as labels, but in a label-free context they only interact with the proteins noncovalently, mainly through electrostatic and hydrophobic interactions. Thus, external dyes have a lower risk of structurally disrupting PPIs than covalently attached labels.[170]

The fluorescence properties (intensity, emission maximum, lifetime) of the dyes depend on the viscosity, temperature, and polarity of their environment, mainly due to solvent relaxation and twisted intramolecular charge transfer (TICT). In solvent relaxation, polar solvent molecules surrounding the excited dye are aligned so that the energy level of the excited state is lower than in non-polar solvents. As a result, the dye emission is observed at longer wavelengths when measured in polar solvents compared to non-polar solvents.[170] In TICT, an electron is transferred within the dye from a donor group to an acceptor group due to conformational changes (e.g., twists) in the dye molecule. This transfer reduces the energy level of the excited state. TICT may also lead to excitation relaxation through routes other than fluorescence, decreasing the dye quantum yield. Like solvent relaxation, TICT is more prominent in polar than non-polar solvents, and it may also promote solvent relaxation.[170–172]

There are several types of external fluorescent dyes with different mechanisms, such as rotational and polarity sensitive dyes. Rotational dyes, such as Thioflavin T, 9-(dicyanovinyl)-julolidine, and Proteostat, are more affected by the viscosity of their environment than the polarity. They function through the TICT principle and produce more signal when their surroundings become more rigid. The rigidity changes can be caused by solvent properties, but also by protein interactions. In the study of PPIs, rotational dyes are mostly used for studying protein fibrillation and aggregation, because the protein complexes are very large and thus drastically change the viscosity of the dye microenvironment (Fig. 11A).[172–176]

Another group of external dyes is more sensitive to the polarity of the environment. Examples of such dyes are 1-anilinonaphthalene-8-sulfonate (ANS), SYPRO Orange, and Nile Red. These dyes produce a low signal in an aqueous environment because the high polarity leads to solvent relaxation and/or quantum yield loss through TICT. When soluble proteins are denatured, their inner hydrophobic amino acids are exposed and offer a non-polar binding environment for the dyes. Upon binding, the dyes are protected from the effects of the polar solvent, and their fluorescence increases.[170] Polarity-sensitive dyes can detect PPIs when the interaction exposes hydrophobic areas of the protein. For example, aggregation often leads to substantial changes in the structure of the proteins and enables the dye binding.[177] However, PPIs do not always reveal the hydrophobic structures to such extent that dye binding is possible. Therefore, polarity sensitive dyes are often used for PPI detection in the thermal shift assay (TSA) format, also known as differential scanning fluorimetry (DSF).[178,179]

In DSF assays, denaturing the proteins with elevated temperatures enables the binding of polarity-sensitive dyes, producing progressively more signal when the temperature increases and the denaturation proceeds. Individual proteins have their characteristic T_m values that can be obtained from the half point of the melting curve (Fig. 11B).[180,181] Protein complexes are often more stable than individual proteins, causing a measurable increase in the T_m (Fig. 11C).[178,179] The binding affinities of PPIs may be determined by monitoring the T_m values with several concentrations of one interaction partner.[178]

DSF measurements are high-throughput-compatible because they can be performed in a microtiter plate format, and the fluorescence signals can be monitored with common fluorescence intensity plate readers. If the dye has suitable excitation and emission wavelengths, the DSF assay can even be performed using a quantitative polymerase chain reaction (qPCR) instrument. This setup enables simultaneous temperature ramping and fluorescence measurement. SYPRO Orange, for example, has optical properties compatible with the standard filters found in most qPCR devices. The disadvantage is the low sensitivity of the dyes: the required sample concentration is in the micromolar range, which leads to high protein consumption.

[178,179,182,183] Furthermore, the DSF approach is not suitable for all proteins, as complex formation does not always affect the protein T_m. The proteins of interest might also not produce adequate thermal curves in the first place. In addition, surfactants pose a major issue for measurements with polarity-sensitive external dyes, as the dyes often bind to the micelles formed by the surfactant molecules. As surfactants are often found in protein storage buffers, sample dilution might be required to avoid the adverse effects and obtain reliable results. Viscosity-sensitive external dyes are less affected by surfactants than polarity-sensitive dyes, although high concentrations of some detergents, such as polysorbate, can still interfere with the measurement.[184]

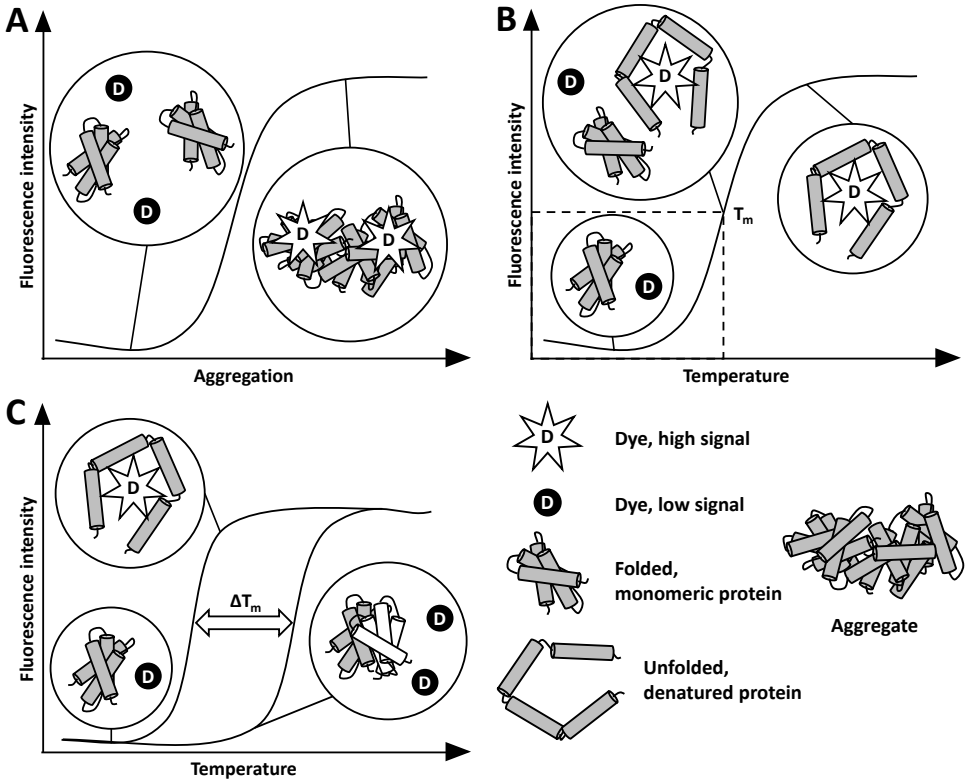

Figure 11. The use of external dyes in PPI research. **A.** Rotationally sensitive dyes usually produce low signal when they are combined with native, monomeric proteins. Upon protein aggregation, the microenvironment of the dyes becomes more rigid, leading to fluorescence intensity increase. **B.** Proteins are denatured when subjected to high temperatures, and their internal hydrophobic amino acids are exposed. Polarity-sensitive dyes are protected from the effects of the polar solvent upon binding to the hydrophobic areas and produce increased fluorescence signal at the measured wavelength. The T_m, at which 50 % of the protein is in the denatured form, can be calculated from the obtained melting curve. **C.** DSF can be used to observe PPIs based on their effect on the protein thermal stability. A T_m shift is observed when the proteins are monitored together if the proteins interact and the complex has different thermal stability compared to the individual proteins.

2.6.3 Intrinsic fluorescence

Besides using conjugated labels or external dyes, it is possible to study PPIs using the fluorescence naturally produced by the studied proteins. Proteins have intrinsic fluorescence properties if they contain the aromatic amino acids phenylalanine, tyrosine, or tryptophan, which can be excited at UV wavelengths.[185] Out of these three amino acids, phenylalanine has a low quantum yield, and tyrosine fluorescence is often naturally quenched. Tryptophan, on the other hand, has a sufficient quantum yield and, notably, different fluorescence lifetimes as determined by the non-covalent interactions and polarity in the immediate vicinity of the side chain. The environment also affects the tryptophan fluorescence emission maximum: lower polarity leads to emission at shorter wavelengths. Thus, if protein binding changes the tryptophan environment, it is possible to observe PPIs through intrinsic fluorescence.[186,187] Intrinsic fluorescence can also be utilized in DSF assays instead of external dyes for measuring and comparing the thermal stability of individual proteins and protein complexes. Tryptophan fluorescence is suitable for DSF assays because denaturation exposes the inner tryptophan residues to the polar solvent, redshifting the emission. The changes in the signal intensity are often observed at wavelengths of 330 and 350 nm, and their ratio.[188]

Intrinsic fluorescence assays are not applicable to all situations, as they rely on the studied proteins containing tryptophans and the PPI changing the environment of these tryptophans. Interpreting the data is challenging, because many different factors, from the presence of charged groups to the composition of the solvent, can change the local tryptophan environment.[189] On the other hand, the DSF assays require that the proteins and the complex produce thermal curves and that the interaction affects the thermal stability, which is not always the case. Although intrinsic fluorescence is utilized in PPI research, it is perhaps more useful in studying the structure of individual proteins.

2.6.4 Circular dichroism spectroscopy

Circular dichroism spectroscopy (CD) is mainly used for analyzing protein secondary structure, but it can also be applied to studying PPIs. In CD, circularly polarized ultraviolet (UV) light interacts with the peptide bonds, aromatic amino acid residues, and disulfide bridges of proteins.[190] Light interacts differently with asymmetric molecules, such as the secondary structure of proteins, depending on whether the circular polarization of the light is left- or right-handed. If the polarization directions are not equal in the light reflected from a sample, the light becomes elliptically polarized, and the changes are quantified by the CD detector. Different secondary structures produce distinct CD bands at given wavelengths, so

the protein secondary structure can be inferred from the spectra (Fig. 12A). However, CD cannot resolve the protein structure in a more detailed level.[191–193]

PPIs are detected based on the structural changes of the interacting proteins compared to the individual ones: if the interaction affects the structure of the optically active groups of the proteins, the CD spectrum changes (Fig. 12B). If there is no conformational change, PPIs can usually be detected based on the differences in the protein stability. Often, proteins are more stable in complex than individually, so denaturants or elevated temperatures have a different effect on the protein secondary structure based on the interaction status. CD can also be used to obtain dissociation and association constants by titrating the interacting proteins.[194] CD is suitable for analyzing proteins and protein complexes over a wide size range and can even be utilized in aggregation monitoring.[195]

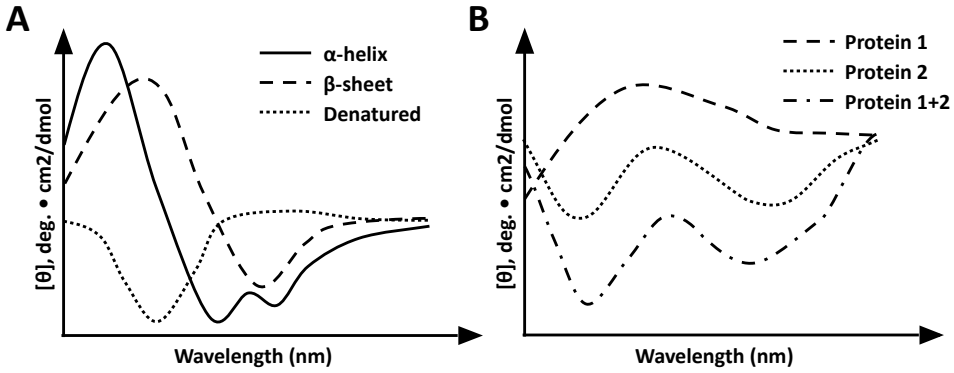

Figure 12. Schematic representation of circular dichroism data. **A.** Typical CD spectra of α-helices, β-sheets, and unstructured (denatured) proteins. **B.** The spectrum produced by the protein complex differs from those of the individual proteins, enabling PPI detection.

The sample requirement of CD assays is in the micromolar concentration range, and the sample concentration should be determined accurately prior to the CD measurement to enable reliable interpretation of the structural data. The buffer composition must also be carefully considered when measuring in the far-UV region (<260 nm), because several commonly used buffer components, such as NaCl, absorb light at these wavelengths.[190] Traditionally, the throughput of CD has been low, but in recent years the it has been increased through automation and the use of flow cells.[196,197]

2.6.5 Nuclear magnetic resonance spectroscopy

When it comes to structural data, CD has a low resolution and only provides information on the secondary structure. There are also methods for resolving protein

complex structures in greater detail, such as nuclear magnetic resonance (NMR) spectroscopy. NMR can measure the structure of fully soluble proteins at the atomic level, in a near-physiological environment. Notably, it can also determine the structures of weakly interacting protein complexes that have dissociation constants of 10^{-4} M or higher.[198]

NMR monitors how magnetically active nuclei absorb electromagnetic radiation on the radio frequency when exposed to a strong magnetic field.[199] Under the effect of the magnetic field and electromagnetic radiation, nuclei have their own characteristic resonance frequency that is determined by the environment of the nucleus, i.e., the bonds to other atoms and the atoms that are within 5 Å from the resonating nucleus. Even otherwise identical nuclei give different signals, i.e., chemical shifts, at different positions in the protein structure, producing a distinct NMR spectrum for each protein. PPIs change the nuclei environment at the protein-protein interface and can therefore be monitored by recording the changes through chemical shift perturbation analysis.[200–202]

Not all nuclei can be measured with NMR, however, as the observed isotopes must contain an odd number of protons. For hydrogen, the most common isotope (^{1}H) meets this demand, but the most abundant isotopes of, for example, carbon and nitrogen have an even number of protons. The less common variants ^{13}C and ^{15}N, which are often used in NMR measurements, must be integrated to the studied proteins through isotope enrichment. The isotope-enriched proteins are produced in cells grown in a media with, for example, only ^{15}N available instead of the more common ^{14}N. The isotope enrichment does not require any external conjugation to the protein and it very rarely affects the protein functionality. However, the use of recombinant proteins with appropriate isotopes complicates sample preparation. On the other hand, relying on the readily available ^{1}H may lead to interference from the water molecules of the solvent. Another disadvantage of NMR is that a very high sample concentration is required, often in the millimolar concentration range. The protein complex size is also a limiting factor, with the upper size limit of 80–90 kDa making it more feasible to study only fragments of the interacting proteins instead of whole proteins.[200,203] Although NMR is a powerful method for acquiring information on PPIs, the structure of the PPI interface, and the kinetics, the method is the most suitable for detailed studies of a specific, known protein-protein pair with suitable properties instead of screening through a large number of potential interactions.

2.6.6 X-ray crystallography

Like NMR, X-ray crystallography is a method than can resolve protein and protein complex structures in great detail. In X-ray crystallography, that the studied protein

complex must first be crystallized through vapor diffusion or by introducing a precipitant into the solution, for example. The measurement is performed by monitoring the diffraction of X-rays from the crystallized structure. The diffraction pattern changes based on the electron densities of the sample, so the 3D structure of the protein complex can be inferred from the pattern.[204,205]

X-ray crystallography has an advantage over NMR, in that the size of the protein complex is not a limiting factor, so it is therefore possible to determine the structure of entire protein complexes. The need for crystallization, however, severely limits the usability of the method. A very high (saturated) protein concentration, often in the millimolar range, is required for crystallization, which leads to high sample consumption. Additionally, not all proteins—and particularly not all protein complexes—can be crystallized or form crystals of sufficiently high quality.[206,207] Crystal formation is especially hard to achieve with weakly interacting proteins.[198] In addition, it may be challenging to distinguish the protein-protein interface from the connections formed due to crystallization.[208]

2.6.7 Cryogenic electron microscopy

Single-particle cryogenic electron microscopy (cryo-EM) is another method that is able to determine the structure of protein-protein complexes in very high, even atomic, resolution. In addition, cryo-EM also enables visualization of the samples.[209] The protein complexes are applied onto EM grids and subsequently frozen to make it possible for the proteins to withstand the vacuum of the electron microscope. The freezing is performed by rapidly plunging the grids into liquid ethane, and the protein complexes are frozen onto the holey carbon surface of the EM grid in random orientations. The grid is then imaged with an electron microscope, in which an electron beam is focused on the sample and the image forms based on how the sample scatters the electrons. In single-particle cryo-EM, several randomly oriented particles are imaged in 2D, then computationally aligned and combined to obtain the 3D structure of the complex. Biological samples are sensitive to radiation, which limits the possible strength of the electron beam during the measurement. A lower electron dose does not damage the sample as much, but also leads to a low signal-to-noise ratio with conventional EM cameras. Obtaining the atomic resolution has been possible only after the introduction of direct electron detection devices.[210]

Cryo-EM sample volumes are in the microliter range, and the concentration requirement is in the nanomolar or micromolar area, so the method consumes less sample than NMR or X-ray crystallography.[211] Crucially, cryo-EM does not require crystallization, unlike X-ray crystallography, and the method enables determining the structure of very large protein pairs or even multiprotein complexes, unlike NMR. Thus, cryo-EM fills a gap between X-ray crystallography and NMR by

making it possible to determine the structure of large protein complexes that cannot be crystallized. Cryo-EM has a lower size limit of about 50 kDa, however, which limits the ability to obtain the structures of individual proteins.[212] Fixing the proteins into the EM grid also means that determining dynamic structures is often not viable. Furthermore, variations in the sample preparation process may affect the obtained results. In addition, the atomic resolution has only been achieved very recently, and before this the protein structures have been obtained with the resolution of 3–4 Å.[209] The main disadvantage of cryo-EM is that, even when the lower resolution suffices and cutting-edge devices are not needed, the required instrumentation is specialized, expensive, and often not readily available.

2.6.8 Scattering

Measuring the intensity of light scattering of proteins provides information on protein size and molecular weight, and both static light scattering (SLS) and dynamic light scattering (DLS) are utilized in PPI studies. In both methods, a monochromatic light of high intensity is focused into the protein sample, and the intensity of the scattered light is monitored.[213,214] PPIs are detected based on the scattering changes, as the protein complexes have a larger size and distribute differently in the solution compared to individual proteins. Scattering methods can detect size changes in the nanometer range, so it may be possible to study the binding between two proteins.[215] However, light scattering is often applied to studying the aggregation of proteins, as the drastic particle size changes caused by aggregation are relatively easy to detect.[216]

In SLS, scattering is monitored continuously at one or several angles, and the mean intensity is recorded. Measurements are performed with a range of protein concentrations to obtain reliable data.[217] In DLS, the measurement is performed several times in very short intervals, and light scattered from the proteins arrives to the detector in different phases depending on the positions of scattering particles. The phases of the scattered photons may be destructive or constructive compared to each other, creating a distinct interference pattern that reflects the position of the particles in the moment of the measurement, and sequential measurements produce different interference patterns. Small proteins have fast diffusion and cause rapid intensity changes at the detector, whereas large proteins or protein complexes cause slower changes. Diffusion coefficients can be calculated through the autocorrelation function based on the intensity fluctuations and their rate, and the hydrodynamic radii (i.e., size) of proteins can be detected. Scattering measurements enable PPI detection because protein complexes have larger hydrodynamic radii compared to individual proteins (Fig. 13). The more there are particles of certain size, the more light is scattered, which leads to increased signal intensity.[214]

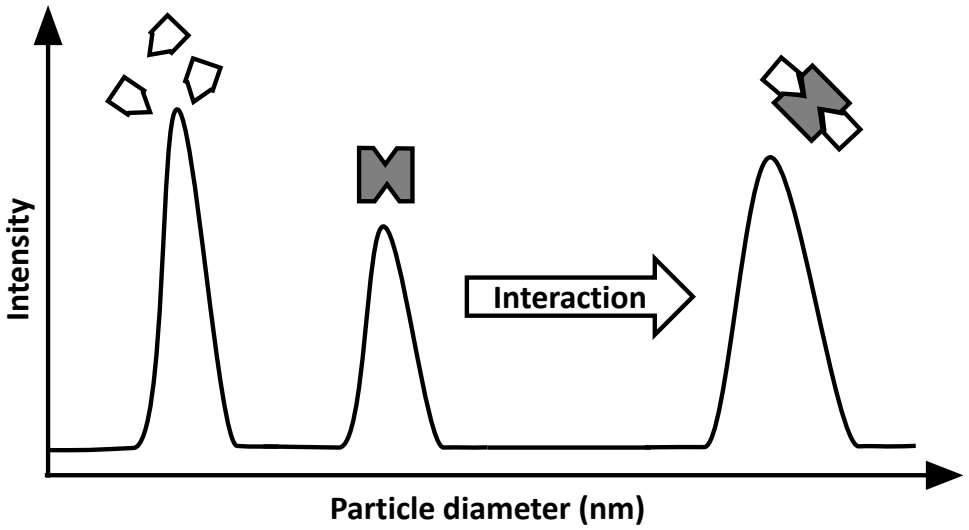

Figure 13. Schematic representation of scattering data. PPIs can be detected based on the increased diameter of the protein complex compared to that of the individual proteins.

Scattering studies enable determining the stoichiometry and dissociation constants of PPIs.[215,218,219] The detection limits depend on the size of the studied particles, but individual large proteins (e.g., antibodies) can be detected in the nanomolar concentration range.[216,219] The traditional cuvette format of the scattering measurements restricts the throughput, but improvements have been made by developing approaches that are compatible with microtiter plates or capillaries.[219,220] SLS is able to determine particle size down to 10 nm when measurements at multiple angles are used, meaning that the method cannot define the size of small, individual proteins. DLS, on the other hand, can determine hydrodynamic radii even below 1 nm.[214,216] However, both SLS and DLS have limitations, such as sensitivity to dust or other contaminating particles in the solution. Additionally, scattering is a qualitative method and does not enable quantifying of the protein complexes. There are also issues with the reproducibility, especially in the case of non-spherical and polydisperse particles.[221] To obtain reliable results, the algorithms applied to calculating the protein sizes must be carefully chosen based on the properties of the sample, such as concentration, polydispersity, and viscosity.[215,216]

2.7 Summary

In conclusion, there are a wide variety of methods for studying and monitoring PPIs in a label-free manner using purified proteins. The properties of the introduced methods are summarized in Table 1. Each method has a different measurement

principle, its own strengths and weaknesses, and is suitable for different purposes. In the context of drug development, for example, techniques with high throughput, such as BLI and external dyes, might be suitable for the initial screening of large protein libraries. Once potential binder molecules have been found, they may be further studied with medium-throughput methods, such as SPR, to obtain the most promising drug candidates with the highest affinities and specificities. Characterizing the complex structure and binding mechanics in detail with NMR, cryo-EM, ITC, and other low-throughput methods becomes viable after narrowing the studied interactions to only a handful. Some methods, such as SPR, may also be used in several levels of the drug development process, which facilitates the comparison of the results between different stages.

Among the label-free methods introduced in this thesis, the surface-based assays generally have better sensitivity than the solution-based assays, and thus require less sample material. Some, such as BLI and RWG, are easily manufactured in an HTS-compatible format. Nowadays, it is also possible to perform the detection of resonance-, polarization, and interference-based optical methods, such as SPR and ellipsometry, in an imaging format, often in combination with protein microarrays. This drastically improves the throughput compared to the traditional instruments. However, conjugating one of the studied proteins to a solid surface may distort the results. The surface itself can cause issues such as steric hindrance and electrostatic repulsion, and the effects may be different for each studied protein, requiring careful optimization.[222] Immobilizing charged proteins might pose specific challenges, depending on the surface type.[223] Regardless of the charge, binding proteins to a surface can render their interaction sites inaccessible, especially when the proteins are adsorbed to the sensor non-specifically. A balance must also be found with the liquid flow rate to ensure that concentration gradients are avoided and the liquid flow does not disrupt the interaction.[224,225] In a sense, conjugation to a solid surface is akin to labeling the molecules, and has many of the same disadvantages.

Solution-based label-free methods, on the other hand, are fully conjugation-free. Thus, they enable studying PPIs under conditions that more closely resemble the physiological environment, and some methods provide extremely detailed information about the interactions. For example, NMR and cryo-EM are excellent tools for studying the protein complex structure, and calorimetry yields information on the thermostability and reaction energetics. Unfortunately, most solution-based methods have a significantly lower sensitivity than surface-based methods, with detection limits in the micromolar range or higher. This limits the HTS capabilities of the methods, even when the assay setup and instrumentation would allow a high throughput. High protein concentration can also affect the properties of the protein in the solution and lead to concentration-dependent shifts in the measured T_m or the formation of undesired artefacts, such as aggregates. Thus, there is a niche to be

filled for solution-based PPI analysis techniques with improved sensitivity and HTS compatibility.

As for the current trends in label-free PPI research, SPR and calorimetry seem to be holding their positions as the gold standard methods, even though both are already decades old and provide only low to medium throughput. Of course, these techniques have been improved over the years by developing new sensor materials and setups, and there are ongoing efforts to increase their throughput. However, when it comes to PPI screening, the microarray format holds perhaps the most promise, as it intrinsically has a very high throughput, and instruments suited for the microarray imaging may become more commonplace in the future. In the structural level of PPI studies, cryo-EM already stands to surpass NMR and X-ray crystallography, both of which face limitations regarding either the protein complex size or the crystallization requirement. So far, price has been a limiting issue with cryo-EM, but the technology required to reach atomic resolution will likely become less expensive in the coming years.

Table 1. Summary of label-free methods for studying PPIs with purified proteins.

Method	Surface-free	Sensi-tivity	Through-put	Measures	Properties
SPR	No	pM-nM	High*	Binding	Gold standard of surface-based methods.
RWG	No	pM-nM	High	Binding	Microtiter plate format.
Ellipsometry	No	pM	High*	Binding	Measures both amplitude and phase of light; more detailed information than SPR.
TIRE	No	pM	High*	Binding	Combines ellipsometry and SPR.
DPI	No	<pM	Low	Binding, conformation	Measures both mass and thickness of protein layer.
BLI	No	nM	High	Binding	Microtiter plate format.
QCM-D	No	pM	Medium	Binding, conformation	Provides information also on adsorbed water.
EIS	No	aM-fM	High	Binding	Extremely sensitive but prone to interference.
ITC	Yes	μM	Low	Binding, thermodynamics	Monitors reaction enthalpy and stoichiometry.
DSC	Yes	μM	Low	Thermal stability	Thermal ramping.
External dyes	Yes	μM	High	Thermal stability	Thermal ramping. Microtiter plate format.
Intrinsic fluorescence	Yes	μM	High	Thermal stability, structure	Relies on tryptophan at convenient locations. Microtiter plate format.
CD	Yes	μM	Medium	Structure, thermal stability	Mainly for studying protein secondary structure.
NMR	Yes	mM	Low	Structure	Suitable for known protein pairs.
X-ray crystallography	Yes	mM	Low	Structure	Requires crystallization.
Cryo-EM	Yes	nM-μM	Low	Structure	Enables visualization.
Scattering	Yes	nM	High	Size	Primarily used for aggregation monitoring. Microtiter plate format.

*High throughput in a microarray setting.

3 Aims of the Study

The main objective of this PhD work was to develop a novel label-free, homogenous, sensitive, easy-to-use platform for studying proteins in several concepts and situations *in vitro*. The principle and functionality of the method were initially established by measuring protein thermal stability and PLIs, and the assay was then applied to monitoring PPIs. In addition to detecting PPIs between two different interaction partners—both 1:1 pairs and protein complexes—the method was demonstrated for monitoring antibody aggregation in an *in vitro* setting.

The aims of the original publications were:

I To introduce the Protein-Probe method and establish its functionality by monitoring protein thermal profiles and ligand stabilization.

II To demonstrate the Protein-Probe method in studying the interactions of protein pairs and multiprotein complexes.

III To apply the Protein-Probe method for studying the stability and aggregation of diagnostic and therapeutic antibodies.

IV To study the functionality of thermal shift assays using KRAS and its interaction partners as models.

4 Materials and Methods

For more details, please refer to the original publications.

4.1 Luminescence and absorbance measurements

Time-resolved luminescence (TRL) measurements were performed with Victor 1420 multilabel counter (PerkinElmer; excitation 340 nm, emission 615 nm) (**I**) and Tecan Spark 20M (Tecan; excitation 340 nm, emission 620 nm) (**I-IV**), with 400–800 µs delay time and 400 µs integration time. Europium excitation spectra (250–500 nm; emission monitored at 620 nm) and emission spectra (550–800 nm; excitation at 340 nm), as well as 1,1,3,3,3′,3′-hexamethylindodicarbocyanine (HIDC) excitation spectra (450–680 nm, emission monitored at 700 nm), emission spectra (630–850 nm, excitation at 618 nm), and absorbance spectra (400–750 nm) were monitored with Tecan Spark 20M (**II, III**). Luminescence lifetimes were monitored with Varian Cary Eclipse Fluorescence spectrophotometer (Agilent Technologies) using 340 nm excitation, 615 nm emission, 0.1 ms delay and gate times, and the total measurement time of 3 ms (**II, III**). FRET measurements were performed using Tecan Infinite200Pro (Tecan) (530 nm excitation, 590 nm emission) (**II**). SYPRO Orange (excitation 485 nm, emission 590 nm) (**I-IV**) and ANS (excitation 350 nm, emission 490 nm) (**IV**) luminescence was monitored with Tecan Spark 20M. Thermal ramping was performed using PTC-100 and PTC-200 Peltier Thermal Cycler (MJ Research) (**I-IV**). Absorbance measurements were performed on transparent 96-well plates (TOMTEC Plastics) (**III**). Black OptiPlate 384-well plates (PerkinElmer) (**I-IV**) and black or white low volume 384-well plates (Corning) (**II, IV**) were used for room temperature (RT) assays. Black Framestar 96- or 384-well plates (4titude) were used for thermal ramping studies (**I-IV**).

4.2 Assay buffers

The assay buffers were selected based on the specific requirements of the tested proteins. The buffers used in the main experiments are listed in Table 2. Formulation buffers, which were chosen according to the suggestions and specifications provided by a commercial partner, are listed in Table 3.

Table 2. Compositions of the main assay buffers.

Buffer	Components
Buffer 1 (**I, III**)	0.1x phosphate-buffered saline (PBS), 0.001 % (v/v) Triton X-100
Buffer 2 (**II, IV**)	10 mM HEPES (pH 7.5), 0.001 % (v/v) Triton X-100, 1 mM $MgCl_2$, 20 mM NaCl
Buffer 3 (**II**)	10 mM HEPES (pH 7.5), 0.001 % (v/v) Triton X-100
Buffer 4 (**II**)	20 mM HEPES (pH 7.5), 100 mM KCl, 1 mM $MgCl_2$
Buffer 5 (**IV**)	10 mM HEPES (pH 7.5), 0.001 % (v/v) Triton X-100, 20 mM NaCl
Buffer 6 (**IV**)	10 mM HEPES (pH 7.5), 0.001 % (v/v) Triton X-100, 1 mM EDTA, 20 mM NaCl
Buffer 7 (**II, IV**)	20 mM HEPES (pH 7.5), 1 mM MgCl2¬, 10 mM NaCl, 0.01 % (v/v) Triton-X 100, 0.005 % (w/v) γ-globulins
Modulation solution base (**I-IV**)	7.7 mM Na_2HPO_4, 6.1 mM citric acid, pH 4, 0.01% Triton X-100

Table 3. Compositions of formulation buffers (**III**).

Buffer	Base buffer	pH	Excipient
Buffer 8	PBS	7.2	NA
Buffer 9	Citrate-phosphate buffer	4	0.9 % (w/v) NaCl
Buffer 10	Citrate-phosphate buffer	5	0.9 % (w/v) NaCl
Buffer 11	Citrate-phosphate buffer	6	0.9 % (w/v) NaCl
Buffer 12	Citrate-phosphate buffer	7	0.9 % (w/v) NaCl
Buffer 13	Citrate-phosphate buffer	8	0.9 % (w/v) NaCl
Buffer 14	Citrate-phosphate buffer	7	0.9 % (w/v) NaCl, 0.02 % (v/v) polysorbate 20
Buffer 15	Citrate-phosphate buffer	7	0.9 % (w/v) NaCl, 0.1 % (v/v) polysorbate 20
Buffer 16	Citrate-phosphate buffer	7	0.9 % (w/v) NaCl, 0.4 % (v/v) polysorbate 20
Buffer 17	Citrate-phosphate buffer	7	0.9 % (w/v) NaCl, 50 mM sucrose
Buffer 18	Citrate-phosphate buffer	7	0.9 % (w/v) NaCl, 150 mM sucrose
Buffer 19	Citrate-phosphate buffer	7	0.9 % (w/v) NaCl, 500 mM sucrose
Buffer 20	Citrate-phosphate buffer	7	0.9 % (w/v) NaCl, 30 mM sorbitol
Buffer 21	Citrate-phosphate buffer	7	0.9 % (w/v) NaCl, 100 mM sorbitol
Buffer 22	Citrate-phosphate buffer	7	0.9 % (w/v) NaCl, 300 mM sorbitol

4.3 Protein-Probe preparation and characterization

4.3.1 Europium-labeled peptide

A nonadentate Eu^{3+}-chelate, {2,2',2",2'"-{[4'-(4'"-isothiocyanatophenyl)-2,2',6',2"-terpyridine-6,6"-diyl]bis(methylene-nitrilo)}tetrakis(acetate)}europium(III) (QRET Technologies) was conjugated to the N-terminus of the sensing peptide sequence (NH2-EYEEEEEVEEEVEEE; Pepmic) (**I-IV**). Isothiocyanate-activated Eu^{3+}-chelate (1 mg) was dissolved in 100 µL of MilliQ H_2O and combined with 0.5 mg of the peptide in 100 µL of pyridine/H_2O/triethylamine (9:1.5:0.1 ratio). The reaction was incubated 18 h at RT, then purified with reverse-phase adsorption chromatography using Dionex Ultimate 3000 LC system (Dionex, Thermo Fisher Scientific) with Ascentis RP-amide C18 column (Supelco Analytical, Sigma Aldrich). The eluent (50 mM TEAAc pH 7.0:ACN 100%) was used in a linear gradient (1 ml/min from 10:90 to 50:50 in 17 min). The Eu-probe concentration was determined by comparing the TRL signal of the probe to a Eu^{3+}-standard (DELFIA, PerkinElmer) and assuming the ratio of Eu^{3+}-chelate and peptide was 1:1.

4.3.2 Modulation solution and the Protein-Probe

The modulation solution base was prepared by combining 0.2 M Na_2HPO_4 and 0.1 M citric acid in different ratios to achieve the desired pH values, diluting the phosphate-citrate buffer 1/10, and supplementing it with 0.01 % (v/v) Triton X-100. The combination of Na_2HPO_4 and citric acid was chosen because it enabled preparing buffers in the desired pH range. To prepare the modulation solution, 3.5 or 4 µM HIDC was added. The Protein-Probe solution was made by supplementing the modulation solution with 1–1.5 nM Eu-probe. (**I-IV**) Unless otherwise specified, the sample volume was 8 µL, the Protein-Probe solution volume was 65 µL, and samples were prepared into Buffer 1 and assayed in triplicates. The TRL or luminescence signals were monitored after 5 min incubation at RT.

The effect of modulation solution pH on the stability and TRL signal level of the Eu-probe was studied by monitoring the Eu-probe in pH 2–10 modulation solution without HIDC several times during a 130 min incubation. (**I**) An IgG_1 monoclonal antibody (mAb; 80 nM, T_m 75.7 °C) was incubated for 3 min at RT or 80 °C (full denaturation) and combined with the Protein-Probe solution (3.5 µM HIDC, pH 2–10), followed by monitoring the TRL signals. All subsequent assays were performed with the modulation solution buffered to pH 4. The Protein-Probe sensitivity was compared to SYPRO Orange by monitoring denatured IgG_1 mAb (0–5 µM) (**I**), GDP-loaded KRAS (0–15 µM, Buffer 2) (**II**), and trastuzumab (0–6 µM) (**III**). SYPRO Orange was added in 2 µL, to 1x final concentration.

The excitation and emission spectra of the Eu-probe (1 nM) and HIDC (3.5 µM) were monitored both with and without denatured anti-CRP mAb (30 nM)/CRP (50 nM) complex (**II**) and 1 µM aggregated trastuzumab (**III**). The lifetimes of Eu-probe (50 nM) and Protein-Probe solution (50 nM Eu-probe and 2–3.5 µM HIDC) were monitored both with and without denatured 1 µM anti-CRP mAb/0.2 µM CRP (**II**) and 1 µM aggregated trastuzumab (**III**).

4.4 Thermal ramping assays

The Protein-Probe solution contained 3–4 µM HIDC and 1 nM Eu-probe. SYPRO Orange was added in 12 µL (single step) or 2 µL (two-step) to the final concentrations of 5x and 1x, respectively. ANS was used in the final concentration of 10 µM. The tested temperatures were between 35 and 95 °C and 2–5 °C intervals were used. The samples were incubated for 3 min at each temperature and the Protein-Probe solution was added thereafter. SYPRO Orange assays were performed similarly in two steps, or the sample and SYPRO Orange were combined prior to the heating, followed by luminescence measurement. ANS assays were performed in one step, with the sample and ANS both added before the heating.

Protein-Probe measurements. The thermal curves of all murine monoclonal antibodies (mAb1-mAb26, 80 nM, 2–3 replicates) (**III**), trastuzumab (80–2000 nM) (**III**), malate dehydrogenase (100 nM) (**I**), carbonic anhydrase (CA; 200 nM) with and without acetazolamide (AZA, 0–10 µM) (**I**), and SA (400 nM) with or without biotin (0–20 µM) were monitored in Buffer 1 (**I**). The CA/AZA and SA/biotin titrations were performed by combining 4 µL CA or SA with 4 µL of AZA or biotin, respectively. The samples were incubated for 3 min at 70 °C (CA) or 90 °C (SA), followed by the TRL signal measurement.

CRP (0–50 nM) and anti-CRP mAb (IgG_1, T_m 70.9 °C, 0–30 nM) were monitored in Buffer 3, individually or in combination. The individual and combined thermal curves of eukaryotic initiation factor 4A (eIF4A; 75 or 150 nM), eukaryotic translation initiation factor 4H (eIF4H; 500 or 1000 nM), and programmed cell death protein 4 (PDCD4; 75– 300 nM or 2 µM) were monitored in Buffer 4. In addition, eIF4A was monitored in Buffer 4 supplemented with 0.001 % Triton X-100. (**III**)

The thermal curves of 50–100 nM KRAS (GDP-KRAS, 5'-guanylyl imidodiphosphate (GMPPNP)-KRAS, and mutants G13D, G12D, G12C, Q61L, and Q61R), and designed ankyrin repeat protein (DARPin) K27 (100 nM) were monitored in Buffer 2. KRAS mutants G13D and Q61R were also monitored in Buffers 5 and 6. Wild type (WT) KRAS or G12C were monitored in thermal ramping in combination with DARPins K27 (100 nM), K13 (0–200 nM), K19 (0–500 nM); inhibitors ARS-853 (0–5000 nM), ARS-1620 (0–5000 nM), AMG-510 (0–100 nM), and MRTX849 (0–100 nM); and GDP (0–900 µM), GTP (10 µM), and adenosine

triphosphate (ATP; 10 μM) in Buffer 2. KRAS G12C (50 nM) was also combined with DARPin K13 (50 nM) and AMG-510 (0–900 nM), MRTX849 (0–900 nM), ARS853 (0–20 μM), and ARS1620 (0–20 μM) in thermal ramping, in Buffer 2. (**IV**)

SYPRO Orange and ANS measurements. The thermal curves of 2 μM IgG_1 mAb (**I**), 2 μM eIF4A, 2 μM PDCD4 (**II**), and 2 μM trastuzumab (**III**), as well as 6 μM KRAS (WT or G12C mutant) with AMG-510 (0–20 μM), MRTX849 (0–20 μM), ARS853 (20 μM), and ARS1620 (20 μM) (**IV**) were measured using SYPRO Orange. The thermal stability of 6 μM KRAS was also monitored with 0–20 μM AMG-510 and MRTX849 using ANS. (**IV**) Trastuzumab, eIF4A, and KRAS and its binding partners were monitored using a single step protocol, whereas the IgG_1 thermal curve was measured using the two-step protocol, in which the SYPRO Orange solution was added after the sample incubation at an elevated temperature.

4.5 Room temperature assays

Assaying protein interactions. The affinities of inhibitors AMG-510 and MRTX849, and DARPins K13, K19, and K27 were monitored in a quenching resonance energy transfer (QRET) assay in Buffer 7 in a final volume of 15 μL. (**II, IV**) KRAS mutant G12C or KRAS WT were incubated for 5 min with the inhibitors (0.03–10 000 nM) or DARPins (1–1000 nM), respectively. K27 (2–6000nM), as well as GDP (2–6000nM), was incubated with both GDP- and GMPPNP-loaded KRAS. The QRET detection solution (2.5 μM modulator MT2, 10 nM Eu^{3+}-GTP) was added, and the Eu^{3+}-GTP association was initiated with SOS^{cat} (10 nM). The TRL signal was monitored multiple times over 60 min. The eIF4A activity and specificity to eIF4H was monitored in FRET assays. (**II**) eIF4A (1.5 μM, 3 μL) and eIF4H (1.5 μM, 3 μL) were combined with pre-annealed Cy3-/BHQ2-RNA complex (50 nM, 2 μL) and Cy3-RNA-complementary DNA (1 μM) with or without PDCD4 (0–10 μM, 2 μL), followed by helicase reaction initiation by Mg^{2+} (2 mM)/ATP (5 mM) complex (2 μL). The FRET signals were monitored every 5 min for 45 min.

Monitoring multiprotein complexes. Biotinylated bovine serum albumin (bio-BSA, 20 nM) was assayed with SA (0–600 nM) in Buffer 3, with BSA (20 nM) as a negative control. (**II**) The Protein-Probe solution contained 6 μM HIDC and 4.5 nM Eu-probe. The interaction was confirmed by titrating the combination of 20 nM bio-BSA and 200 nM SA with 0–10 μM biotin. The interactions between CRP (0–100 nM) and anti-CRP mAb or two non-specific mAbs (0–500 nM) were monitored in Buffer 3, using Protein-Probe containing 3.5 μM HIDC and 1 nM Eu-probe. (**II**)

Monitoring protein aggregation. Trastuzumab (32 μM) was stored at 60 °C for 13 days, during which samples (2 μM) were monitored multiple times using the Protein-Probe, SYPRO Orange, and UV250. (**III**) The samples were incubated with SYPRO Orange (2 μL, 1x final concentration) or the Protein-Probe (3.5 μM HIDC,

1 nM Eu-probe) for 5 min before monitoring the luminescence or TRL signals. The absorbance at 250 nm was measured in quartz cuvettes, using 400 µL volume. Aggregate formation was also confirmed in native PAGE experiments on an 8 % tris-glycine gel with native, partially, or fully aggregated mAbs (5 µg/lane). The electrophoresis was performed according to the manufacturer's instructions. Trastuzumab, mAb2, and mAb4 were aggregated by incubating the proteins for 3 min at 85 °C (100 % aggregated) and mixed with intact mAbs to monitor the Protein-Probe sensitivity for aggregation as the percentage of spiked aggregate. (**III**) The final concentration was 6 µM throughout the mAb aggregate series from 0 to 10 %. The Protein-Probe, containing 4 µM HIDC and 1.5 nM Eu-probe, was combined with 6 µL of samples. The background samples with baseline aggregation ("0 %") were measured with six replicates, whereas the other samples were measured in triplicates. Six mAbs (30–34 µM) were stressed by storing them at -20, 4, 35, or 45 °C for three weeks, then monitored at RT and elevated temperatures using the Protein-Probe as described in section 4.4. Trastuzumab, mAb1, and mAb11 were diluted to 6 µM to Buffers 8–22 (Table 4) and stored for four days at 65 °C (trastuzumab) or 45 °C (mAb1 and mAb11). mAb12-mAb17 were stored in Buffers 9–13 for four days at 45 °C. The samples were diluted 1/10 to MilliQ H_2O and (using 4 µL sample) combined with the Protein-Probe solution in four replicates. The plate was briefly mixed and TRL signals were monitored multiple times during 60 min.

4.6 Data processing

The signal-to-background (S/B) ratios were calculated as μ_{max}/μ_{min} and the coefficient of variation as $(\sigma/\mu) \times 100$. In these formulas, μ is the mean value and σ is the standard deviation (SD). The denaturation temperatures, detection limits, half maximal effectivity concentration (EC_{50}), and half maximal inhibitory concentration (IC_{50}) values were calculated based on the fitted data using standard sigmoidal and linear fitting functions. The data were analyzed using Origin 2016 (OriginLab, Northampton, MA).

5 Results and Discussion

5.1 Principle of the Protein-Probe method

The studies included in this doctoral work developed and utilized the Protein-Probe method, which was introduced in Publication **I** and then applied to monitoring various proteins and their interactions under different conditions (**II-IV**). At the core of the Protein-Probe method is the Eu-probe: a peptide conjugated with a Eu^{3+}-chelate. The peptide moiety of the Eu-probe binds to denatured and aggregated proteins, but not significantly to intact, native, individual proteins. The exact mechanism of the Eu-probe interaction has not been determined, but the probe is assumed to bind to the hydrophobic regions that often become accessible after the unfolding/denaturation of soluble proteins. The Eu-probe binding is improved when the probe is protonated, and therefore the assays are performed in a modulation solution that has a low pH. The modulation solution also contains a quencher molecule, HIDC. When the Eu-probe is added, the solution is referred to as the Protein-Probe.

The Eu^{3+}-chelate has two components: a lanthanide ion, Eu^{3+}, and an organic chelate moiety coordinating the ion. As lanthanide ions absorb light weakly, the chelate structure is required to effectively gather the excitation energy. The chelate also protects the ion from the quenching effect of water.[61] Excitation of the chelate leads to a conversion from the singlet state to the triplet state through intersystem crossing, followed by energy transfer to the lanthanide ion. The lanthanide ion is excited, and the return to ground state is observed as emission.[226] The excitation wavelength is chosen based on the properties of the organic chelate and the emission wavelength is dictated by the lanthanide ion, so the apparent Stokes shift is substantial, and crosstalk of the excitation and emission light is avoided.[61,226] The Eu-probe is excited at 340 nm and the emission is measured at approximately 620 nm. The absorption maximum of HIDC is 636 nm, and therefore HIDC effectively absorbs and quenches the Eu-probe emission inf the Protein-Probe solution (Fig. 14).

Lanthanide ion emission decays in milliseconds, unlike that of conventional fluorophores, whose lifetimes are in the nanosecond scale. In a time-resolved assay, the measurement gate to the detector is opened 400 µs after the excitation pulse and closed again after another 400 µs, for example. Thus, autofluorescence from plastic

materials, biological samples, or other sources does not interfere with the measurement, and the assay sensitivity is improved. The quenching effect of HIDC considerably shortens the emission lifetime of the Eu-probe, typically from 1 ms to ~0.1 ms. As a result, very low TRL signal is observed when the Eu-probe is free in the Protein-Probe solution. However, when the Eu-probe binds to a partially or fully denatured protein, the energy transfer from the Eu-chelate to HIDC is prevented, and the emission lifetime is prolonged. Thus, a high TRL signal is monitored during the chosen measurement window. This provides the basis for the Protein-Probe method.

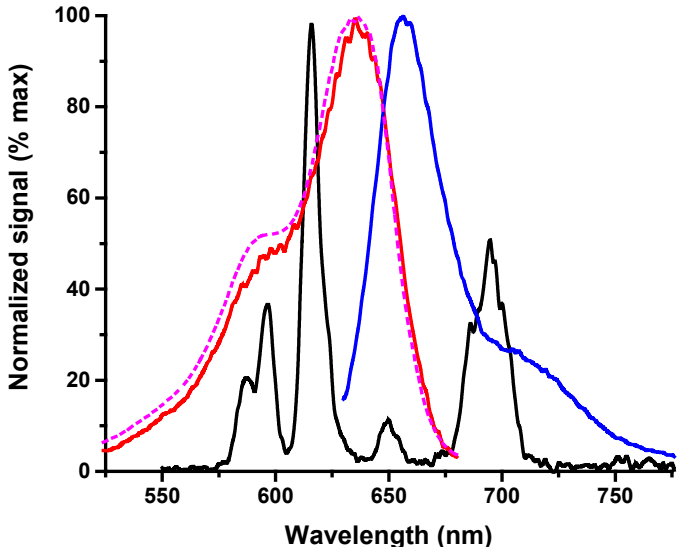

Figure 14. HIDC effectively absorbs the Eu-probe emission. The emission spectrum of the Eu-probe (black) and HIDC excitation (red), emission (blue), and absorbance (magenta, dashed line) spectra were monitored, and the results demonstrate that the Eu-probe emission maximum overlaps with HIDC excitation and absorbance wavelengths. Thus, HIDC effectively quenches the Eu-probe emission.

5.2 Proof-of-concept protein thermal stability and PLI studies

To demonstrate the functionality and principle of the Protein-Probe technique, the method was first applied to monitoring the thermal denaturation of individual proteins in a similar fashion to commonly used external dyes such as SYPRO Orange and ANS. The Protein-Probe produces low TRL signal when the proteins are in their native form, denaturation is observed as a signal increase, and the melting curve eventually saturates when the protein is fully denatured. The T_m of the protein can

be determined using a sigmoidal fit, and the obtained value provides information on the thermal stability of the protein.[180,227] In addition to the thermal profiling of individual proteins, the Protein-Probe method was applied to studying PLIs in thermal shift measurements. PLIs can affect the protein stability and cause a shift in the T_m, so they may be detected by comparing the melting temperatures of the individual proteins and the complexes (Fig. 15).[183]

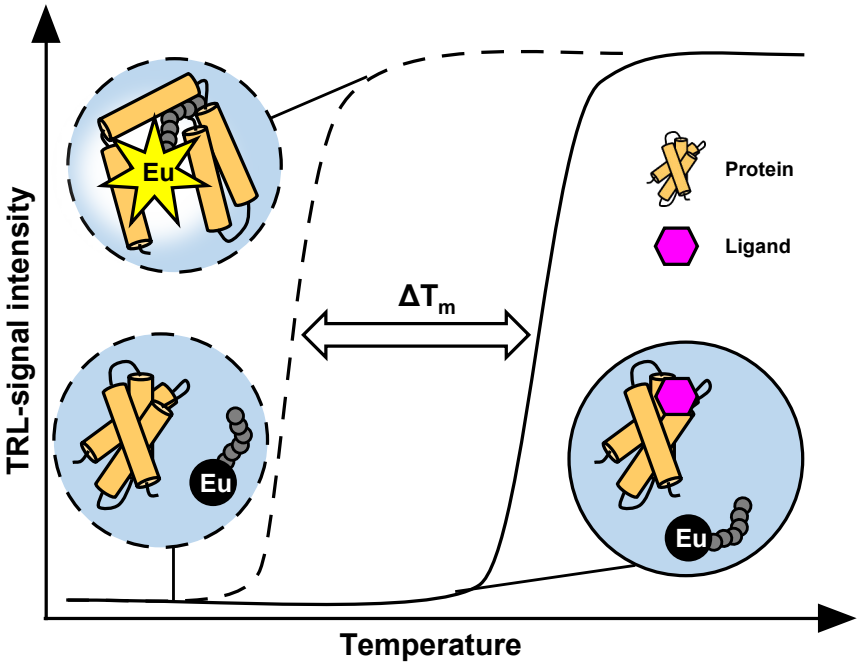

Figure 15. The principle of the Protein-Probe method for monitoring protein thermal denaturation and PLIs. The Eu-probe does not bind significantly to individual, native proteins, and the free Eu-probe produces low TRL signal in the modulation solution. Binding to the inner hydrophobic regions of denatured proteins protects the Eu-probe from the quenching effect, and protein thermal curves can be monitored. Proteins have their characteristic melting temperatures (dashed line), which may be affected by ligand binding (solid line). Thus, PLIs can be detected as shifts in the melting temperature.

The Protein-Probe method was optimized in denaturation experiments with individual proteins. The pH of the modulation solution was tested from 2 to 10 without and with IgG_1 mAb (80 nM). The optimum pH for the method sensitivity was found to be 4, based on the S/B (heat-denatured/native mAb) and signal stability over time. (**I**) Thus, all the following tests were performed in modulation solution buffered to pH 4. Triton X-100 was also found to improve the S/B of the method and was therefore included in the modulation solution base buffer. The sensitivity of the Protein-Probe method evaluated by comparing it to SYPRO Orange, which is a popular external dye in thermal stability experiments. The Protein-Probe was found

to have 30- to 100-fold higher sensitivity than SYPRO Orange, when fully denatured IgG_1 mAb (**I**), KRAS (**II**), and trastuzumab (**III**) were titrated. This high sensitivity makes it possible to use nanomolar protein concentrations in the Protein-Probe assays. The T_m values obtained with the Protein-Probe were also found to be in a good agreement with those measured with SYPRO Orange, as demonstrated with, e.g., IgG_1 mAb (**I**) and trastuzumab (**III**).

Next, the complete thermal curves and T_m values of several individual proteins were measured with the Protein-Probe. For malate dehydrogenase, CA, and SA, the calculated respective T_m values of 44.6 ± 0.5, 67.9 ± 0.9, and 75.7 ± 0.1 °C were comparable to the literature values.[228–230] (**I**) The T_m values measured for 2 μM PDCD4 using the Protein-Probe (59.7 ± 0.1 °C) and SYPRO Orange (60.0 ± 0.3 °C) were in good agreement. The thermal curves of eIF4A were measured in 150 nM with the Protein-Probe and in 2 μM with SYPRO Orange, and the resulting T_m values were 54.5 ± 0.1 °C and 50.3 ± 0.1 °C, respectively. (**II**) The minor difference in these values may be related to the use of different protein concentrations in the assays. Analyzing 26 different mAbs yielded melting curves and characteristic T_m values for all of them. The T_m values of mAb1-mAb3 were monitored from two separate batches, and the batch-to-batch variation was found to be insignificant, indicating good reproducibility of the Protein-Probe measurements (Fig. 16A). (**III**)

The Protein-Probe was also applied to measuring the thermal profiles of WT and mutant KRAS to see if stability differences could be detected. (**IV**) The melting curves of WT KRAS and five mutants were observed with the Protein-Probe, and mutants G13D (T_m 47.7 ± 0.4 °C) and Q61R (T_m 66.5 ± 0.5 °C) had a clearly different thermal stability compared to WT KRAS (T_m 60.1 ± 0.3 °C). This was likely due to the differences in their intrinsic nucleotide exchange activity, which is known to affect GTPase stability; G13D has a rapid nucleotide exchange rate, whereas Q61-mutants has a very low activity.[231,232]

Mg^{2+} maintains the stable, nucleotide-bound form of KRAS, so the effect of removing Mg^{2+} from the buffer was studied in Protein-Probe assays with G13D and Q61R KRAS. (**IV**) G13D was destabilized equally by removing the Mg^{2+} and adding 1 mM EDTA (T_m values 43.4 ± 0.6 and 43.6 ± 0.8 °C, respectively), whereas Q61R yielded T_m values of 59.2 ± 0.7 °C without Mg^{2+} and 50.6 ± 1.0 °C with 1 mM EDTA (Fig. 16B). The large T_m difference can be explained by the low nucleotide exchange activity of Q61R, as EDTA is required to bring this mutant to a fully nucleotide-free state. It was also observed that adding 10 μM GDP stabilized the G13D mutant greatly (ΔT_m >10 °C) and had a moderate stabilizing effect on the WT KRAS but did not affect the T_m of KRAS Q61R. Similar results were obtained with GTP, whereas ATP had no effect on the KRAS stability. (**IV**) Different GTP-analogs were shown to stabilize KRAS to different extents. (**IV**) These results further corroborate the observation that the stabilization of KRAS is related to nucleotide binding, and

altogether the findings demonstrate that the Protein-Probe method is useful for monitoring protein stability changes caused by the buffer composition.

Interestingly, it was observed that the protein concentration affects the T_m values observed with the Protein-Probe. For example, trastuzumab produced T_m values of 76.3 ± 0.6 and 81.0 ± 0.2 °C when measured in 2000 and 80 nM concentrations, respectively (**III**), and the T_m values obtained for 50 nM KRAS (WT, Q61R, Q61L) were 8.4–11.8 °C higher than those observed with 1250 nM samples. (**IV**) This might be due to the sensitivity of the Protein-Probe method: 10 % denaturation, for example, produces a higher number of denatured protein molecules at a micromolar concentration than it does at nanomolar protein amounts. Therefore, detectable signal (and, thus, a melting curve) may be obtained earlier when the protein concentration is high. This means that the T_m values obtained with the Protein-Probe at low concentrations may not always precisely match with those determined by reference methods requiring more protein. Nevertheless, the results obtained with the individual proteins demonstrate that the Protein-Probe method can be applied to measuring the thermal denaturation and melting temperature of a wide variety of proteins, which provides the basis for the technique.

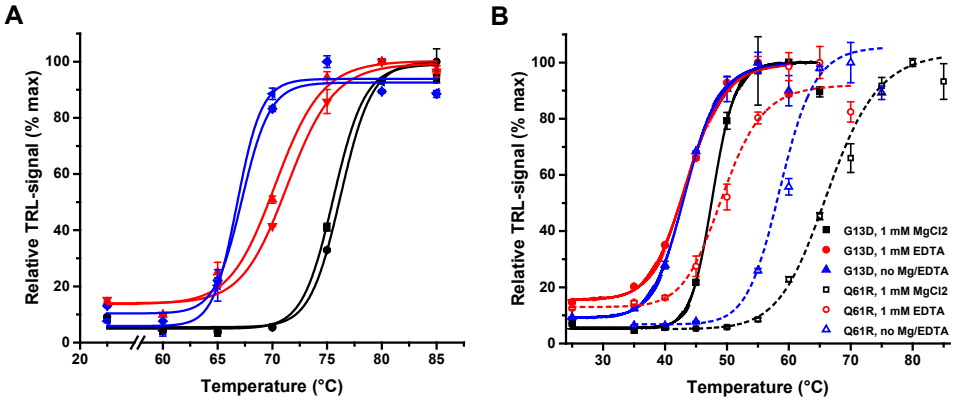

Figure 16. The Protein-Probe can be used to monitor protein thermal stability. **A.** The thermal curves of three mAbs were monitored using two batches from each mAb. There was little difference between the batches, but a characteristic T_m was observed for all three mAbs (mAb1, red; mAb2, black; mAb3, blue). **B.** The buffer composition affected the stability of KRAS mutants G13D and Q61R. Removing Mg^{2+} from the buffer destabilized KRAS, as Mg^{2+} promotes maintaining the nucleotide-bound stable form of the protein. The extent of the destabilization depended on the intrinsic nucleotide activity of the protein, and achieving the nucleotide-free state with the less-active mutant Q61R required EDTA in the buffer. Data represent mean ± SD (n=3)

In the next phase, the Protein-Probe suitability for studying PLIs in TSA format was evaluated. Combining 200 nM CA with AZA at 70 °C and 400 nM SA with biotin at 95 °C in a Protein-Probe assay yielded EC_{50} values of 248 and 597 nM, respectively. Based on these results, saturating ligand concentrations (5 µM AZA

and 10 µM biotin) were monitored with CA and SA in a thermal ramping assay. (**I**) A thermal shift was observed with both proteins when the ligands were present (Fig. 17A). For CA, the ΔT_m was 2.1 °C, which is in accordance with literature values.[229] For SA, the precise ΔT_m could not be determined due to instrumental limitations, as the T_m of the SA-biotin complex is higher than 100 °C.[230] In the Protein-Probe assay, at ΔT_m of over 15 °C was observed.

The Protein-Probe was also applied to studying the interactions of KRAS mutant G12C and small molecular inhibitors. (**IV**) Many promising KRAS G12C inhibitors have been developed, including ARS853, ARS1620, AMG-510, and MRTX849.[56,233–235] Out of these four inhibitors, AMG-510 and MRTX849 have the highest affinities to KRAS G12C, and their IC_{50} values were determined to be 20.7 ± 1.2 and 6.9 ± 0.8 nM, respectively. The interaction of KRAS G12C and 100 nM AMG-510 or MRTX849 resulted in clear thermal shifts in Protein-Probe assays, with thermal shifts of 24.8 and 15.6 °C, respectively (Fig. 17B). The interactions of KRAS G12C and ARS853 or ARS1620 were also detected as a T_m shift with the Protein-Probe, with maximum stabilization achieved with 5 µM inhibitors. The Protein-Probe results were confirmed to be accurate by monitoring the binding and thermal shift with the reference methods, SYPRO Orange and ANS. It was somewhat difficult to confirm the binding of AMG-510 and MRTX849, as especially AMG-510 reduced the obtained luminescence signals at the selected micromolar

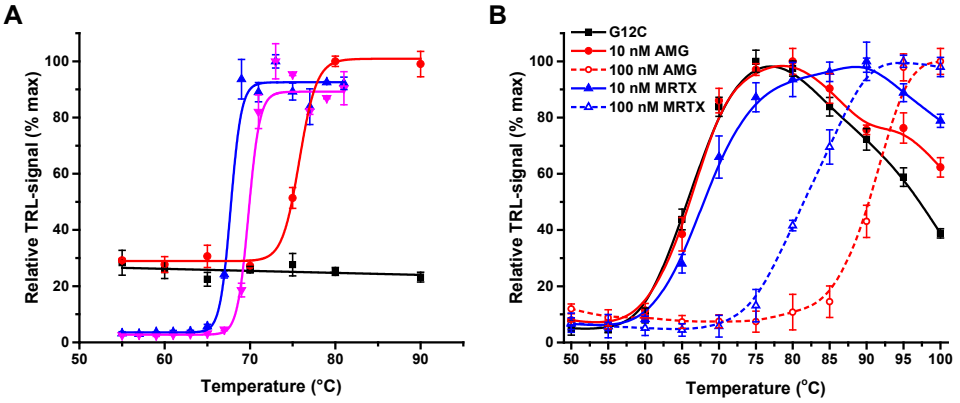

Figure 17. The Protein-Probe enables monitoring PLIs based on a T_m shift. **A.** The thermal profiles of 200 nM CA and 400 nM SA were monitored with their ligands (5 µM AZA and 10 µM biotin, respectively). In both cases, a thermal shift was observed, indicating binding. With CA, a thermal shift of 2.1 °C was detected. With SA and biotin, the ΔT_m was over 15 °C. **B.** KRAS mutant G12C (50 nM) was monitored with two covalently binding inhibitors, AMG-510 and MRTX849 (10 or 100 nM). The 10 nM concentration was insufficient to cause a major T_m shift, but the interaction with 100 nM AMG-510 and MRTX849 increased the T_m of KRAS G12C by 24.8 and 15.6 °C, respectively. Data represent mean ± SD (n=3)

concentrations. High AMG-510 and MRTX849 concentrations also affected the Protein-Probe method, but because the improved sensitivity of the method allowed the use of nanomolar inhibitor, this was not an issue. Based on the results of the PLI experiments, the Protein-Probe is suitable for monitoring the interaction between proteins and small molecular ligands, as observed from changes in the T_m.

5.3 PPI studies

The Protein-Probe was applied to monitoring PPIs in thermal ramping experiments, utilizing the same T_m-shift principle as with PLIs (Fig. 15). WT KRAS was studied with an artificial binder molecule, DARPin K27, which is known to be specific to the inactive GDP-bound form of KRAS. (**II**) First, it was determined that the K27 affinity for GDP-KRAS was lower than 50 nM, and that K27 did not significantly bind to KRAS loaded with GMPPNP. GMPPNP, which is a GTP analog, was used owing to its better stability compared to GTP. When monitored with the Protein-Probe in thermal ramping, GDP-KRAS and GMPPNP-KRAS produced thermal curves with and without K27, whereas no clear thermal curve was measured for individual K27. This was not unexpected, as DARPins are known to have high thermal stability, with melting temperatures exceeding 100 °C.[236,237] The interaction between GDP-KRAS and K27 was clearly detectable from a thermal shift of 8.7 °C. With GMPPNP-KRAS, the addition of K27 led to an insignificant thermal shift, indicating no interaction (Fig. 18A).

Interestingly, two other DARPins, K13 and K19, blocked KRAS nucleotide exchange in QRET assays with IC_{50} values of 177 ± 5.2 and 164 ± 1.6 nM, respectively, but did not affect the T_m of KRAS when monitored with the Protein-Probe. (**IV**) However, it was hypothesized that the interaction between KRAS and K13 or K19 could be detected in a competitive TSA format, as the binding area of K13 and K19 overlaps with the binding site of covalent KRAS G12C inhibitors. Thus, complex formation with K13 or K19 was expected to decrease the substantial stabilizing effect of covalent inhibitors such as AMG-510 and MRTX849 (Fig. 18B). In thermal ramping assays, K13 completely blocked the stabilization by 100 nM AMG-510 and reduced the stabilizing effect of 300 and 900 nM inhibitor (Fig. 17B). Similar results were obtained with MRTX849, ARS853, and ARS1620. (**IV**) This demonstrates that the competitive approach enables the monitoring of PPIs based on thermal profiles, even when the interaction does not induce a thermal shift.

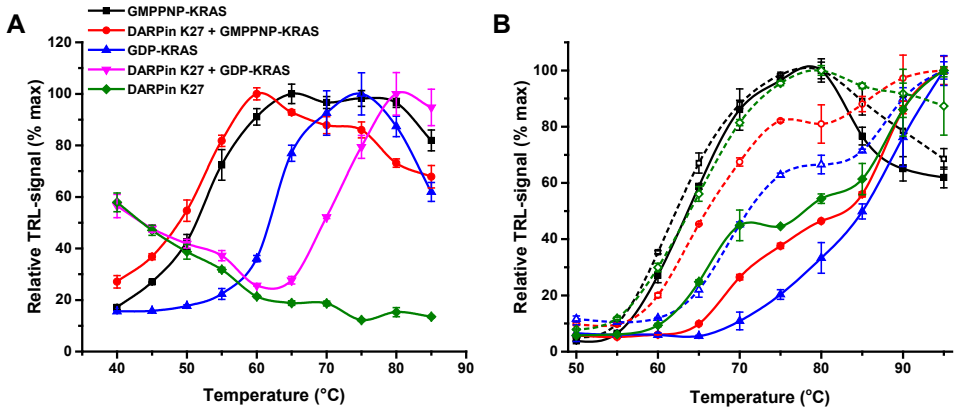

Figure 18. PPIs were observed with the Protein-Probe based on changes in the T_m. **A.** When 100 nM DARPin K27 was monitored with 50 nM GDP-KRAS, the 8.7 °C thermal shift indicated that selective binding took place. For 50 nM GMPPNP-KRAS the ΔT_m was negligible, as the DARPin did not bind this form. **B.** KRAS G12C (50 nM, black) was measured with AMG-510 (100 nM, green; 300 nM, red, 900 nM, blue) without (solid lines) and with (dashed lines) 50 nM DARPin K13. The complex formation between KRAS G12C and K13 did not affect the KRAS T_m. However, K13 did block the KRAS G12C/AMG-510 interaction, making it possible to detect K13 binding based on the thermal profile. Data represent mean ± SD (n=3)

Other protein pairs were found that also did not produce a T_m shift as a result of interaction. For example, the binding of eIF4A and its modulators, eIF4H and PDCD4 did not yield clear changes in the T_m values. (**II**) In this case, a different approach was taken from the competitive TSA. After confirming in FRET assays that the activity of eIF4A was induced by eIF4H and inhibited by PDCD4, the interactions were studied in thermal ramping with the Protein-Probe by combining 75 nM eIF4A with 0.5 and 1 µM eIF4H (Fig. 19A) and 75–300 nM PDCD4 (Fig. 19B). The individual proteins produced only low to moderate TRL signal, but the complexes gave clear thermal curves. Both protein pairs produced the highest S/B ratios at 65 °C regardless of the concentrations, when the TRL signal of the complex was compared to individual PDCD4 or eIF4H. The maximum S/B values obtained this way were between 4.0 and 10.5. Combining the non-interacting proteins PDCD4 and eIF4H did not lead to a signal increase at any temperature. These results demonstrate that it is possible to monitor PPI pair formation also by comparing the TRL signals of the complex and individual proteins at elevated temperatures.

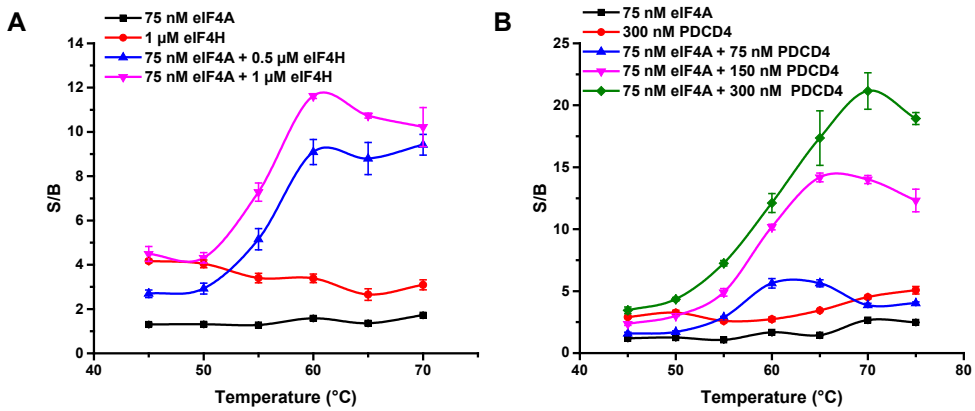

Figure 19. PPIs were observed based on TRL signal increase at elevated temperatures. **A.** The interaction of 75 nM eIF4A and 0.5 or 1 µM eIF4H was observed in thermal ramping. The individual proteins produced only low to moderate TRL signal at all temperatures. When eIF4A and eIF4H were combined, clear thermal curves were detected. Thus, the binding can be monitored based on the elevated signal at high temperatures. **B.** The interaction between 75 nM eIF4A and 75–300 nM PDCD4 was also observed based on the signal increase at elevated temperatures. Especially 150 and 300 nM PDCD4 yielded a high signal in combination with eIF4A in thermal ramping. Data represent the S/B ratio compared to buffer (mean ± SD, n=3).

Next, multiprotein complexes were studied using bio-BSA/SA and CRP/anti-CRP mAb interactions as models. (**II**) In both cases, large complexes are formed: SA has four binding sites for biotin, and CRP has five binding sites for the mAbs. As more than one biotin is conjugated to the BSA and antibodies have two antigen binding sites, the formation of large protein networks is also possible. We hypothesized that the Protein-Probe could be applied to sensing the structural changes upon complex formation also at RT, due to the large size of multiprotein complexes (Fig. 20). However, complex formation at RT leads to less dramatic changes than the complete denaturation of proteins, so it was assumed that relatively high protein concentrations would be required to provide enough binding surfaces for the Eu-probe.

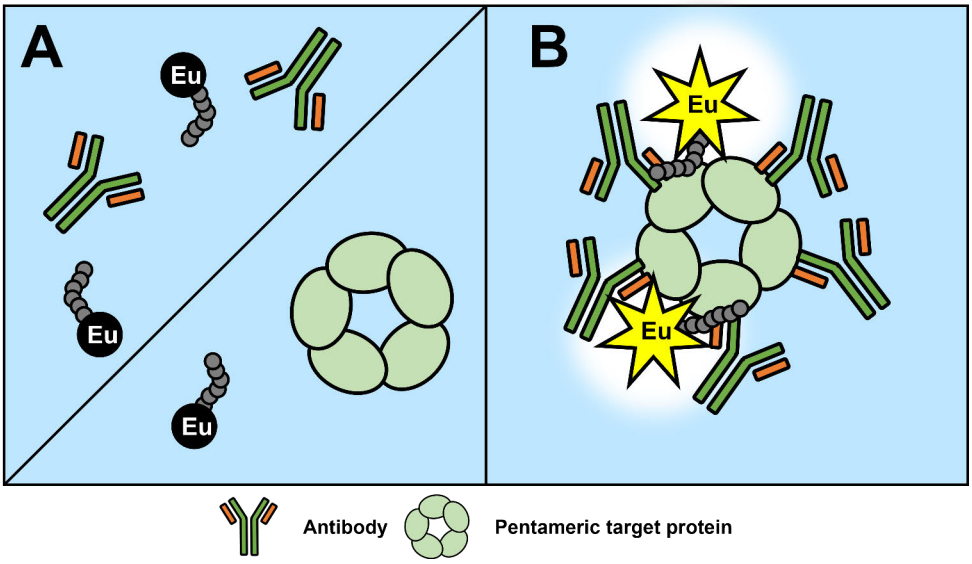

Figure 20. Measuring PPIs of large complexes with the Protein-Probe at RT. **A.** The Protein-Probe does not bind significantly to the individual proteins, leading to TRL signal quenching in the modulation solution. **B.** The formation of large protein complexes leads to structural modifications and an increase in the protein surface area, which enable Eu-probe binding. Thus, a high TRL signal is observed after complex formation.

SA and biotin bind with femtomolar affinity, which makes the interaction effectively irreversible.[238] Therefore, bio-BSA/SA was a suitable proof-of-concept pair for the first tests. (**II**) Titrating 20 nM bio-BSA with 0–600 nM SA and monitoring the interaction with the Protein-Probe led to elevated TRL signals at increasing SA concentrations. Similar titration using SA and non-biotinylated BSA did not produce a signal increase. When the interaction between 200 nM SA and 20 nM bio-BSA was blocked with 0–10 µM biotin, the S/B ratio of the reactions with 0 and 10 µM biotin was 34, and an IC_{50} value of 306 ± 4 nM was observed. This indicated that free biotin blocks the interaction and confirmed that the observed high TRL signal resulted from the formation of the bio-BSA/SA complex.

The interaction between the second large protein complex model, CRP and anti-CRP mAb, also had a very high, picomolar affinity.[239] CRP (0–100 nM) was combined with three mAbs (0–500 nM): a specific anti-CRP mAb and two non-specific control mAbs. (**II**) The binding of CRP and the anti-CRP mAb was observed as elevated TRL signals at the RT measurement, similarly to bio-BSA and SA. The maximum S/B ratio was 4.3, as calculated by comparing the signal of the mAb/CRP complex to that of the individual mAb (Fig. 21A). This ratio was achieved with 100 nM anti-CRP mAb and 20 nM CRP. At the higher mAb concentrations, the S/B values decreased because the TRL signal of the individual mAb increased. The highest S/B ratios across all the concentrations were achieved when the mAb:CRP

ratio was 5:1, which was expected based on the pentameric structure of CRP. When CRP was combined with the non-specific mAbs, no significant S/B increases were observed, confirming that only specific interactions were monitored (Fig. 21B).

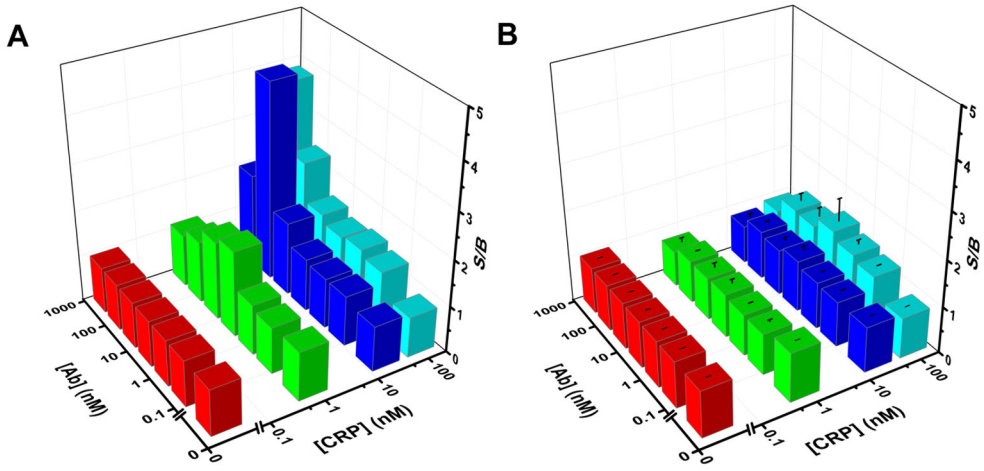

Figure 21. The interaction of CRP and mAbs was monitored at RT using the Protein-Probe. **A.** An increased S/B ratio was observed upon combining 0–100 nM CRP with 0–500 nM anti-CRP mAb. The highest S/B value within each mAb concentration was obtained at mAb:CRP ratio of 5:1. The maximum S/B ratio was produced by 100 nM mAb in complex with 20 nM CRP. **B.** When CRP was combined with two non-specific, non-interacting mAbs, the increase in the S/B ratio was negligible, which demonstrates the specificity of the method. The S/B ratios of the two non-specific mAbs, presented here as averages with error bars, were highly similar. Data are presented as S/B ratios (mAb/CRP complex vs. individual mAb average TRL signals) (n=3).

The CRP/anti-CRP mAb interactions were also monitored in thermal ramping with the Protein-Probe, but clear T_m changes were not detected. (**II**) Thus, the complex was tested using a similar assay format as with eIF4A by combining low concentrations (0–10 nM) of CRP and mAbs at elevated temperatures. At these concentrations, individual CRP was undetectable at all temperatures, and the individual mAbs produced low to moderate TRL signal. At 90 °C, the CRP/anti-CRP mAb combination produced up to 7-fold higher specific signal compared to a non-specific control mAb with CRP. Thus, increasing the assay temperature may enable monitoring multiprotein complexes with the Protein-Probe with improved sensitivity and less sample materials.

5.4 Aggregation studies

As it was demonstrated that the Protein-Probe can be applied to monitoring large protein complexes, we turned our attention to another PPI type: aggregation. One theory is that protein aggregation is often mediated by the hydrophobic core areas of proteins binding together, which leads to the formation of large, disordered clumps of protein.[240] Because the Eu-probe binds to hydrophobic areas, we hypothesized that the Protein-Probe method could also be used for detecting protein aggregation (Fig. 22). All aggregation studies were performed in Publication **III**.

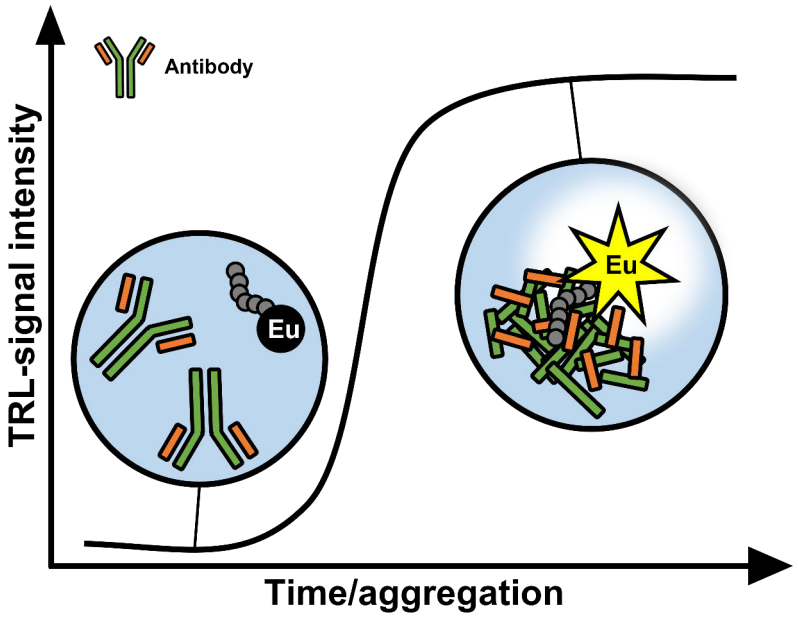

Figure 22. Aggregation monitoring with the Protein-Probe. Proteins such as mAbs have a tendency to aggregate over time. The Protein-Probe does not interact significantly with the native, monomeric mAbs, but aggregation compromises the mAb structure and exposes the hydrophobic core areas for Eu-probe binding. The protection from the modulation solution leads to a high TRL signal, and thus protein aggregation can be detected with the Protein-Probe.

Aggregation can cause problems with protein-based drugs, including therapeutic mAbs. The aggregation of a drug can endanger patient safety due to increased immunogenicity and reduce the efficacy of the drug molecule as a result of losing the binding activity, so it is important to carefully monitor the stability and integrity of therapeutic proteins.[241] Trastuzumab, a therapeutic mAb commonly used in breast cancer treatment, and several murine mAbs were studied to demonstrate the Protein-Probe suitability for detecting protein aggregation. First, the mAbs were intentionally aggregated and the aggregation was monitored as a function of time

and concentration. The Protein-Probe was then applied to monitoring mAb aggregation under thermal stress and in different storage buffer compositions.

The Protein-Probe sensitivity to aggregation was compared to two reference methods, SYPRO Orange and UV250, which are both suitable for monitoring protein aggregation.[242,243] Trastuzumab (32 µM) was stored at 60 °C for 13 days, and several samples were taken during this time to be analyzed in 2 µM with all three methods. The detection limits, calculated as S/B = 3 compared to intact trastuzumab, were 18 h, 123 h, and 205 h for the Protein-Probe, SYPRO Orange, and UV250, respectively (Fig. 23A). The Protein-Probe achieved an analytical limit of detection of only 1.2 h when calculated using 3*SD of the intact trastuzumab. The early detection limit implies that the Protein-Probe method could be suitable for detecting very early aggregation, potentially even at the nucleation phase. The sensitivity of the Protein-Probe method was further studied by performing a percentual aggregation titration. Intact trastuzumab and two other mAbs were titrated with 0–10 % heat-aggregated mAb, keeping the total concentration at 6 µM. The Protein-Probe detected aggregation below 0.1 %, and a linear range of 0.04–3.3 % was achieved with all three mAbs (Fig. 23B).

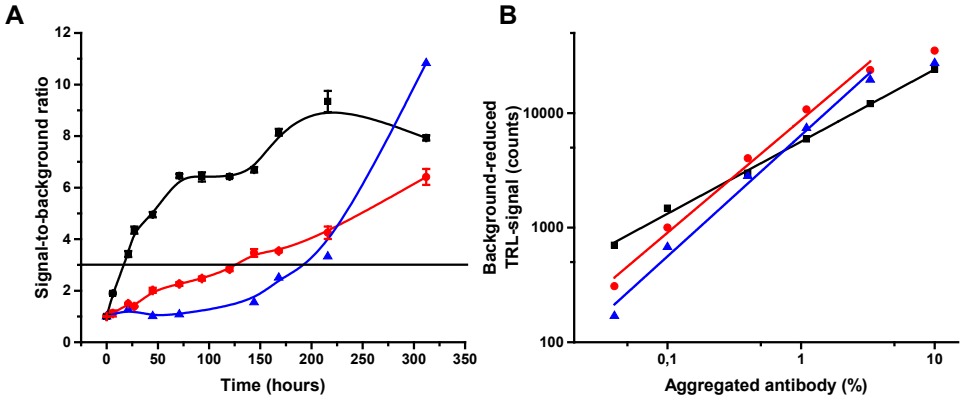

Figure 23. The Protein-Probe enabled early and sensitive detection of mAb aggregation. **A.** Aggregation was monitored as a function of time with the Protein-Probe (black), SYPRO Orange (red), and UV250 (blue). Trastuzumab (32 µM) was stored at 60 °C for 13 days, and the aggregation was monitored at various time points from 2 µM samples. The detection limits (S/B = 3, horizontal line) for the Protein-Probe, SYPRO Orange, and UV250 were 18, 123, and 205 h, respectively. Data are presented as the S/B ratio of trastuzumab stored at 60 °C and intact trastuzumab stored at 4 °C (mean ± SD, n=3). **B.** The Protein-Probe sensitivity to aggregation was tested by titrating intact mAbs with their aggregated counterparts. Trastuzumab (red), mAb2 (black), and mAb4 (blue) were monitored in 6 µM with 0–10 % aggregated mAb. Aggregation below 0.1 % was monitored with the Protein-Probe for all mAbs. Data are presented as background (monomeric mAb) reduced average signals (sample n=3, background n=6).

Next, six mAbs (30–34 µM) with melting temperatures from 60.4 ± 0.3 to 82.7 ± 0.2 °C were stored for three weeks at -20, 4, 35, or 45 °C, and the aggregation was subsequently monitored in 80 nM concentration using the Protein-Probe. Out of these six mAbs, two were aggregated at all storage temperatures, as indicated by the high S/B ratios compared to buffer. Usually, mAbs are stable at -20 and 4 °C for several months, but in this case these results were not unexpected, as we purposely included mAbs that were already in poor condition before the experiment. Two mAbs yielded low S/B ratios regardless of the storage temperature, i.e., had a low aggregation tendency. The remaining two mAbs gave high S/B ratios only after storage at 45 °C, seemingly being susceptible to aggregation only at an elevated temperature (Fig. 24A). The results obtained with the Protein-Probe were also confirmed with PAGE using mAb4 and mAb10. Fully aggregated mAbs, which produced very high TRL signal with the Protein-Probe, were not able to enter the gel, whereas intact mAbs produced low TRL signal and clear PAGE bands. Partial aggregation resulted in both a band on the gel and accumulation at the edge of the loading well, as well as moderate TRL signal levels.

Monitoring the melting curves of the six thermally stressed mAbs (80 nM) with the Protein-Probe revealed that partial aggregation did not affect the T_m of the mAbs. Total aggregation, on the other hand, made it impossible to obtain the T_m value, because the TRL signal was already saturated at RT. It was also observed that the T_m values of the mAbs did not directly predict their tendency to aggregate. For example, mAb5 only aggregated at 45 °C and had a T_m of 60.4 ± 0.3 °C, whereas mAb6 aggregated at all temperatures and had a T_m of 68.8 ± 0.4 °C. Thus, there seemed to be no evident link between protein thermal stability and aggregation.

In the next step, storage buffer formulation tests were performed. Buffer composition is a major aspect in maintaining mAb stability during extended storage, and therefore it is of high importance to determine the optimal storage buffer. In our study, trastuzumab, mAb1, and mAb11 (6 µM) were stored for four days in 15 different buffers (Table 3). PBS was chosen as the reference buffer, as it is an often-used—if not ideal—buffer for the long-term storage of commercial mAbs. In addition, mAb12-mAb17 (two IgG_1, two IgG_{2a}, and two chimeric mAbs) were stored in buffers 9–13. All mAbs were kept at 45 °C to accelerate the aggregation, except trastuzumab, which has a higher thermal stability. To ensure that changes would be observed within the same incubation period as with the other mAbs, 65 °C was chosen for trastuzumab incubation.

When buffers with pH 4–8 were tested, trastuzumab aggregation was reduced with increasing pH, and the lowest amount of aggregation was achieved in the pH 8 buffer. This was slightly surprising, as a more acidic pH was expected to be more suitable based on the isoelectric point of trastuzumab (~8.7).[244] mAb1 and mAb11 were the most stable at pH 7, but less aggregation was observed at pH 4 compared

to pH 5 (Fig. 24B). However, the same tendency was not detected with the other tested mAbs. With mAb12-mAb17, the minimum amount of aggregation was achieved at pH 6 or 7, further demonstrating that near-neutral pH is optimal for storage. Thus, pH 7 phosphate-citrate + 0.9 % (w/v) NaCl was chosen as the base buffer for excipient testing.

The storage buffers of protein drugs often contain additives that improve the stability of the product. In this study, we chose to test pH 7 phosphate-citrate buffer supplemented with a detergent (0.02–0.4 % (v/v) polysorbate-20), a disaccharide (50–500 mM sucrose), and a polyol (30–300 mM sorbitol), which are all used as excipients in mAb storage solutions.[245] Polysorbate-20 had no effect on trastuzumab stability but increased the aggregation of mAb1 and mAb11 compared to the pH 7 phosphate-citrate buffer. Sucrose and sorbitol, on the other hand, improved the stability of all three mAbs, especially at high concentrations. The lowest level of aggregation was monitored when the mAbs were stored in the buffer containing 300 mM sorbitol, implying that this was the optimal buffer composition out of the tested excipients (Fig. 24B).

The buffers were prepared according to the specifications of a commercial partner, and the chosen compositions are not very widely used for formulation testing. Therefore, the results obtained in this study concerning the aggregation propensity of these mAbs may not be widely applicable to mAb manufacturing. However, the goal of establishing the Protein-Probe as a suitable method for aggregation studies, in addition to monitoring PPIs between two different proteins, was achieved with this model setting.

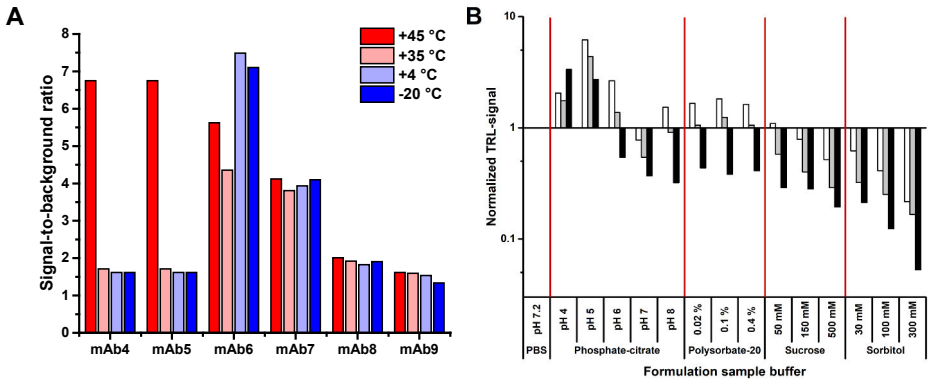

Figure 24. mAb aggregation caused by non-optimal storage conditions was monitored with the Protein-Probe. **A.** Six mAbs (32–24 µM) were stored at -20, 4, 35, and 45 °C for three weeks, then monitored with the Protein-Probe in 80 nM. Clear differences were observed in their inherent stabilities, with some mAbs aggregating under all storage temperatures and others appearing resistant to aggregation even at elevated temperatures. Data represent S/B ratios compared to buffer, calculated from average TRL signals (n=2). **B.** mAb1 (white), mAb11 (grey), and trastuzumab (black) (6 µM) were stored in 15 formulation buffers for 4 days at an elevated temperature, then monitored with the Protein-Probe after 1/10 dilution. PBS-normalized values >1 indicate increased aggregation compared to storage in PBS, and values <1 indicate increased stability. The lowest level of aggregation was monitored in near-neutral pH, and out of the tested excipients, 300 nM sorbitol had the most prominent stabilizing effect on all mAbs. Data represent PBS-normalized mean values (n=4).

6 Summary and Conclusions

Proteins make life possible, and their normal function is enabled by PPIs. PPIs are an important target in both fundamental research, such as studying the normal function of the cell, and in applied research, such as in screening for new drug compounds to treat different diseases. A wide variety of methods exists for studying, analyzing, and screening PPIs. However, techniques that provide high sensitivity without the requirement of conjugating the interacting proteins to label molecules or solid surfaces are still lacking.

In this doctoral study a novel, solution-based, label-free method was developed and applied to monitoring protein stability and interactions. The Protein-Probe method is based on a Eu-chelate-labeled sensing peptide, called the Eu-probe. The Eu-probe does not bind significantly to low concentrations of native, individual proteins, in which case a low TRL signal is observed due to the quenching effects of the modulation solution. Binding to denatured or aggregated proteins protects the Eu-probe from the quenching and results in a high TRL signal.

The Protein-Probe method was introduced in Publication **I**, where it was used to monitor the melting curves of several individual proteins. CA and SA were also studied with their ligands, and ligand binding was successfully monitored based on thermal stability changes. The Protein-Probe was able to monitor proteins at low nanomolar concentrations, unlike the established TSA methods, such as SYPRO Orange or ANS. This reduced the sample consumption and the risk of sample aggregation.

In Publication **II**, the Protein-Probe was applied to studying PPIs. The interaction of KRAS and an artificial binder molecule, DARPin K27, was successfully monitored based on the T_m shift. It was also demonstrated that the interaction may be monitored based on the high TRL signal produced by the protein complex but not the individual proteins. This was shown with eIF4A and two of its binding partners, eIF4H and PDCD4. The same principle was also demonstrated to be functional for detecting large protein complexes: CRP/anti-CRP mAb and SA/bio-BSA. The capability to measure PPIs independently of a thermal shift makes the Protein-Probe a versatile method.

The Protein-Probe technique was used to monitor mAb aggregation in Publication **III**. The Protein-Probe was proven to detect aggregation significantly earlier than the SYPRO Orange and UV250 reference methods. Clear differences were observed in the aggregation tendencies of several heat-stressed mAb samples, and the effects of pH and excipients on aggregation were studied in a storage buffer formulation test. Although the Protein-Probe is, unlike some traditional aggregation detection methods, not yet capable of determining the size of the aggregates, it still provides a sensitive, high-throughput alternative for methods such as rotationally sensitive dyes and DLS.

In publication **IV**, the TSA concept and factors affecting the results were evaluated by studying KRAS with the Protein-Probe and other TSA methods. The buffer composition and sample protein concentration were demonstrated to affect protein thermal stability. The results show that comparison between T_m values obtained from different TSA studies is difficult, even when using the same method, and close attention must be paid to the assay details. The binding of KRAS mutant G12C and several covalent inhibitors was also successfully monitored with the Protein-Probe. The ability to use low inhibitor concentrations made it possible to avoid the inhibitor-induced signal loss observed with the reference methods. PPIs between KRAS and DARPins were monitored both in conventional thermal shift measurements and in a competitive TSA format, which demonstrated yet another assay design in which the Protein-Probe can be utilized.

In conclusion, the developed Protein-Probe method fills the niche for a sensitive, label-free method for protein stability and interaction studies. The method has nanomolar sensitivity, an improvement over the micromolar concentration requirements of several currently available solution-based methods. The Protein-Probe technique can be easily applied to monitor a wide variety of proteins and interaction types with only minimal modifications to the assay protocol or buffers. Samples can be considerably diluted, so the components of protein storage buffers do not easily interfere with measurements. The homogeneous, easy-to-use format and compatibility with microtiter plates of several sizes mean that the Protein-Probe method has great potential for HTS.

The Protein-Probe requires a modulation solution with low pH to function, because protonation of the carboxylic groups is required with the current peptide structure of the Eu-probe. Unfortunately, low pH might affect the studied proteins by opening the structure and may even denature sensitive proteins. In addition, although the Protein-Probe method is versatile, the probe structure may lead to bias for certain interaction types while missing others. In assays performed at RT, a signal increase is not obtained if the interaction does not lead to at least partial unfolding, i.e., reveal enough hydrophobic structures. For example, the aggregation of non-unfolded, native proteins may be difficult to detect. On the other hand, proteins that

have hydrophobic amino acids on the surface can produce elevated TRL signal even before denaturation. Regarding protein stability, only issues such as aggregation or thermal instability are currently detected with the Protein-Probe method, whereas other quality concerns, such as deamidation, cannot be monitored. Developing novel peptide probe structures might make the assays functional in a more neutral pH and enable monitoring interaction types and stability issues beyond those detected with the current probe. With the current system, protein concentration and assay buffer composition can also influence the T_m values, and this must be considered when the assays are planned, and kept in mind when experimental results are compared within assays or methods.

Perhaps the most significant property of the current Protein-Probe method is that the thermal assays must be performed using a two-step protocol: first, the samples are heated, and then the Protein-Probe solution is added, as heating negatively affects the modulation solution. The two-step protocol complicates the assay, requires extra work, and increases the sample requirement. Ideally, the assay would be performed in one step, using a qPCR instrument for the detection. New modulator molecule structures might help achieve this goal, especially when combined with novel peptide probes. Furthermore, the method suitability for measuring chemical denaturation should be further investigated, as this approach would not require incubation at elevated temperatures. The method development is ongoing, and promising preliminary results have been acquired with concepts such as a one-step thermal assay protocol using a FRET approach. Thus, the work continues toward an improved assay setup for detecting PPIs in a label-free manner.

Acknowledgements

This doctoral thesis work was carried out in the Detection Technology group of the Department of Chemistry at the University of Turku during the years 2019–2021. First, I want to gratefully acknowledge the financial support for this work from the Finnish Concordia Fund and Emil Aaltonen Foundation. I would like to thank the heads of the department, Prof. Pasi Virta, Prof. Juha-Pekka Salminen, and Prof. Carita Kvarnström, for giving me the opportunity to perform my doctoral studies at the Department of Chemistry. My sincere gratitude goes also to Prof. Hanns-Christian Mahler and Prof. Kevan Shokat for providing insightful feedback on the thesis, and Prof. Ali Tavassoli for agreeing to be my opponent.

My deepest gratitude goes to my supervisors Docent Harri Härmä and Dr. Kari Kopra, who offered me invaluable support and guidance along the way and made this journey possible for me by sharing their knowledge. This thesis wouldn't exist without their ideas and insight. I would like to offer my special thanks to all my co-authors, who greatly improved the quality of my manuscripts: Prof. Martin Bushell, Prof. John Le Quesne, Prof. Andreas Plückthun, Dr. Ville Eskonen, Dr. William Gillette, Dr. Morteza Malakoutikhah, Dr. Kenneth Westover, Nazia Hassan, Jelena Jakovleva, Jonas Kapp, Taru Kariniemi, Randa Mahran, and Emmiliisa Vuorinen.

Furthermore, I'd like to specifically thank the people I've worked with in the Detection Technology lab. Morteza, thanks for the talks about life in Finland. I think I, too, learned at thing or two about Finnish grammar. Ville, despite repeatedly implying that you hate helping people you still helped me with all the questions I had, so thanks for that. Nazia and Randa, I'm glad I got to meet you both, and I wish you the best of luck on your journey. You can do it! Thank you also for all the students that chose to do some lab work with us and made it possible for me to improve my skills as an instructor. Titta, Suvituuli, Milja, and Juho, I hope your MSc projects go well. Jenni, Juuso, and Eemeli, good luck with your BSc work. Huda, it was such a pleasure to work with you, but I'm even more grateful that we became friends outside of work, too. Your motivation, kindness, and good heart will carry you wherever you want to go. An honorable mention goes out also for past office mates: Adefunke and Ashwini. Maybe I should also say: sorry for the distraction. Hopefully the chocolate made up for it.

I am also especially grateful to our technical staff: Kirsi Laaksonen, who kept us supplied with all the tubes and reagents we could hope for; Mauri Nauma, who saved our cells multiple times, and Kari Loikas, who provided us all the computers and displays that we needed (and we needed many).

I would like to thank my dear friends outside the Department of Chemistry, too. Anna-Sofia and Sanna especially for providing me with company and conversations so far removed from the lab environment that I could forget the thesis for a while. Kiitos koiralenkeistä! Maria, we've had a long road together at UTU and even before it, and in the future, we'll again be working in almost adjacent buildings. Somehow, I'm not surprised—but I am glad. I'm looking forward to our future riding trips and dog walks. Saara, you get a copy of the thesis specifically so you can show it to Hilla and assure her that even if her godmother knows nothing about children, she's ridiculously overqualified in other areas. Linda, thank you for letting me be your maid of honor—yet another thing that helped me take my mind off from the thesis crises. And Lu, I'd like to extend thanks to you and your whole family for providing us excellent food and keeping us fed also when the campus restaurants were closed. A special thanks for all the extra cashews. I want to thank Annu and Cy, too, for being such kind, encouraging people. Let's meet in person again soon! Also, I feel that the MBD -16 group deserves a mention here. I'm not particularly active in the chat, but we've had some fun times!

My thanks also go to my parents, Eino and Päivi, who most of the time had no idea what I was doing but were really encouraging anyway. The two adorable dogs they got during the time I was doing my thesis proved to be a very welcome distraction from the realities of the world. In addition, I want to thank my fiancé, Jani, who also had no idea what I was doing most of the time, but still managed to see me through my meltdowns admirably. You're able to make me laugh even on the worst days.

Lastly, I wish to extend my deep gratitude (and also maybe a little bit of blame) to my dearest labmate, Emmi. The one functioning PhD student finally evolved into two graduated ones! If it weren't for you, I probably wouldn't have started this journey. If it weren't for you, I *definitely* wouldn't have finished it.

Oh, and to anyone reading this: thanks for picking up a copy of my thesis!

And: never believe you're not enough.

22.11.2021

Salla Valtonen

References

(1) Braun, P.; Gingras, A. C. History of Protein-Protein Interactions: From Egg-White to Complex Networks. *Proteomics* **2012**, *12* (10), 1478–1498. https://doi.org/10.1002/pmic.201100563.

(2) Ivanov, A. A.; Khuri, F. R.; Fu, H. Targeting Protein-Protein Interactions as an Anticancer Strategy. *Trends Pharmacol. Sci.* **2013**, *34* (7), 393–400. https://doi.org/10.1016/j.tips.2013.04.007.

(3) Ponomarenko, E.; Poverennaya, E.; Ilgisonis, E.; Pyatnitskiy, M.; Kopylov, A.; Zgoda, V.; Lisitsa, A.; Archakov, A. The Size of the Human Proteome: The Width and Depth. *Int. J. Anal. Chem.* **2016**, *2016*. https://doi.org/10.1155/2016/7436849.

(4) Nelson, D. L.; Cox, M. M. *Lehninger Principles of Biochemistry: 6th Edition*; Macmillan Learning, 2012.

(5) Gutteridge, A.; Thornton, J. M. Understanding Nature's Catalytic Toolkit. *Trends Biochem. Sci.* **2005**, *30* (11), 622–629. https://doi.org/10.1016/j.tibs.2005.09.006.

(6) Mann, M.; Jensen, O. N. Proteomic Analysis of Post-Translational Modifications. *Nat. Biotechnol.* **2003**, *21* (3), 255–261. https://doi.org/10.1038/nbt0303-255.

(7) File:Protein structure (full).png - Wikipedia https://en.wikipedia.org/wiki/File:Protein_structure_(full).png (accessed Apr 19, 2021).

(8) Levitt, M.; Chothia, C. Structural Patterns in Globular Proteins. *Nature* **1976**, *261* (5561), 552–558. https://doi.org/10.1038/261552a0.

(9) Kaplan, D. L. Fibrous Proteins - Silk as a Model System. *Polym. Degrad. Stab.* **1998**, *59* (1–3), 25–32. https://doi.org/10.1016/s0141-3910(97)00000-1.

(10) Kang, M. K.; Tullman-Ercek, D. Engineering Expression and Function of Membrane Proteins. *Methods* **2018**, *147*, 66–72. https://doi.org/10.1016/j.ymeth.2018.04.014.

(11) Tanford, C. Protein Denaturation. *Adv. Protein Chem.* **1968**, *23* (C), 121–282. https://doi.org/10.1016/S0065-3233(08)60401-5.

(12) Daniel, R. M.; Dines, M.; Petach, H. H. The Denaturation and Degradation of Stable Enzymes at High Temperatures. *Biochem. J.* **1996**, *317* (Pt 1), 1. https://doi.org/10.1042/BJ3170001.

(13) Roberts, C. J. Therapeutic Protein Aggregation: Mechanisms, Design, and Control. *Trends Biotechnol.* **2014**, *32* (7), 372. https://doi.org/10.1016/J.TIBTECH.2014.05.005.

(14) Bemporad, F.; De Simone, A.; Chiti, F.; Dobson, C. M. Characterizing Intermolecular Interactions That Initiate Native-Like Protein Aggregation. *Biophys. J.* **2012**, *102* (11), 2595–2604. https://doi.org/10.1016/J.BPJ.2012.03.057.

(15) Ciechanover, A.; Kwon, Y. T. a. Degradation of Misfolded Proteins in Neurodegenerative Diseases: Therapeutic Targets and Strategies. *Exp. Mol. Med.* **2015**, *47* (3), e147. https://doi.org/10.1038/emm.2014.117.

(16) Tittelmeier, J.; Nachman, E.; Nussbaum-Krammer, C. Molecular Chaperones: A Double-Edged Sword in Neurodegenerative Diseases. *Front. Aging Neurosci.* **2020**, *12*. https://doi.org/10.3389/fnagi.2020.581374.

(17) Brundin, P.; Melki, R.; Kopito, R. Prion-like Transmission of Protein Aggregates in Neurodegenerative Diseases. *Nat. Rev. Mol. Cell Biol.* **2010**, *11* (4), 301–307. https://doi.org/10.1038/nrm2873.

(18) Aloy, P.; Russell, R. B. Ten Thousand Interactions for the Molecular Biologist. *Nat. Biotechnol.* **2004**, *22* (10), 1317–1321. https://doi.org/10.1038/nbt1018.
(19) Garma, L.; Mukherjee, S.; Mitra, P.; Zhang, Y. How Many Protein-Protein Interactions Types Exist in Nature? *PLoS One* **2012**, *7* (6). https://doi.org/10.1371/journal.pone.0038913.
(20) Mosca, R.; Céol, A.; Stein, A.; Olivella, R.; Aloy, P. 3did: A Catalog of Domain-Based Interactions of Known Three-Dimensional Structure. *Nucleic Acids Res.* **2014**, *42* (D1). https://doi.org/10.1093/nar/gkt887.
(21) Nooren, I. M. A.; Thornton, J. M. Diversity of Protein-Protein Interactions. *EMBO J.* **2003**, *22* (14), 3486–3492. https://doi.org/10.1093/emboj/cdg359.
(22) Avruch, J.; Khokhlatchev, A.; Kyriakis, J. M.; Luo, Z.; Tzivion, G.; Vavvas, D.; Zhang, X.-F. Ras Activation of the Raf Kinase: Tyrosine Kinase Recruitment of the MAP Kinase Cascade. *Recent Prog. Horm. Res.* **2001**, *56*, 127–155. https://doi.org/10.1210/RP.56.1.127.
(23) Molina, J. R.; Adjei, A. A. The Ras/Raf/MAPK Pathway. *J. Thorac. Oncol.* **2006**, *1* (1), 7–9. https://doi.org/10.1016/S1556-0864(15)31506-9.
(24) Wang, W.; Roberts, C. J. Protein Aggregation – Mechanisms, Detection, and Control. *Int. J. Pharm.* **2018**, *550* (1–2), 251–268. https://doi.org/10.1016/J.IJPHARM.2018.08.043.
(25) 3did - Results https://3did.irbbarcelona.org/dispatch.php?type=interaction&value1=RBD&type1=domain&value2=Ras&type2=domain (accessed Aug 18, 2021).
(26) Ofran, Y.; Rost, B. Analysing Six Types of Protein-Protein Interfaces. *J. Mol. Biol.* **2003**, *325* (2), 377–387. https://doi.org/10.1016/S0022-2836(02)01223-8.
(27) Headd, J. J.; Andrew Ban, Y. E.; Brown, P.; Edelsbrunner, H.; Vaidya, M.; Rudolph, J. Protein-Protein Interfaces: Properties, Preferences, and Projections. **2007**. https://doi.org/10.1021/pr070018.
(28) Hwang, H.; Vreven, T.; Janin, J.; Weng, Z. Protein-Protein Docking Benchmark Version 4.0. *Proteins Struct. Funct. Bioinforma.* **2010**, *78* (15), 3111–3114. https://doi.org/10.1002/prot.22830.
(29) Tran, T. H.; Chan, A. H.; Young, L. C.; Bindu, L.; Neale, C.; Messing, S.; Dharmaiah, S.; Taylor, T.; Denson, J.-P.; Esposito, D.; Nissley, D. V.; Stephen, A. G.; McCormick, F.; Simanshu, D. K. KRAS Interaction with RAF1 RAS-Binding Domain and Cysteine-Rich Domain Provides Insights into RAS-Mediated RAF Activation. *Nat. Commun. 2021 121* **2021**, *12* (1), 1–16. https://doi.org/10.1038/s41467-021-21422-x.
(30) Chakrabarti, P.; Janin, J. Dissecting Protein-Protein Recognition Sites. *Proteins Struct. Funct. Genet.* **2002**, *47* (3), 334–343. https://doi.org/10.1002/prot.10085.
(31) Liddington, R. C. Structural Basis of Protein-Protein Interactions. In *Protein-Protein Interactions: Methods and Applications: Second Edition*; Springer New York, 2015; Vol. 1278, pp 3–22. https://doi.org/10.1007/978-1-4939-2425-7_1.
(32) Bogan, A. A.; Thorn, K. S. Anatomy of Hot Spots in Protein Interfaces. *J. Mol. Biol.* **1998**, *280* (1), 1–9. https://doi.org/10.1006/jmbi.1998.1843.
(33) Talley, K.; Alexov, E. On the PH-Optimum of Activity and Stability of Proteins. *Proteins Struct. Funct. Bioinforma.* **2010**, *78* (12), n/a-n/a. https://doi.org/10.1002/prot.22786.
(34) Roberts, D.; Keeling, R.; Tracka, M.; Van Der Walle, C. F.; Uddin, S.; Warwicker, J.; Curtis, R. The Role of Electrostatics in Protein-Protein Interactions of a Monoclonal Antibody. *Mol. Pharm.* **2014**, *11* (7), 2475–2489. https://doi.org/10.1021/mp5002334.
(35) Pasquier, C.; Vazdar, M.; Forsman, J.; Jungwirth, P.; Lund, M. Anomalous Protein-Protein Interactions in Multivalent Salt Solution. *J. Phys. Chem. B* **2017**, *121* (14), 3000–3006. https://doi.org/10.1021/acs.jpcb.7b01051.
(36) Song, W. J.; Sontz, P. A.; Ambroggio, X. I.; Tezcan, F. A. Metals in Protein-Protein Interfaces. *Annu. Rev. Biophys.* **2014**, *43* (1), 409–431. https://doi.org/10.1146/annurev-biophys-051013-023038.

(37) Blanco, M. A.; Perevozchikova, T.; Martorana, V.; Manno, M.; Roberts, C. J. Protein-Protein Interactions in Dilute to Concentrated Solutions: α-Chymotrypsinogen in Acidic Conditions. *J. Phys. Chem. B* **2014**, *118* (22), 5817–5831. https://doi.org/10.1021/jp412301h.

(38) Saluja, A.; Kalonia, D. S. Nature and Consequences of Protein-Protein Interactions in High Protein Concentration Solutions. *Int. J. Pharm.* **2008**, *358* (1–2), 1–15. https://doi.org/10.1016/j.ijpharm.2008.03.041.

(39) Moor, N. A.; Lavrik, O. I. Protein–Protein Interactions in DNA Base Excision Repair. *Biochem.* **2018**, *83* (4), 411–422. https://doi.org/10.1134/S0006297918040120.

(40) Grifo, J. A.; Tahara, S. M.; Morgan, M. A.; Shatkin, A. J.; Merrick, W. C. New Initiation Factor Activity Required for Globin MRNA Translation. *J. Biol. Chem.* **1983**, *258* (9), 5804–5810. https://doi.org/10.1016/S0021-9258(20)81965-6.

(41) Jackson, R. J.; Hellen, C. U. T.; Pestova, T. V. The Mechanism of Eukaryotic Translation Initiation and Principles of Its Regulation. *Nat. Rev. Mol. Cell Biol. 2010 112* **2010**, *11* (2), 113–127. https://doi.org/10.1038/nrm2838.

(42) Schuster-Böckler, B.; Bateman, A. Protein Interactions in Human Genetic Diseases. *Genome Biol.* **2008**, *9* (1), R9. https://doi.org/10.1186/gb-2008-9-1-r9.

(43) Garcia, C. K.; Wilund, K.; Arca, M.; Zuliani, G.; Fellin, R.; Maioli, M.; Calandra, S.; Bertolini, S.; Cossu, F.; Grishin, N.; Barnes, R.; Cohen, J. C.; Hobbs, H. H. Autosomal Recessive Hypercholesterolemia Caused by Mutations in a Putative LDL Receptor Adaptor Protein. *Science (80-.).* **2001**, *292* (5520), 1394–1398. https://doi.org/10.1126/science.1060458.

(44) Udhane, S. S.; Parween, S.; Kagawa, N.; Pandey, A. V. Altered CYP19A1 and CYP3A4 Activities Due to Mutations A115V, T142A, Q153R and P284L in the Human P450 Oxidoreductase. *Front. Pharmacol.* **2017**, *8* (AUG). https://doi.org/10.3389/fphar.2017.00580.

(45) Ptashne, M. Binding Reactions: Epigenetic Switches, Signal Transduction and Cancer. *Curr. Biol.* **2009**, *19* (6), R234–R241. https://doi.org/10.1016/j.cub.2009.02.015.

(46) Bergoug, M.; Doudeau, M.; Godin, F.; Mosrin, C.; Vallée, B.; Bénédetti, H. Neurofibromin Structure, Functions and Regulation. *Cells* **2020**, *9* (11). https://doi.org/10.3390/CELLS9112365.

(47) Wells, J. A.; McClendon, C. L. Reaching for High-Hanging Fruit in Drug Discovery at Protein-Protein Interfaces. *Nature* **2007**, *450* (7172), 1001–1009. https://doi.org/10.1038/nature06526.

(48) Cochran, A. G. Antagonists of Protein-Protein Interactions. *Chem. Biol.* **2000**, *7* (4), R85–R94. https://doi.org/10.1016/S1074-5521(00)00106-X.

(49) Pawson, T.; Nash, P. Assembly of Cell Regulatory Systems through Protein Interaction Domains. *Science (80-.).* **2003**, *300* (5618), 445–452. https://doi.org/10.1126/science.1083653.

(50) Raj, M.; Bullock, B. N.; Arora, P. S. Plucking the High Hanging Fruit: A Systematic Approach for Targeting Protein-Protein Interactions. *Bioorganic Med. Chem.* **2013**, *21* (14), 4051–4057. https://doi.org/10.1016/j.bmc.2012.11.023.

(51) Morelli, X.; Bourgeas, R.; Roche, P. Chemical and Structural Lessons from Recent Successes in Protein-Protein Interaction Inhibition (2P2I). *Curr. Opin. Chem. Biol.* **2011**, *15* (4), 475–481. https://doi.org/10.1016/j.cbpa.2011.05.024.

(52) Le, J. Drug Bioavailability - Clinical Pharmacology - MSD Manual Professional Edition https://www.msdmanuals.com/professional/clinical-pharmacology/pharmacokinetics/drug-bioavailability (accessed Aug 18, 2021).

(53) Uprety, D.; Adjei, A. A. KRAS: From Undruggable to a Druggable Cancer Target. *Cancer Treat. Rev.* **2020**, *89*, 102070. https://doi.org/10.1016/J.CTRV.2020.102070.

(54) Moore, A. R.; Rosenberg, S. C.; McCormick, F.; Malek, S. RAS-Targeted Therapies: Is the Undruggable Drugged? *Nat. Rev. Drug Discov.* **2020**, *19* (8), 533. https://doi.org/10.1038/S41573-020-0068-6.

(55) FDA grants accelerated approval to sotorasib for KRAS G12C mutated NSCLC | FDA https://www.fda.gov/drugs/resources-information-approved-drugs/fda-grants-accelerated-approval-sotorasib-kras-g12c-mutated-nsclc (accessed Aug 20, 2021).

(56) Canon, J.; Rex, K.; Saiki, A. Y.; Mohr, C.; Cooke, K.; Bagal, D.; Gaida, K.; Holt, T.; Knutson, C. G.; Koppada, N.; Lanman, B. A.; Werner, J.; Rapaport, A. S.; San Miguel, T.; Ortiz, R.; Osgood, T.; Sun, J.-R.; Zhu, X.; McCarter, J. D.; Volak, L. P.; Houk, B. E.; Fakih, M. G.; O'Neil, B. H.; Price, T. J.; Falchook, G. S.; Desai, J.; Kuo, J.; Govindan, R.; Hong, D. S.; Ouyang, W.; Henary, H.; Arvedson, T.; Cee, V. J.; Lipford, J. R. The Clinical KRAS(G12C) Inhibitor AMG 510 Drives Anti-Tumour Immunity. *Nat. 2019 5757781* **2019**, *575* (7781), 217–223. https://doi.org/10.1038/s41586-019-1694-1.

(57) Ostrem, J. M.; Peters, U.; Sos, M. L.; Wells, J. A.; Shokat, K. M. K-Ras(G12C) Inhibitors Allosterically Control GTP Affinity and Effector Interactions. *Nat. 2013 5037477* **2013**, *503* (7477), 548–551. https://doi.org/10.1038/nature12796.

(58) Garlick, J. M.; Sturlis, S. M.; Bruno, P. A.; Yates, J. A.; Peiffer, A. L.; Liu, Y.; Goo, L.; Bao, L.; Salle, S. N. De; Tamayo-Castillo, G.; Charles L. Brooks, I.; Merajver, S. D.; Mapp, A. K. Norstictic Acid Is a Selective Allosteric Transcriptional Regulator. *J. Am. Chem. Soc.* **2021**, *143* (25), 9297–9302. https://doi.org/10.1021/JACS.1C03258.

(59) Toseland, C. P. Fluorescent Labeling and Modification of Proteins. *J. Chem. Biol.* **2013**, *6* (3), 85. https://doi.org/10.1007/S12154-013-0094-5.

(60) Stryer, L.; Haugland, R. P. Energy Transfer: A Spectroscopic Ruler. *Proc. Natl. Acad. Sci. U. S. A.* **1967**, *58* (2), 719–726. https://doi.org/10.1073/pnas.58.2.719.

(61) Lakowicz, J. R. *Principles of Fluorescence Spectroscopy*; Springer, 2006. https://doi.org/10.1007/978-0-387-46312-4.

(62) Shrestha, D.; Jenei, A.; Nagy, P.; Vereb, G.; Szöllősi, J. Understanding FRET as a Research Tool for Cellular Studies. *Int. J. Mol. Sci.* **2015**, *16* (4), 6718–6756. https://doi.org/10.3390/ijms16046718.

(63) Erickson, M. G.; Alseikhan, B. A.; Peterson, B. Z.; Yue, D. T. Preassociation of Calmodulin with Voltage-Gated Ca2+ Channels Revealed by FRET in Single Living Cells. *Neuron* **2001**, *31* (6), 973–985. https://doi.org/10.1016/S0896-6273(01)00438-X.

(64) Udenfriend, S.; Gerber, L.; Nelson, N. Scintillation Proximity Assay: A Sensitive and Continuous Isotopic Method for Monitoring Ligand/Receptor and Antigen/Antibody Interactions. *Anal. Biochem.* **1987**, *161* (2), 494–500. https://doi.org/10.1016/0003-2697(87)90479-9.

(65) Cook, N.; Harris, A.; Hopkins, A.; Hughes, K. Scintillation Proximity Assay (SPA) Technology to Study Biomolecular Interactions. *Curr. Protoc. Protein Sci.* **2002**, *Chapter 19*. https://doi.org/10.1002/0471140864.ps1908s27.

(66) Ullman, E. F.; Kirakossian, H.; Switchenko, A. C.; Ishkanian, J.; Ericson, M.; Wartchow, C. A.; Pirio, M.; Pease, J.; Irvin, B. R.; Singh, S.; Singh, R.; Patel, R.; Dafforn, A.; Davalian, D.; Skold, C.; Kurn, N.; Wagner, D. B. Luminescent Oxygen Channeling Assay (LOCI): Sensitive, Broadly Applicable Homogeneous Immunoassay Method. *Clin. Chem.* **1996**, *42* (9), 1518–1526. https://doi.org/10.1093/clinchem/42.9.1518.

(67) Taouji, S.; Dahan, S.; Bosse, R.; Chevet, E. Current Screens Based on the AlphaScreen™ Technology for Deciphering Cell Signalling Pathways. *Curr. Genomics* **2009**, *10* (2), 93–101. https://doi.org/10.2174/138920209787847041.

(68) A Practical Guide to Working with AlphaScreen.

(69) Lewis, A. C. F.; Saeed, R.; Deane, C. M. Predicting Protein-Protein Interactions in the Context of Protein Evolution. *Mol. Biosyst.* **2009**, *6* (1), 55–64. https://doi.org/10.1039/b916371a.

(70) Nielsen, P. J.; Trachsel, H. The Mouse Protein Synthesis Initiation Factor 4A Gene Family Includes Two Related Functional Genes Which Are Differentially Expressed. *EMBO J.* **1988**, *7* (7), 2097–2105. https://doi.org/10.1002/J.1460-2075.1988.TB03049.X.

(71) Galicia-Vázquez, G.; Cencic, R.; Robert, F.; Agenor, A. Q.; Pelletier, J. A Cellular Response Linking EIF4AI Activity to EIF4AII Transcription. *RNA* **2012**, *18* (7), 1373–1384. https://doi.org/10.1261/RNA.033209.112.

(72) Meijer, H. A.; Kong, Y. W.; Lu, W. T.; Wilczynska, A.; Spriggs, R. V.; Robinson, S. W.; Godfrey, J. D.; Willis, A. E.; Bushell, M. Translational Repression and EIF4A2 Activity Are Critical for MicroRNA-Mediated Gene Regulation. *Science (80-.).* **2013**, *340* (6128), 82–85. https://doi.org/10.1126/SCIENCE.1231197.

(73) Teng, S.; Madej, T.; Panchenko, A.; Alexov, E. Modeling Effects of Human Single Nucleotide Polymorphisms on Protein-Protein Interactions. *Biophys. J.* **2009**, *96* (6), 2178–2188. https://doi.org/10.1016/j.bpj.2008.12.3904.

(74) Shin, W. H.; Christoffer, C. W.; Kihara, D. In Silico Structure-Based Approaches to Discover Protein-Protein Interaction-Targeting Drugs. *Methods* **2017**, *131*, 22–32. https://doi.org/10.1016/j.ymeth.2017.08.006.

(75) Truong, K.; Ikura, M. The Use of FRET Imaging Microscopy to Detect Protein-Protein Interactions and Protein Conformational Changes in Vivo. *Current Opinion in Structural Biology*, 2001, *11*, 573–578. https://doi.org/10.1016/S0959-440X(00)00249-9.

(76) Yan, Y.; Marriott, G. Analysis of Protein Interactions Using Fluorescence Technologies. *Curr. Opin. Chem. Biol.* **2003**, *7* (5), 635–640. https://doi.org/10.1016/j.cbpa.2003.08.017.

(77) Manko, H.; Normant, V.; Perraud, Q.; Steffan, T.; Gasser, V.; Boutant, E.; Réal, É.; Schalk, I. J.; Mély, Y.; Godet, J. Flim-Fret Measurements of Protein-Protein Interactions in Live Bacteria. *J. Vis. Exp.* **2020**, *2020* (162), 1–21. https://doi.org/10.3791/61602.

(78) Albertazzi, L.; Arosio, D.; Marchetti, L.; Ricci, F.; Beltram, F. Quantitative FRET Analysis With the E ^{0} GFP-MCherry Fluorescent Protein Pair. *Photochem. Photobiol.* **2009**, *85* (1), 287–297. https://doi.org/10.1111/j.1751-1097.2008.00435.x.

(79) Magde, D.; Elson, E. L.; Webb, W. W. Fluorescence Correlation Spectroscopy. II. An Experimental Realization. *Biopolymers* **1974**, *13* (1), 29–61. https://doi.org/10.1002/BIP.1974.360130103.

(80) Baum, M.; Erdel, F.; Wachsmuth, M.; Rippe, K. Retrieving the Intracellular Topology from Multi-Scale Protein Mobility Mapping in Living Cells. *Nat. Commun.* **2014**, *5*. https://doi.org/10.1038/NCOMMS5494.

(81) Schwille, P.; Meyer-Almes, F.; Rigler, R. Dual-Color Fluorescence Cross-Correlation Spectroscopy for Multicomponent Diffusional Analysis in Solution. *Biophys. J.* **1997**, *72* (4), 1878–1886. https://doi.org/10.1016/S0006-3495(97)78833-7.

(82) Fields, S.; Song, O. K. A Novel Genetic System to Detect Protein-Protein Interactions. *Nature* **1989**, *340* (6230), 245–246. https://doi.org/10.1038/340245a0.

(83) Stynen, B.; Tournu, H.; Tavernier, J.; Van Dijck, P. Diversity in Genetic In Vivo Methods for Protein-Protein Interaction Studies: From the Yeast Two-Hybrid System to the Mammalian Split-Luciferase System. *Microbiol. Mol. Biol. Rev.* **2012**, *76* (2), 331–382. https://doi.org/10.1128/mmbr.05021-11.

(84) Formstecher, E.; Aresta, S.; Collura, V.; Hamburger, A.; Meil, A.; Trehin, A.; Reverdy, C.; Betin, V.; Maire, S.; Brun, C.; Jacq, B.; Arpin, M.; Bellaiche, Y.; Bellusci, S.; Benaroch, P.; Bornens, M.; Chanet, R.; Chavrier, P.; Delattre, O.; Doye, V.; Fehon, R.; Faye, G.; Galli, T.; Girault, J. A.; Goud, B.; de Gunzburg, J.; Johannes, L.; Junier, M. P.; Mirouse, V.; Mukherjee, A.; Papadopoulo, D.; Perez, F.; Plessis, A.; Rossé, C.; Saule, S.; Stoppa-Lyonnet, D.; Vincent, A.; White, M.; Legrain, P.; Wojcik, J.; Camonis, J.; Daviet, L. Protein Interaction Mapping: A Drosophila Case Study. *Genome Res.* **2005**, *15* (3), 376–384. https://doi.org/10.1101/gr.2659105.

(85) Nakayama, M.; Kikuno, R.; Ohara, O. Protein-Protein Interactions between Large Proteins: Two-Hybrid Screening Using a Functionally Classified Library Composed of Long CDNAs. *Genome Res.* **2002**, *12* (11), 1773–1784. https://doi.org/10.1101/gr.406902.

(86) Sidhu, S. S.; Fairbrother, W. J.; Deshayes, K. Exploring Protein-Protein Interactions with Phage Display. *ChemBioChem* **2003**, *4* (1), 14–25. https://doi.org/10.1002/cbic.200390008.

(87) Mullen, L. M.; Nair, S. P.; Ward, J. M.; Rycroft, A. N.; Henderson, B. Phage Display in the Study of Infectious Diseases. *Trends Microbiol.* **2006**, *14* (3), 141–147. https://doi.org/10.1016/j.tim.2006.01.006.

(88) Sundell, G. N.; Ivarsson, Y. Interaction Analysis through Proteomic Phage Display. *Biomed Res. Int.* **2014**, *2014*. https://doi.org/10.1155/2014/176172.

(89) Bazan, J.; Całkosiñski, I.; Gamian, A. Phage Displaya Powerful Technique for Immunotherapy: 1. Introduction and Potential of Therapeutic Applications. *Hum. Vaccines Immunother.* **2012**, *8* (12), 1817–1828. https://doi.org/10.4161/hv.21703.

(90) Iqbal, H.; Akins, D. R.; Kenedy, M. R. Co-Immunoprecipitation for Identifying Protein-Protein Interactions in Borrelia Burgdorferi. In *Methods in Molecular Biology*; Humana Press Inc., 2018; Vol. 1690, pp 47–55. https://doi.org/10.1007/978-1-4939-7383-5_4.

(91) Free, R. B.; Hazelwood, L. A.; Sibley, D. R. Identifying Novel Protein-Protein Interactions Using Co-Immunoprecipitation and Mass Spectroscopy. *Curr. Protoc. Neurosci.* **2009**, *0 5* (SUPPL. 46), Unit. https://doi.org/10.1002/0471142301.ns0528s46.

(92) Puig, O.; Caspary, F.; Rigaut, G.; Rutz, B.; Bouveret, E.; Bragado-Nilsson, E.; Wilm, M.; Séraphin, B. The Tandem Affinity Purification (TAP) Method: A General Procedure of Protein Complex Purification. *Methods* **2001**, *24* (3), 218–229. https://doi.org/10.1006/meth.2001.1183.

(93) Roux, K. J.; Kim, D. I.; Raida, M.; Burke, B. A Promiscuous Biotin Ligase Fusion Protein Identifies Proximal and Interacting Proteins in Mammalian Cells. *J. Cell Biol.* **2012**, *196* (6), 801. https://doi.org/10.1083/JCB.201112098.

(94) Wittig, I.; Schägger, H. Features and Applications of Blue-Native and Clear-Native Electrophoresis. *Proteomics* **2008**, *8* (19), 3974–3990. https://doi.org/10.1002/PMIC.200800017.

(95) Wittig, I.; Schägger, H. Native Electrophoretic Techniques to Identify Protein–Protein Interactions. *Proteomics* **2009**, *9* (23), 5214–5223. https://doi.org/10.1002/PMIC.200900151.

(96) Wu, Y.; Li, Q.; Chen, X.-Z. Detecting Protein–Protein Interactions by Far Western Blotting. *Nat. Protoc. 2007 212* **2007**, *2* (12), 3278–3284. https://doi.org/10.1038/nprot.2007.459.

(97) Fägerstam, L. G.; Frostell-Karlsson, Å.; Karlsson, R.; Persson, B.; Rönnberg, I. Biospecific Interaction Analysis Using Surface Plasmon Resonance Detection Applied to Kinetic, Binding Site and Concentration Analysis. *J. Chromatogr. A* **1992**, *597* (1–2), 397–410. https://doi.org/10.1016/0021-9673(92)80137-J.

(98) Johnsson, B.; Löfås, S.; Lindquist, G. Immobilization of Proteins to a Carboxymethyldextran-Modified Gold Surface for Biospecific Interaction Analysis in Surface Plasmon Resonance Sensors. *Anal. Biochem.* **1991**, *198* (2), 268–277. https://doi.org/10.1016/0003-2697(91)90424-R.

(99) Han, Y.; Gao, Y.; He, T.; Wang, D.; Guo, N.; Zhang, X.; Chen, S.; Wang, H. PD-1/PD-L1 Inhibitor Screening of Caffeoylquinic Acid Compounds Using Surface Plasmon Resonance Spectroscopy. *Anal. Biochem.* **2018**, *547*, 52–56. https://doi.org/10.1016/j.ab.2018.02.003.

(100) Cheng, X.; Veverka, V.; Radhakrishnan, A.; Waters, L. C.; Muskett, F. W.; Morgan, S. H.; Huo, J.; Yu, C.; Evans, E. J.; Leslie, A. J.; Griffiths, M.; Stubberfield, C.; Griffin, R.; Henry, A. J.; Jansson, A.; Ladbury, J. E.; Ikemizu, S.; Carr, M. D.; Davis, S. J. Structure and Interactions of the Human Programmed Cell Death 1 Receptor. *J. Biol. Chem.* **2013**, *288* (17), 11771–11785. https://doi.org/10.1074/jbc.M112.448126.

(101) Wegner, G. J.; Lee, H. J.; Marriott, G.; Corn, R. M. Fabrication of Histidine-Tagged Fusion Protein Arrays for Surface Plasmon Resonance Imaging Studies of Protein - Protein and Protein - DNA Interactions. *Anal. Chem.* **2003**, *75* (18), 4740–4746. https://doi.org/10.1021/ac0344438.

(102) Nikolovska-Coleska, Z. Studying Protein-Protein Interactions Using Surface Plasmon Resonance. *Methods Mol. Biol.* **2015**, *1278*, 109–138. https://doi.org/10.1007/978-1-4939-2425-7_7.

(103) Ziblat, R.; Lirtsman, V.; Davidov, D.; Aroeti, B. Infrared Surface Plasmon Resonance: A Novel Tool for Real Time Sensing of Variations in Living Cells. *Biophys. J.* **2006**, *90* (7), 2592. https://doi.org/10.1529/BIOPHYSJ.105.072090.

(104) Schneider, C. S.; Bhargav, A. G.; Perez, J. G.; Wadajkar, A. S.; Winkles, J. A.; Woodworth, G. F.; Kim, A. J. Surface Plasmon Resonance as a High Throughput Method to Evaluate Specific and Non-Specific Binding of Nanotherapeutics. *J. Control. Release* **2015**, *219*, 331–344. https://doi.org/10.1016/j.jconrel.2015.09.048.

(105) Minh Hiep, H.; Endo, T.; Kerman, K.; Chikae, M.; Kim, D. K.; Yamamura, S.; Takamura, Y.; Tamiya, E. A Localized Surface Plasmon Resonance Based Immunosensor for the Detection of Casein in Milk. *Sci. Technol. Adv. Mater.* **2007**, *8* (4), 331–338. https://doi.org/10.1016/j.stam.2006.12.010.

(106) Kushwaha, A. S.; Kumar, A.; Kumar, R.; Srivastava, S. K. A Study of Surface Plasmon Resonance (SPR) Based Biosensor with Improved Sensitivity. *Photonics Nanostructures - Fundam. Appl.* **2018**, *31*, 99–106. https://doi.org/10.1016/j.photonics.2018.06.003.

(107) Abbas, A.; Linman, M. J.; Cheng, Q. Sensitivity Comparison of Surface Plasmon Resonance and Plasmon-Waveguide Resonance Biosensors. *Sensors Actuators, B Chem.* **2011**, *156* (1), 169–175. https://doi.org/10.1016/j.snb.2011.04.008.

(108) Miles, A. High-Throughput SPR Screening and Characterization of Small Molecules Binding to Protein Targets.

(109) Cunningham, B.; Li, P.; Lin, B.; Pepper, J. Colorimetric Resonant Reflection as a Direct Biochemical Assay Technique. *Sensors Actuators, B Chem.* **2002**, *81* (2–3), 316–328. https://doi.org/10.1016/S0925-4005(01)00976-5.

(110) Cunningham, B. T.; Li, P.; Schulz, S.; Lin, B.; Baird, C.; Gerstenmaier, J.; Genick, C.; Wang, F.; Fine, E.; Laing, L. Label-Free Assays on the BIND System. *J. Biomol. Screen.* **2004**, *9* (6), 481–490. https://doi.org/10.1177/1087057104267604.

(111) De Flaviis, F. Guided Waves. In *The Electrical Engineering Handbook*; Elsevier Inc., 2005; pp 539–551. https://doi.org/10.1016/B978-012170960-0/50041-4.

(112) Hu, D.; Fry, S. R.; Huang, J. X.; Ding, X.; Qiu, L.; Pan, Y.; Chen, Y.; Jin, J.; McElnea, C.; Buechler, J.; Che, X.; Cooper, M. A. Comparison of Surface Plasmon Resonance, Resonant Waveguide Grating Biosensing and Enzyme Linked Immunosorbent Assay (ELISA) in the Evaluation of a Dengue Virus Immunoassay. *Biosens. 2013, Vol. 3, Pages 297-311* **2013**, *3* (3), 297–311. https://doi.org/10.3390/BIOS3030297.

(113) Paulsen, M.; Jahns, S.; Gerken, M. Intensity-Based Readout of Resonant-Waveguide Grating Biosensors: Systems and Nanostructures. *Photonics Nanostructures - Fundam. Appl.* **2017**, *26*, 69–79. https://doi.org/10.1016/j.photonics.2017.07.003.

(114) Rich, R. L.; Myszka, D. G. Higher-Throughput, Label-Free, Real-Time Molecular Interaction Analysis. *Anal. Biochem.* **2007**, *361* (1), 1–6. https://doi.org/10.1016/j.ab.2006.10.040.

(115) Mandenius, C. F.; Welin, S.; Danielsson, B.; Lundström, I.; Mosbach, K. The Interaction of Proteins and Cells with Affinity Ligands Covalently Coupled to Silicon Surfaces as Monitored by Ellipsometry. *Anal. Biochem.* **1984**, *137* (1), 106–114. https://doi.org/10.1016/0003-2697(84)90354-3.

(116) Kodera, S.; Okajima, T.; Iwabuki, H.; Kitaguchi, D.; Kuroda, S.; Yoshinobu, T.; Tanizawa, K.; Futai, M.; Iwasaki, H. Detection of Protein-Protein Interactions on SiO2/Si Surfaces by Spectroscopic Ellipsometry. *Anal. Biochem.* **2003**, *321* (1), 65–70. https://doi.org/10.1016/S0003-2697(03)00422-6.

(117) Mora, M. F.; Wehmeyer, J. L.; Synowicki, R.; Garcia, C. D. Investigating Protein Adsorption via Spectroscopic Ellipsometry. *Biol. Interact. Mater. Surfaces* **2009**, 19. https://doi.org/10.1007/978-0-387-98161-1_2.

(118) Li, K.; Wang, S.; Wang, L.; Yu, H.; Jing, N.; Xue, R.; Wang, Z. Fast and Sensitive Ellipsometry-Based Biosensing. *Sensors (Switzerland)* **2018**, *18* (1). https://doi.org/10.3390/s18010015.

(119) Kariper, I. A.; Üstündağ, Z.; Caglayan, M. O. A Sensitive Spectrophotometric Ellipsometry Based Aptasensor for the Vascular Endothelial Growth Factor Detection. *Talanta* **2021**, *225*, 121982. https://doi.org/10.1016/j.talanta.2020.121982.

(120) Nabok, A.; Tsargorodskaya, A. The Method of Total Internal Reflection Ellipsometry for Thin Film Characterisation and Sensing. *Thin Solid Films* **2008**, *516* (24), 8993–9001. https://doi.org/10.1016/j.tsf.2007.11.077.

(121) Kriechbaumer, V.; Nabok, A.; Mustafa, M. K.; Al-Ammar, R.; Tsargorodskaya, A.; Smith, D. P.; Abell, B. M. Analysis of Protein Interactions at Native Chloroplast Membranes by Ellipsometry. *PLoS One* **2012**, *7* (3), 34455. https://doi.org/10.1371/journal.pone.0034455.

(122) Asinovski, L.; Beaglehole, D.; Clarkson, M. T. Imaging Ellipsometry: Quantitative Analysis. *Phys. status solidi* **2008**, *205* (4), 764–771. https://doi.org/10.1002/pssa.200777855.

(123) Nabok, A. V.; Tsargorodskaya, A.; Hassan, A. K.; Starodub, N. F. Total Internal Reflection Ellipsometry and SPR Detection of Low Molecular Weight Environmental Toxins. *Appl. Surf. Sci.* **2005**, *246* (4), 381–386. https://doi.org/10.1016/J.APSUSC.2004.11.084.

(124) Cross, G. H.; Reeves, A. A.; Brand, S.; Popplewell, J. F.; Peel, L. L.; Swann, M. J.; Freeman, N. J. A New Quantitative Optical Biosensor for Protein Characterisation. *Biosens. Bioelectron.* **2003**, *19* (4), 383–390. https://doi.org/10.1016/S0956-5663(03)00203-3.

(125) Escorihuela, J.; González-Martínez, M. Á.; López-Paz, J. L.; Puchades, R.; Maquieira, Á.; Gimenez-Romero, D. Dual-Polarization Interferometry: A Novel Technique to Light up the Nanomolecular World. *Chem. Rev.* **2015**, *115* (1), 265–294. https://doi.org/10.1021/cr5002063.

(126) Zhao, X.; Pan, F.; Cowsill, B.; Lu, J. R.; Garcia-Gancedo, L.; Flewitt, A. J.; Ashley, G. M.; Luo, J. Interfacial Immobilization of Monoclonal Antibody and Detection of Human Prostate-Specific Antigen. *Langmuir* **2011**, *27* (12), 7654–7662. https://doi.org/10.1021/la201245q.

(127) Balhara, V.; Deshmukh, S. S.; Kálmán, L.; Kornblatt, J. A. The Interaction of Streptococcal Enolase with Canine Plasminogen: The Role of Surfaces in Complex Formation. *PLoS One* **2014**, *9* (2), e88395. https://doi.org/10.1371/journal.pone.0088395.

(128) Swann, M. J.; Peel, L. L.; Carrington, S.; Freeman, N. J. Dual-Polarization Interferometry: An Analytical Technique to Measure Changes in Protein Structure in Real Time, to Determine the Stoichiometry of Binding Events, and to Differentiate between Specific and Nonspecific Interactions. *Anal. Biochem.* **2004**, *329* (2), 190–198. https://doi.org/10.1016/j.ab.2004.02.019.

(129) Song, H. Y.; Zhou, X.; Hobley, J.; Su, X. Comparative Study of Random and Oriented Antibody Immobilization as Measured by Dual Polarization Interferometry and Surface Plasmon Resonance Spectroscopy. *Langmuir* **2012**, *28* (1), 997–1004. https://doi.org/10.1021/la202734f.

(130) Sonesson, A. W.; Callisen, T. H.; Brismar, H.; Elofsson, U. M. A Comparison between Dual Polarization Interferometry (DPI) and Surface Plasmon Resonance (SPR) for Protein Adsorption Studies. *Colloids Surfaces B Biointerfaces* **2007**, *54* (2), 236–240. https://doi.org/10.1016/J.COLSURFB.2006.10.028.

(131) Kumaraswamy, S.; Tobias, R. Label-Free Kinetic Analysis of an Antibody-Antigen Interaction Using Biolayer Interferometry. In *Protein-Protein Interactions: Methods and Applications: Second Edition*; Springer New York, 2015; Vol. 1278, pp 165–182. https://doi.org/10.1007/978-1-4939-2425-7_10.

(132) Yang, D.; Singh, A.; Wu, H.; Kroe-Barrett, R. Comparison of Biosensor Platforms in the Evaluation of High Affinity Antibody-Antigen Binding Kinetics. *Anal. Biochem.* **2016**, *508*, 78–96. https://doi.org/10.1016/J.AB.2016.06.024.

(133) Dennison, S. M.; Reichartz, M.; Seaton, K. E.; Dutta, S.; Wille-Reece, U.; Hill, A. V. S.; Ewer, K. J.; Rountree, W.; Sarzotti-Kelsoe, M.; Ozaki, D. A.; Alam, S. M.; Tomaras, G. D. Qualified Biolayer Interferometry Avidity Measurements Distinguish the Heterogeneity of Antibody Interactions with Plasmodium Falciparum Circumsporozoite Protein Antigens . *J. Immunol.* **2018**, *201* (4), 1315–1326. https://doi.org/10.4049/jimmunol.1800323.

(134) Roederer, J. E.; Bastiaans, G. J. Microgravimetric Immunoassay with Piezoelectric Crystals. *Anal. Chem.* **1983**, *55* (14), 2333–2336. https://doi.org/10.1021/ac00264a030.

(135) Li, X.; Song, S.; Pei, Y.; Dong, H.; Aastrup, T.; Pei, Z. Oriented and Reversible Immobilization of His-Tagged Proteins on Two- and Three-Dimensional Surfaces for Study of Protein-Protein Interactions by a QCM Biosensor. *Sensors Actuators, B Chem.* **2016**, *224*, 814–822. https://doi.org/10.1016/j.snb.2015.10.096.

(136) Wu, C.; Li, X.; Song, S.; Pei, Y.; Guo, L.; Pei, Z. QCM Biosensor Based on Polydopamine Surface for Real-Time Analysis of the Binding Kinetics of Protein-Protein Interactions. *Polymers (Basel).* **2017**, *9* (10), 482. https://doi.org/10.3390/polym9100482.

(137) Heller, G. T.; Mercer-Smith, A. R.; Johal, M. S. Quartz Microbalance Technology for Probing Biomolecular Interactions. *Methods Mol. Biol.* **2015**, *1278*, 153–164. https://doi.org/10.1007/978-1-4939-2425-7_9.

(138) McMillan, D. G. G.; Marritt, S. J.; Firer-Sherwood, M. A.; Shi, L.; Richardson, D. J.; Evans, S. D.; Elliott, S. J.; Butt, J. N.; Jeuken, L. J. C. Protein-Protein Interaction Regulates the Direction of Catalysis and Electron Transfer in a Redox Enzyme Complex. *J. Am. Chem. Soc.* **2013**, *135* (28), 10550–10556. https://doi.org/10.1021/ja405072z.

(139) Salmain, M.; Ghasemi, M.; Boujday, S.; Spadavecchia, J.; Técher, C.; Val, F.; Le Moigne, V.; Gautier, M.; Briandet, R.; Pradier, C. M. Piezoelectric Immunosensor for Direct and Rapid Detection of Staphylococcal Enterotoxin A (SEA) at the Ng Level. *Biosens. Bioelectron.* **2011**, *29* (1), 140–144. https://doi.org/10.1016/j.bios.2011.08.007.

(140) Marx, K. A. Quartz Crystal Microbalance: A Useful Tool for Studying Thin Polymer Films and Complex Biomolecular Systems at the Solution - Surface Interface. *Biomacromolecules* **2003**, *4* (5), 1099–1120. https://doi.org/10.1021/bm020116i.

(141) Modin, C.; Stranne, A. L.; Foss, M.; Duch, M.; Justesen, J.; Chevallier, J.; Andersen, L. K.; Hemmersam, A. G.; Pedersen, F. S.; Besenbacher, F. QCM-D Studies of Attachment and Differential Spreading of Pre-Osteoblastic Cells on Ta and Cr Surfaces. *Biomaterials* **2006**, *27* (8), 1346–1354. https://doi.org/10.1016/J.BIOMATERIALS.2005.09.022.

(142) Ogi, H.; Nagai, H.; Fukunishi, Y.; Yanagida, T.; Hirao, M.; Nishiyama, M. Multichannel Wireless-Electrodeless Quartz-Crystal Microbalance Immunosensor. *Anal. Chem.* **2010**, *82* (9), 3957–3962. https://doi.org/10.1021/AC100527R.

(143) Shen, H.; Zhou, T.; Hu, J. A High-Throughput QCM Chip Configuration for the Study of Living Cells and Cell-Drug Interactions. *Anal. Bioanal. Chem.* **2017**, *409* (27), 6463–6473. https://doi.org/10.1007/s00216-017-0591-4.

(144) QSense Pro - Nanoscience Instruments https://www.nanoscience.com/products/quartz-crystal-microbalance/qsense-pro/ (accessed Apr 9, 2021).

(145) Huang, J.; Lin, Q.; Yu, J.; Ge, S.; Li, J.; Yu, M.; Zhao, Z.; Wang, X.; Zhang, X.; He, X.; Yuan, L.; Yin, H.; Osa, T.; Chen, K.; Chen, Q. Comparison of a Resonant Mirror Biosensor (IAsys) and a Quartz Crystal Microbalance (QCM) for the Study on Interaction between Paeoniae Radix 801 and Endothelin-1. *Sensors* **2008**, *8* (12), 8275–8290. https://doi.org/10.3390/s8128275.

(146) Lisdat, F.; Schäfer, D. The Use of Electrochemical Impedance Spectroscopy for Biosensing. *Anal. Bioanal. Chem.* **2008**, *391* (5), 1555–1567. https://doi.org/10.1007/s00216-008-1970-7.

(147) Katz, E.; Willner, I. Probing Biomolecular Interactions at Conductive and Semiconductive Surfaces by Impedance Spectroscopy: Routes to Impedimetric Immunosensors, DNA-Sensors, and Enzyme Biosensors. *Electroanalysis* **2003**, *15* (11), 913–947. https://doi.org/10.1002/elan.200390114.

(148) Zamfir, L. G.; Puiu, M.; Bala, C. Advances in Electrochemical Impedance Spectroscopy Detection of Endocrine Disruptors. *Sensors (Switzerland)* **2020**, *20* (22), 1–21. https://doi.org/10.3390/s20226443.

(149) Daniels, J. S.; Pourmand, N. Label-Free Impedance Biosensors: Opportunities and Challenges. *Electroanalysis* **2007**, *19* (12), 1239–1257. https://doi.org/10.1002/elan.200603855.

(150) He, J.; Bahr, J.; Chisholm, B. J.; Li, J.; Chen, Z.; Balbyshev, S. N.; Bonitz, V.; Bierwagen, G. P. Combinatorial Materials Research Applied to the Development of New Surface Coatings X: A High-Throughput Electrochemical Impedance Spectroscopy Method for Screening Organic

Coatings for Corrosion Inhibition. *J. Comb. Chem.* **2008**, *10* (5), 704–713. https://doi.org/10.1021/cc8000458.

(151) Zhang, F.; Lin, L. X.; Wang, G. W.; Hu, R.; Lin, C. J.; Chen, Y. A High-Throughput Electrochemical Impedance Spectroscopy Evaluation of Bioresponsibility of the Titanium Microelectrode Array Integrated with Hydroxyapatite and Silver. *Electrochim. Acta* **2012**, *85*, 152–161. https://doi.org/10.1016/j.electacta.2012.08.033.

(152) Kostal, E.; Kasemann, S.; Dincer, C.; Partel, S. Impedimetric Characterization of Interdigitated Electrode Arrays for Biosensor Applications. *Proceedings* **2018**, *2* (13), 899. https://doi.org/10.3390/proceedings2130899.

(153) Bogomolova, A.; Komarova, E.; Reber, K.; Gerasimov, T.; Yavuz, O.; Bhatt, S.; Aldissi, M. Challenges of Electrochemical Impedance Spectroscopy in Protein Biosensing. *Anal. Chem.* **2009**, *81* (10), 3944–3949. https://doi.org/10.1021/ac9002358.

(154) Zhu, H.; Bilgin, M.; Bangham, R.; Hall, D.; Casamayor, A.; Bertone, P.; Lan, N.; Jansen, R.; Bidlingmaier, S.; Houfek, T.; Mitchell, T.; Miller, P.; Dean, R. A.; Gerstein, M.; Snyder, M. Global Analysis of Protein Activities Using Proteome Chips. *Science (80-.).* **2001**, *293* (5537), 2101–2105. https://doi.org/10.1126/science.1062191.

(155) Melton, L. Proteomics in Multiplex. *Nature* **2004**, *429* (6987), 101–107. https://doi.org/10.1038/429101a.

(156) Schweitzer, B.; Predki, P.; Snyder, M. Microarrays to Characterize Protein Interactions on a Whole-Proteome Scale. *Proteomics* **2003**, *3* (11), 2190–2199. https://doi.org/10.1002/pmic.200300610.

(157) Ray, S.; Mehta, G.; Srivastava, S. Label-Free Detection Techniques for Protein Microarrays: Prospects, Merits and Challenges. *Proteomics* **2010**, *10* (4), 731–748. https://doi.org/10.1002/pmic.200900458.

(158) Lausted, C.; Hu, Z.; Hood, L. Quantitative Serum Proteomics from Surface Plasmon Resonance Imaging. *Mol. Cell. Proteomics* **2008**, *7* (12), 2464–2474. https://doi.org/10.1074/mcp.M800121-MCP200.

(159) Pierce, M. M.; Raman, C. S.; Nall, B. T. Isothermal Titration Calorimetry of Protein-Protein Interactions. *Methods A Companion to Methods Enzymol.* **1999**, *19* (2), 213–221. https://doi.org/10.1006/meth.1999.0852.

(160) Chiu, M.; Prenner, E. Differential Scanning Calorimetry: An Invaluable Tool for a Detailed Thermodynamic Characterization of Macromolecules and Their Interactions. In *Journal of Pharmacy and Bioallied Sciences*; Wolters Kluwer -- Medknow Publications, 2011; Vol. 3, pp 39–59. https://doi.org/10.4103/0975-7406.76463.

(161) Wiseman, T.; Williston, S.; Brandts, J. F.; Lin, L. N. Rapid Measurement of Binding Constants and Heats of Binding Using a New Titration Calorimeter. *Anal. Biochem.* **1989**, *179* (1), 131–137. https://doi.org/10.1016/0003-2697(89)90213-3.

(162) Privalov, P. L.; Plotnikov, V. V.; Filimonov, V. V. Precision Scanning Microcalorimeter for the Study of Liquids. *J. Chem. Thermodyn.* **1975**, *7* (1), 41–47. https://doi.org/10.1016/0021-9614(75)90079-8.

(163) Jelesarov, I.; Bosshard, H. R. Isothermal Titration Calorimetry and Differential Scanning Calorimetry as Complementary Tools to Investigate the Energetics of Biomolecular Recognition. *J. Mol. Recognit.* **1999**, *12* (1), 3–18. https://doi.org/10.1002/(SICI)1099-1352(199901/02)12:1<3::AID-JMR441>3.0.CO;2-6.

(164) Cooper, M. A. Label-Free Screening of Bio-Molecular Interactions. *Anal. Bioanal. Chem.* **2003**, *377* (5), 834–842. https://doi.org/10.1007/s00216-003-2111-y.

(165) Durowoju, I. B.; Bhandal, K. S.; Hu, J.; Carpick, B.; Kirkitadze, M. Differential Scanning Calorimetry — A Method for Assessing the Thermal Stability and Conformation of Protein Antigen. *J. Vis. Exp.* **2017**, *2017* (121). https://doi.org/10.3791/55262.

(166) Schaefer, J. V.; Sedlák, E.; Kast, F.; Nemergut, M.; Plückthun, A. Modification of the Kinetic Stability of Immunoglobulin G by Solvent Additives. *MAbs* **2018**, *10* (4), 607. https://doi.org/10.1080/19420862.2018.1450126.

(167) Torres, F. E.; Recht, M. I.; Coyle, J. E.; Bruce, R. H.; Williams, G. Higher Throughput Calorimetry: Opportunities, Approaches and Challenges. *Curr. Opin. Struct. Biol.* **2010**, *20* (5), 598–605. https://doi.org/10.1016/j.sbi.2010.09.001.

(168) Torres, F. E.; Kuhn, P.; De Bruyker, D.; Bell, A. G.; Wolkin, M. V.; Peeters, E.; Williamson, J. R.; Anderson, G. B.; Schmitz, G. P.; Recht, M. I.; Schweizer, S.; Scott, L. G.; Ho, J. H.; Elrod, S. A.; Schultz, P. G.; Lerner, R. A.; Bruce, R. H. Enthalpy Arrays. *Proc. Natl. Acad. Sci. U. S. A.* **2004**, *101* (26), 9517–9522. https://doi.org/10.1073/pnas.0403573101.

(169) Duff, M. R.; Jr.; Grubbs, J.; Howell, E. E. Isothermal Titration Calorimetry for Measuring Macromolecule-Ligand Affinity. *J. Vis. Exp.* **2011**, *55* (55), 2796. https://doi.org/10.3791/2796.

(170) Hawe, A.; Sutter, M.; Jiskoot, W. Extrinsic Fluorescent Dyes as Tools for Protein Characterization. *Pharm. Res.* **2008**, *25* (7), 1487–1499. https://doi.org/10.1007/s11095-007-9516-9.

(171) Sasaki, S.; Drummen, G. P. C.; Konishi, G. I. Recent Advances in Twisted Intramolecular Charge Transfer (TICT) Fluorescence and Related Phenomena in Materials Chemistry. *J. Mater. Chem. C* **2016**, *4* (14), 2731–2743. https://doi.org/10.1039/c5tc03933a.

(172) Haidekker, M. A.; Brady, T. P.; Lichlyter, D.; Theodorakis, E. A. Effects of Solvent Polarity and Solvent Viscosity on the Fluorescent Properties of Molecular Rotors and Related Probes. *Bioorg. Chem.* **2005**, *33* (6), 415–425. https://doi.org/10.1016/j.bioorg.2005.07.005.

(173) Krebs, M. R. H.; Bromley, E. H. C.; Donald, A. M. The Binding of Thioflavin-T to Amyloid Fibrils: Localisation and Implications. *J. Struct. Biol.* **2005**, *149* (1), 30–37. https://doi.org/10.1016/j.jsb.2004.08.002.

(174) Hawe, A.; Filipe, V.; Jiskoot, W. Fluorescent Molecular Rotors as Dyes to Characterize Polysorbate-Containing IgG Formulations. *Pharm. Res.* **2010**, *27* (2), 314–326. https://doi.org/10.1007/s11095-009-0020-2.

(175) Nagarajan, S.; Lapidus, L. J. Fluorescent Probe DCVJ Shows High Sensitivity for Characterization of Amyloid β-Peptide Early in the Lag Phase. *ChemBioChem* **2017**, *18* (22), 2205–2211. https://doi.org/10.1002/cbic.201700387.

(176) Levine, H. Thioflavine T Interaction with Synthetic Alzheimer's Disease B-amyloid Peptides: Detection of Amyloid Aggregation in Solution. *Protein Sci.* **1993**, *2* (3), 404–410. https://doi.org/10.1002/pro.5560020312.

(177) Finke, J. M.; Jennings, P. A. Early Aggregated States in the Folding of Interleukin-1β. *J. Biol. Phys.* **2001**, *27* (2–3), 119–131. https://doi.org/10.1023/A:1013178505077.

(178) Layton, C. J.; Hellinga, H. W. Quantitation of Protein-Protein Interactions by Thermal Stability Shift Analysis. *Protein Sci.* **2011**, *20* (8), 1439–1450. https://doi.org/10.1002/pro.674.

(179) Choudhary, D.; Kumar, A.; Magliery, T. J.; Sotomayor, M. Using Thermal Scanning Assays to Test Protein-Protein Interactions of Inner-Ear Cadherins. *PLoS One* **2017**, *12* (12). https://doi.org/10.1371/journal.pone.0189546.

(180) Ericsson, U. B.; Hallberg, B. M.; DeTitta, G. T.; Dekker, N.; Nordlund, P. Thermofluor-Based High-Throughput Stability Optimization of Proteins for Structural Studies. *Anal. Biochem.* **2006**, *357* (2), 289–298. https://doi.org/10.1016/j.ab.2006.07.027.

(181) Lo, M. C.; Aulabaugh, A.; Jin, G.; Cowling, R.; Bard, J.; Malamas, M.; Ellestad, G. Evaluation of Fluorescence-Based Thermal Shift Assays for Hit Identification in Drug Discovery. *Anal. Biochem.* **2004**, *332* (1), 153–159. https://doi.org/10.1016/j.ab.2004.04.031.

(182) Lang, B. E.; Cole, K. D. Differential Scanning Calorimetry and Fluorimetry Measurements of Monoclonal Antibodies and Reference Proteins: Effect of Scanning Rate and Dye Selection. *Biotechnol. Prog.* **2017**, *33* (3), 677–686. https://doi.org/10.1002/btpr.2464.

(183) Niesen, F. H.; Berglund, H.; Vedadi, M. The Use of Differential Scanning Fluorimetry to Detect Ligand Interactions That Promote Protein Stability. *Nat. Protoc.* **2007**, *2* (9), 2212–2221. https://doi.org/10.1038/nprot.2007.321.
(184) Ablinger, E.; Leitgeb, S.; Zimmer, A. Differential Scanning Fluorescence Approach Using a Fluorescent Molecular Rotor to Detect Thermostability of Proteins in Surfactant-Containing Formulations. *Int. J. Pharm.* **2013**, *441* (1–2), 255–260. https://doi.org/10.1016/J.IJPHARM.2012.11.035.
(185) TEALE, F. W.; WEBER, G. Ultraviolet Fluorescence of the Aromatic Amino Acids. *Biochem. J.* **1957**, *65* (3), 476–482. https://doi.org/10.1042/bj0650476.
(186) Ghisaidoobe, A. B. T.; Chung, S. J. Intrinsic Tryptophan Fluorescence in the Detection and Analysis of Proteins: A Focus on Förster Resonance Energy Transfer Techniques. *Int. J. Mol. Sci.* **2014**, *15* (12), 22518–22538. https://doi.org/10.3390/ijms151222518.
(187) Striebel, H.-M.; Schellenberg, P.; Grigaravicius, P.; Greulich, K. O. Readout of Protein Microarrays Using Intrinsic Time Resolved UV Fluorescence for Label-Free Detection. *Proteomics* **2004**, *4* (6), 1703–1711. https://doi.org/10.1002/pmic.200300705.
(188) Rieser, R.; Penaud-Budloo, M.; Bouzelha, M.; Rossi, A.; Menzen, T.; Biel, M.; Büning, H.; Ayuso, E.; Winter, G.; Michalakis, S. Intrinsic Differential Scanning Fluorimetry for Fast and Easy Identification of Adeno-Associated Virus Serotypes. *J. Pharm. Sci.* **2020**, *109* (1), 854–862. https://doi.org/10.1016/J.XPHS.2019.10.031.
(189) Vivian, J. T.; Callis, P. R. Mechanisms of Tryptophan Fluorescence Shifts in Proteins. *Biophys. J.* **2001**, *80* (5), 2093–2109. https://doi.org/10.1016/S0006-3495(01)76183-8.
(190) Kelly, S. M.; Jess, T. J.; Price, N. C. How to Study Proteins by Circular Dichroism. *Biochim. Biophys. Acta - Proteins Proteomics* **2005**, *1751* (2), 119–139. https://doi.org/10.1016/j.bbapap.2005.06.005.
(191) Holzwarth, G.; Doty, P. The Ultraviolet Circular Dichroism of Polypeptides. *J. Am. Chem. Soc.* **1965**, *87* (2), 218–228. https://doi.org/10.1021/ja01080a015.
(192) Beychok, S. Circular Dichroism of Biological Macromolecules. *Science (80-.).* **1966**, *154* (3754), 1288–1299. https://doi.org/10.1126/science.154.3754.1288.
(193) Greenfield, N.; Fasman, G. D. Computed Circular Dichroism Spectra for the Evaluation of Protein Conformation. *Biochemistry* **1969**, *8* (10), 4108–4116. https://doi.org/10.1021/bi00838a031.
(194) Greenfield, N. J. Circular Dichroism (CD) Analyses of Protein-Protein Interactions. In *Protein-Protein Interactions: Methods and Applications: Second Edition*; Springer New York, 2015; Vol. 1278, pp 239–265. https://doi.org/10.1007/978-1-4939-2425-7_15.
(195) Joshi, V.; Shivach, T.; Yadav, N.; Rathore, A. S. Circular Dichroism Spectroscopy as a Tool for Monitoring Aggregation in Monoclonal Antibody Therapeutics. *Anal. Chem.* **2014**, *86* (23), 11606–11613. https://doi.org/10.1021/AC503140J.
(196) Fiedler, S.; Cole, L.; Keller, S. Automated Circular Dichroism Spectroscopy for Medium-Throughput Analysis of Protein Conformation. *Anal. Chem.* **2013**, *85* (3), 1868–1872. https://doi.org/10.1021/ac303244g.
(197) Moore-Kelly, C.; Welsh, J.; Rodger, A.; Dafforn, T. R.; Thomas, O. R. T. Automated High-Throughput Capillary Circular Dichroism and Intrinsic Fluorescence Spectroscopy for Rapid Determination of Protein Structure. *Anal. Chem.* **2019**, *91* (21), 13794–13802. https://doi.org/10.1021/acs.analchem.9b03259.
(198) Vaynberg, J.; Qin, J. Weak Protein-Protein Interactions as Probed by NMR Spectroscopy. *Trends Biotechnol.* **2006**, *24* (1), 22–27. https://doi.org/10.1016/j.tibtech.2005.09.006.
(199) Mlynárik, V. Introduction to Nuclear Magnetic Resonance. *Anal. Biochem.* **2017**, *529*, 4–9. https://doi.org/10.1016/J.AB.2016.05.006.
(200) Thompson, P. M.; Beck, M. R.; Campbell, S. L. Protein-Protein Interaction Analysis by Nuclear Magnetic Resonance Spectroscopy. In *Protein-Protein Interactions: Methods and Applications:*

Second Edition; Springer New York, 2015; pp 267–279. https://doi.org/10.1007/978-1-4939-2425-7_16.

(201) O'Connell, M. R.; Gamsjaeger, R.; Mackay, J. P. The Structural Analysis of Proteinâ€“Protein Interactions by NMR Spectroscopy. *Proteomics* **2009**, *9* (23), 5224–5232. https://doi.org/10.1002/pmic.200900303.

(202) Vinogradova, O.; Qin, J. NMR as a Unique Tool in Assessment and Complex Determination of Weak Protein-Protein Interactions. *Top. Curr. Chem.* **2012**, *326*, 35–46. https://doi.org/10.1007/128_2011_216.

(203) Walters, K. J.; Ferentz, A. E.; Hare, B. J.; Hidalgo, P.; Jasanoff, A.; Matsuo, H.; Wagner, G. Characterizing Protein-Protein Complexes and Oligomers by Nuclear Magnetic Resonance Spectroscopy. In *Methods in Enzymology*; Academic Press Inc., 2001; Vol. 339, pp 238–252. https://doi.org/10.1016/S0076-6879(01)39316-3.

(204) Du, Z.; Lee, J. K.; Fenn, S.; Tjhen, R.; Stroud, R. M.; James, T. L. X-Ray Crystallographic and NMR Studies of Protein-Protein and Protein-Nucleic Acid Interactions Involving the KH Domains from Human Poly(C)-Binding Protein-2. *RNA* **2007**, *13* (7), 1043–1051. https://doi.org/10.1261/rna.410107.

(205) Wang, J. H.; Meijers, R.; Xiong, Y.; Liu, J. H.; Sakihama, T.; Zhang, R.; Joachimiak, A.; Reinherz, E. L. Crystal Structure of the Human CD4 N-Terminal Two-Domain Fragment Complexed to a Class II MHC Molecule. *Proc. Natl. Acad. Sci. U. S. A.* **2001**, *98* (19), 10799–10804. https://doi.org/10.1073/pnas.191124098.

(206) Smyth, M. S.; Martin, J. H. J. X Ray Crystallography. *J. Clin. Pathol. - Mol. Pathol.* **2000**, *53* (1), 8–14. https://doi.org/10.1136/mp.53.1.8.

(207) Dessau, M. A.; Modis, Y. Protein Crystallization for X-Ray Crystallography. *J. Vis. Exp.* **2010**, No. 47. https://doi.org/10.3791/2285.

(208) Kobe, B.; Guncar, G.; Buchholz, R.; Huber, T.; Maco, B.; Cowieson, N.; Martin, J. L.; Marfori, M.; Forwood, J. K. Crystallography and Protein-Protein Interactions: Biological Interfaces and Crystal Contacts. *Biochem. Soc. Trans.* **2008**, *36* (6), 1438–1441. https://doi.org/10.1042/BST0361438.

(209) Yip, K. M.; Fischer, N.; Paknia, E.; Chari, A.; Stark, H. Atomic-Resolution Protein Structure Determination by Cryo-EM. *Nat. 2020 5877832* **2020**, *587* (7832), 157–161. https://doi.org/10.1038/s41586-020-2833-4.

(210) Cheng, Y. Single-Particle Cryo-EM—How Did It Get Here and Where Will It Go. *Science (80-.).* **2018**, *361* (6405), 876–880. https://doi.org/10.1126/SCIENCE.AAT4346.

(211) Requirements for Preparation of Cryo-EM Samples A Vital Step in the Cryo-EM Workflow. https://doi.org/10.1016/bs.mie.2016.04.011.

(212) Liu, Y.; Huynh, D. T.; Yeates, T. O. A 3.8 Å Resolution Cryo-EM Structure of a Small Protein Bound to an Imaging Scaffold. *Nat. Commun. 2019 101* **2019**, *10* (1), 1–7. https://doi.org/10.1038/s41467-019-09836-0.

(213) Wyatt, P. J. Light Scattering and the Absolute Characterization of Macromolecules. *Anal. Chim. Acta* **1993**, *272* (1), 1–40. https://doi.org/10.1016/0003-2670(93)80373-S.

(214) Gun'ko, V. M.; Klyueva, A. V.; Levchuk, Y. N.; Leboda, R. Photon Correlation Spectroscopy Investigations of Proteins. *Adv. Colloid Interface Sci.* **2003**, *105* (1–3), 201–328. https://doi.org/10.1016/S0001-8686(03)00091-5.

(215) Stetefeld, J.; McKenna, S. A.; Patel, T. R. Dynamic Light Scattering: A Practical Guide and Applications in Biomedical Sciences. *Biophys. Rev.* **2016**, *8* (4), 409–427. https://doi.org/10.1007/s12551-016-0218-6.

(216) Larkin, M.; Wyatt, P. Light-Scattering Techniques and Their Application to Formulation and Aggregation Concerns. In *Formulation and Process Development Strategies for Manufacturing Biopharmaceuticals*; John Wiley & Sons, Inc.: Hoboken, NJ, USA, 2010; pp 269–305. https://doi.org/10.1002/9780470595886.ch12.

(217) Yadav, S.; Scherer, T. M.; Shire, S. J.; Kalonia, D. S. Use of Dynamic Light Scattering to Determine Second Virial Coefficient in a Semidilute Concentration Regime. *Anal. Biochem.* **2011**, *411* (2), 292–296. https://doi.org/10.1016/j.ab.2010.12.014.
(218) Billinger, E.; Zuo, S.; Lundmark, K.; Johansson, G. Light Scattering Determination of the Stoichiometry for Protease-Potato Serine Protease Inhibitor Complexes. *Anal. Biochem.* **2019**, *582*, 113357. https://doi.org/10.1016/j.ab.2019.113357.
(219) Hanlon, A. D.; Larkin, M. I.; Reddick, R. M. Free-Solution, Label-Free Protein-Protein Interactions Characterized by Dynamic Light Scattering. *Biophys. J.* **2010**, *98* (2), 297–304. https://doi.org/10.1016/j.bpj.2009.09.061.
(220) He, F.; Becker, G. W.; Litowski, J. R.; Narhi, L. O.; Brems, D. N.; Razinkov, V. I. High-Throughput Dynamic Light Scattering Method for Measuring Viscosity of Concentrated Protein Solutions. *Anal. Biochem.* **2010**, *399* (1), 141–143. https://doi.org/10.1016/j.ab.2009.12.003.
(221) Langevin, D.; Raspaud, E.; Mariot, S.; Knyazev, A.; Stocco, A.; Salonen, A.; Luch, A.; Haase, A.; Trouiller, B.; Relier, C.; Lozano, O.; Thomas, S.; Salvati, A.; Dawson, K. Towards Reproducible Measurement of Nanoparticle Size Using Dynamic Light Scattering: Important Controls and Considerations. *NanoImpact* **2018**, *10*, 161–167. https://doi.org/10.1016/J.IMPACT.2018.04.002.
(222) Drake, A. W.; Tang, M. L.; Papalia, G. A.; Landes, G.; Haak-Frendscho, M.; Klakamp, S. L. Biacore Surface Matrix Effects on the Binding Kinetics and Affinity of an Antigen/Antibody Complex. *Anal. Biochem.* **2012**, *429* (1), 58–69. https://doi.org/10.1016/j.ab.2012.06.024.
(223) Khan, S. H.; Farkas, K.; Kumar, R.; Ling, J. A Versatile Method to Measure the Binding to Basic Proteins by Surface Plasmon Resonance. *Anal. Biochem.* **2012**, *421* (2), 385–390. https://doi.org/10.1016/J.AB.2011.12.006.
(224) Myszka, D. G.; He, X.; Dembo, M.; Morton, T. A.; Goldstein, B. Extending the Range of Rate Constants Available from BIACORE: Interpreting Mass Transport-Influenced Binding Data. *Biophys. J.* **1998**, *75* (2), 583–594. https://doi.org/10.1016/S0006-3495(98)77549-6.
(225) Day, Y. S. N.; Baird, C. L.; Rich, R. L.; Myszka, D. G. Direct Comparison of Binding Equilibrium, Thermodynamic, and Rate Constants Determined by Surface- and Solution-Based Biophysical Methods. *Protein Sci.* **2002**, *11* (5), 1017–1025. https://doi.org/10.1110/ps.4330102.
(226) Gudgin Dickson, E. F.; Pollak, A.; Diamandis, E. P. Time-Resolved Detection of Lanthanide Luminescence for Ultrasensitive Bioanalytical Assays. *J. Photochem. Photobiol. B Biol.* **1995**, *27* (1), 3–19. https://doi.org/10.1016/1011-1344(94)07086-4.
(227) Redhead, M.; Satchell, R.; McCarthy, C.; Pollack, S.; Unitt, J. Thermal Shift as an Entropy-Driven Effect. *Biochemistry* **2017**, *56* (47), 6187–6199. https://doi.org/10.1021/acs.biochem.7b00860.
(228) Jaindl, M.; Popp, M. Cyclitols Protect Glutamine Synthetase and Malate Dehydrogenase against Heat Induced Deactivation and Thermal Denaturation. *Biochem. Biophys. Res. Commun.* **2006**, *345* (2), 761–765. https://doi.org/10.1016/j.bbrc.2006.04.144.
(229) Safarian, S.; Bagheri, F.; Moosavi-Movahedi, A. A.; Amanlou, M.; Sheibani, N. Competitive Inhibitory Effects of Acetazolamide upon Interactions with Bovine Carbonic Anhydrase II. *Protein J.* **2007**, *26* (6), 371–385. https://doi.org/10.1007/s10930-007-9073-4.
(230) González, M.; Argaraña, C. E.; Fidelio, G. D. Extremely High Thermal Stability of Streptavidin and Avidin upon Biotin Binding. *Biomol. Eng.* **1999**, *16* (1–4), 67–72. https://doi.org/10.1016/S1050-3862(99)00041-8.
(231) Hunter, J. C.; Manandhar, A.; Carrasco, M. A.; Gurbani, D.; Gondi, S.; Westover, K. D. Biochemical and Structural Analysis of Common Cancer-Associated KRAS Mutations. *Mol. Cancer Res.* **2015**, *13* (9), 1325–1335. https://doi.org/10.1158/1541-7786.MCR-15-0203.
(232) Buhrman, G.; Holzapfel, G.; Fetics, S.; Mattos, C. Allosteric Modulation of Ras Positions Q61 for a Direct Role in Catalysis. *Proc. Natl. Acad. Sci.* **2010**, *107* (11), 4931–4936. https://doi.org/10.1073/PNAS.0912226107.

(233) Patricelli, M. P.; Janes, M. R.; Li, L.-S.; Hansen, R.; Peters, U.; Kessler, L. V.; Chen, Y.; Kucharski, J. M.; Feng, J.; Ely, T.; Chen, J. H.; Firdaus, S. J.; Babbar, A.; Ren, P.; Liu, Y. Selective Inhibition of Oncogenic KRAS Output with Small Molecules Targeting the Inactive State. *Cancer Discov.* **2016**, *6* (3), 316–329. https://doi.org/10.1158/2159-8290.CD-15-1105.

(234) Janes, M. R.; Zhang, J.; Li, L. S.; Hansen, R.; Peters, U.; Guo, X.; Chen, Y.; Babbar, A.; Firdaus, S. J.; Darjania, L.; Feng, J.; Chen, J. H.; Li, S.; Li, S.; Long, Y. O.; Thach, C.; Liu, Y.; Zarieh, A.; Ely, T.; Kucharski, J. M.; Kessler, L. V.; Wu, T.; Yu, K.; Wang, Y.; Yao, Y.; Deng, X.; Zarrinkar, P. P.; Brehmer, D.; Dhanak, D.; Lorenzi, M. V.; Hu-Lowe, D.; Patricelli, M. P.; Ren, P.; Liu, Y. Targeting KRAS Mutant Cancers with a Covalent G12C-Specific Inhibitor. *Cell* **2018**, *172* (3), 578-589.e17. https://doi.org/10.1016/J.CELL.2018.01.006.

(235) Hallin, J.; Engstrom, L. D.; Hargis, L.; Calinisan, A.; Aranda, R.; Briere, D. M.; Sudhakar, N.; Bowcut, V.; Baer, B. R.; Ballard, J. A.; Burkard, M. R.; Fell, J. B.; Fischer, J. P.; Vigers, G. P.; Xue, Y.; Gatto, S.; Fernandez-Banet, J.; Pavlicek, A.; Velastagui, K.; Chao, R. C.; Barton, J.; Pierobon, M.; Baldelli, E.; Patricoin, E. F.; Cassidy, D. P.; Marx, M. A.; Rybkin, I. I.; Johnson, M. L.; Ou, S.-H. I.; Lito, P.; Papadopoulos, K. P.; Jänne, P. A.; Olson, P.; Christensen, J. G. The KRASG12C Inhibitor MRTX849 Provides Insight toward Therapeutic Susceptibility of KRAS-Mutant Cancers in Mouse Models and Patients. *Cancer Discov.* **2020**, *10* (1), 54–71. https://doi.org/10.1158/2159-8290.CD-19-1167.

(236) Kohl, A.; Binz, H. K.; Forrer, P.; Stumpp, M. T.; Plückthun, A.; Grütter, M. G. Designed to Be Stable: Crystal Structure of a Consensus Ankyrin Repeat Protein. *Proc. Natl. Acad. Sci. U. S. A.* **2003**, *100* (4), 1700–1705. https://doi.org/10.1073/pnas.0337680100.

(237) Wu, Y.; Batyuk, A.; Honegger, A.; Brandl, F.; Mittl, P. R. E.; Plückthun, A. Rigidly Connected Multispecific Artificial Binders with Adjustable Geometries. *Sci. Reports 2017 71* **2017**, *7* (1), 1–11. https://doi.org/10.1038/s41598-017-11472-x.

(238) Weber, P. C.; Ohlendorf, D. H.; Wendoloski, J. J.; Salemme, F. R. Structural Origins of High-Affinity Biotin Binding to Streptavidin. *Science (80-.).* **1989**, *243* (4887), 85–88. https://doi.org/10.1126/science.2911722.

(239) Kåpyaho, K.; Tanner, P.; Kårkkåinen, T.; Weber, T. Rapid Determination of C-Reactive Protein by Enzyme Immunoassay Using Two Monoclonal Antibodies. *Scand. J. Clin. Lab. Invest.* **1989**, *49* (4), 389–393. https://doi.org/10.3109/00365518909089112.

(240) Mahler, H. C.; Friess, W.; Grauschopf, U.; Kiese, S. Protein Aggregation: Pathways, Induction Factors and Analysis. *Journal of Pharmaceutical Sciences*. John Wiley and Sons Inc. 2009, pp 2909–2934. https://doi.org/10.1002/jps.21566.

(241) Sauerborn, M.; Brinks, V.; Jiskoot, W.; Schellekens, H. Immunological Mechanism Underlying the Immune Response to Recombinant Human Protein Therapeutics. *Trends Pharmacol. Sci.* **2010**, *31* (2), 53–59. https://doi.org/10.1016/J.TIPS.2009.11.001.

(242) Oshinbolu, S.; Shah, R.; Finka, G.; Molloy, M.; Uden, M.; Bracewell, D. G. Evaluation of Fluorescent Dyes to Measure Protein Aggregation within Mammalian Cell Culture Supernatants. *J. Chem. Technol. Biotechnol.* **2018**, *93* (3), 909–917. https://doi.org/10.1002/jctb.5519.

(243) He, F.; Phan, D. H.; Hogan, S.; Bailey, R.; Becker, G. W.; Narhi, L. O.; Razinkov, V. I. Detection of IgG Aggregation by a High Throughput Method Based on Extrinsic Fluorescence. *J. Pharm. Sci.* **2010**, *99* (6), 2598–2608. https://doi.org/10.1002/jps.22036.

(244) Miranda-Hernández, M. P.; López-Morales, C. A.; Piña-Lara, N.; Perdomo-Abúndez, F. C.; Pérez, N. O.; Revilla-Beltri, J.; Molina-Pérez, A.; Estrada-Marín, L.; Flores-Ortiz, L. F.; Ruiz-Argüelles, A.; Medina-Rivero, E. Pharmacokinetic Comparability of a Biosimilar Trastuzumab Anticipated from Its Physicochemical and Biological Characterization. *Biomed Res. Int.* **2015**, *2015*. https://doi.org/10.1155/2015/874916.

(245) Gervasi, V.; Dall Agnol, R.; Cullen, S.; McCoy, T.; Vucen, S.; Crean, A. Parenteral Protein Formulations: An Overview of Approved Products within the European Union. *European*

Journal of Pharmaceutics and Biopharmaceutics. Elsevier B.V. October 1, 2018, pp 8–24. https://doi.org/10.1016/j.ejpb.2018.07.011.

TURUN
YLIOPISTO
UNIVERSITY
OF TURKU

Painosalama Oy, Turku, Finland 2021

ISBN 978-951-29-8723-8 (PRINT)
ISBN 978-951-29-8724-5 (PDF)
ISSN 0082-7002 (Print)
ISSN 2343-3175 (Online)